CAUSES OF FAILURE OF HIGHWAY CROSS DRAINAGE STRUCTURES

(A CASE STUDY ON SILE RIVER BRIDGE-ARBAMINCH ETHIOPIA)

A THESIS SUBMITTED TO THE SCHOOL OF GRADUATE STUDIES OF ADDIS ABABA UNIVERSITY IN PARTIAL FULFILLMENT OF THE REQUIREMENTS FOR THE DEGREE OF MASTER OF SCIENCE IN CIVIL ENGINEERING

KEFARGACHEW KASSAHUN
ADDIS ABABA UNIVERSITY
ADDIS ABABA INSTITUTE OF TECHNOLOGY

AUGUST-2015
ADDIS ABABA

CAUSES OF FAILURE OF HIGHWAY CROSS DRAINAGE STRUCTURES

(A CASE STUDY ON SILE RIVER BRIDGE -ARBAMINCH ETHIOPIA)

BY

KEFARGACHEW KASSAHUN

A THESIS SUBMITTED TO THE SCHOOL OF GRADUATE STUDIES OF ADDIS ABABA UNIVERSITY IN PARTIAL FULFILLMENT OF THE REQUIREMENTS FOR THE DEGREE OF MASTER OF SCIENCE IN CIVIL ENGINEERING

Dr. ASSIE KEMAL
THESIS ADVISOR

ADDIS ABABA UNIVERSITY
ADDIS ABABA INSTITUTE OF TECHNOLOGY

AUGUST-2015
ADDIS ABABA

CAUSES OF FAILURE OF HIGHWAY CROSS DRAINAGE STRUCTURES

(A CASE STUDY ON SILE RIVER BRIDGE -ARBAMINCH ETHIOPIA)

BY

KEFARGACHEW KASSAHUN

A THESIS SUBMITTED TO THE SCHOOL OF GRADUATE STUDIES OF ADDIS ABABA UNIVERSITY IN PARTIAL FULFILLMENT OF THE REQUIREMENTS FOR THE DEGREE OF MASTER OF SCIENCE IN CIVIL ENGINEERING

<u>Approved by Board of Examiners</u>

Dr. Assie Kemal

…………………………………	……………………………	………………………
Advisor	**Signature**	**Date**

Dr. Ing. Geremew Sahilu

……...…………………………	……………………………	………………………
External Examiner	**Signature**	**Date**

Dr. Yilima Sileshi

…………………………………	……………………………	………………………
Internal Examiner	**Signature**	**Date**

Dr. Esayas G/Yohannes

…………………………………	……………………………	………………………
Chairman	**Signature**	**Date**

DECLARATION

I the undersigned, declare that, this Thesis is my work and all sources of materials used for this Thesis have been duly acknowledged.

Name: *Kefargachew Kassahun*

Signature: ………………………………….

Place: *Addis Ababa University (AAU)*

Addis Ababa Institute of Technology (AAIT)

Date of Submission: *August, 2015*

This Thesis is Dedicated to My Daughters

Ruth & Tsion

ACKNOWLEDGEMENT

I would like to express my deepest gratitude to my advisor, Dr. Assie Kemal, for his excellent guidance, caring, patience, and providing me with an excellent atmosphere for doing research. His guidance helped me in all the time of research and writing this Thesis.

Besides my Thesis advisor, my sincere thanks also goes to Mekari Zemedagegnehu (Highway Engineer-NET Consulting PLC), Engida Zemedagegnehu (Hydro-geologist-Water Works Design & Supervision Enterprise), Esmael Edris (Hydraulics Engineer-China Communication Construction Corporation), Tekilesilassie Nida (Engineer-Ethiopian Roads Authority-Bridge Management Team) and Bamilaku Yilikal (GIS Expert -Road Network Planning Team-ERA).

I would like to thank also the Ethiopian Roads Authority for giving me this chance and covering the cost of my study and research.

Finally, I must express my very profound gratitude to my Family for providing me with unfailing support and continuous encouragement throughout my years of study and through the process of researching and writing this Thesis. This accomplishment would not have been possible without them. Thank you.

ABSTRACT

Highway hydraulic structures perform the vital function of conveying, diverting, or removing surface water from the road right-of-way. In this regard, various types of drainage facilities are required to protect the roads against surface and subsurface water. Among these, Bridges are the most indispensable and expensive highway cross drainage structures that convey storm water under roads.

Bridge sub-structure components; Piers, Abutments and their approach embankments, are damaged by scour during floods. Scour refers to the removal of soil, sand and rocks from around bridge Piers or Abutments by swiftly moving flood current.

The overall objective of the research was to investigate causes of failure of the Sile River Bridge particularly focusing on hydrologic and hydraulic factors.

The SCS Unit Hydrograph Model, HEC-RAS 4.0 Beta, HEC-18 Evaluating Scour at Bridges, Eagle Point Auto CAD-2007 and other supporting soft wares are used to analyze the causes of failure of the Sile River Bridge. Using these models, DEM data, topographic survey data, meteorological and soil are analyzed and the peak discharge, Contraction scour, Local scour at Abutments are estimated and also the adequacy of the bridge opening is checked. The Analyses shows that, there is under estimation of the peak discharge and opening size of the Sile River Bridge. The main failure cause of the Sile River Bridge is Scour both contraction scour at the main channel of the bridge opening area and local scour at the abutments which is estimated about 5.8m total scour depth.

LIST OF ABBREVIATIONS

AASHTO	American Association of State Highway &Transportation
ASTM	American Society for Testing and Materials
BDM	Bridge Design Manual
BMS	Bridge Management System
CAD	Computer Aided Design
C-25	Concrete-25
CSU	Colorado State University
CN	Curve Number
DED	District Engineering Division
DEM	Digital Elevation Model
DS	Design Standard
E	East
ERA	Ethiopian Roads Authority
DDM	Drainage Design Manual
FDOT	Florida Department of Transportation
FHWA	Federal High Way Authority
GIS	Geographic Information System
HEC-RAS	Hydraulic Engineering Circular-River Analysis System
HSG	Hydrologic Soil Group
HS 20-44 Loading	Trucks that pull trailer HS-20 ton semitrailer truck
IDF	Intensity Duration Frequency
ITCZ	Inter Tropical Convergence Zone
HWM	High Water Mark
Km	Kilometer
Km^2	Kilometer Square
m	Meter
masl	Meter above sea level
m/s	Meter per Second
m^3/s	Cubic Meter per Second
mm	Milimeter
MoWIE	Ministry of Water Irrigation and Energy
N	North
NCHRP	National Cooperative Highway Research Program
NMA	National Meteorological Agency
PVC	Poly Vinyl Chloride
RC	Reinforced Concrete
SCS	Soil Conservation Service
SI	International System of Units
SRTM	Shuttle Radar Topography Mission
TCDE	Transport Construction and Design Enterprise
US	United States
USACE	United States Army Corps of Engineers
UTM	Universal Traverse Mercator

LIST OF FIGURES, PHOTOS AND TABLES

LIST OF FIGURES

LIST OF PHOTOS

LIST OF TABLES

TABLE OF CONTENTS

1. BACKGROUND

1.1. General

Roads are the key to the development of an economy. A good road network constitutes the basic infrastructure that accelerates the development process through connectivity and opening up of potential areas to trade and investment. Roads also play a key role in inter-modal transport development establishing links with airports, railway stations and ports. In addition, they have an important role in promoting national integration, which is particularly important in a large country like Ethiopia

In the context of Ethiopia's geography, pattern of settlement and economic activity, transport plays a vital role in facilitating economic development as 95% of the movement of people, and goods is still carried out by road transport(ERA, RSDP, 16 Years Performance Assessment, 2013).

A good road network should constitute the basic infrastructure that accelerates the development process through connectivity and should be built with different structural components. Among these various types of structural components, drainage structures are the key to protect the highway against surface and subsurface water and to provide the required service.

Culverts and Bridges are the major drainage structures that convey storm water under roads. Their purpose is to prevent water from the more frequent storm events from overtopping and crossing the road as such conditions inhibit safe passage of vehicles. Particularly Bridges serve a variety of highway purposes including the elimination of conflicts with traffic and other modes of transportation. Moreover, Bridges enables watercourses to maintain the natural function of flow conveyance and sustaining aquatic life. The use of hydraulic structures can also increase the capital cost of drainage facilities while lowering Operation &Maintenance costs. On the other hand, use of hydraulic structures can reduce initial and future maintenance costs by changing the characteristics of the flow to fit the project needs, and by reducing the size and cost of related facilities.

Hence, the use of hydraulic structures should be limited by careful and thorough hydraulic engineering practices to Locations and Functions justified by prudent planning and design (Hydraulic Design of Safe Bridges, US Department of Transportation, 2012). Moreover, hydraulic structures should be designed to be commensurate with risk, construction cost, importance of the road, economy of maintenance, and legal requirements (Manual for Concrete Bridge Maintenance, ERA, 2010). Contrary to these, though Bridges are important and expensive high-way hydraulic structures, they are vulnerable to failure from flood related causes like overtopping and scour.

Many researches have been conducted during the past but it is still difficult to understand fully all causes of failures of hydrologic and hydraulic factors that affect the performance of highway hydraulic structures in general and Bridges in particular.

Therefore, this research is conducted on the Sile River Bridge which is located approximately at about 523 Km from Addis Ababa and at about 13.6Km from Arbaminch in the South-West direction on the road to Jinka. The Bridge is a single span 20.0m, which was built in 1991 to carry the HS 20-44 loading. However, it is severely affected by scour around the pile, pile cap and abutments. Currently the bridge is hazardous and closed for traffic.

The scope of this research is to assess and analyze the causes of failure of highway cross drainage structures a case of the Sile River Bridge specific to hydrologic and hydraulic factors & to propose appropriate countermeasures & recommendations.

1.2. Description of the Sile River Bridge

The Sile River Bridge is located in the Sodo District in the Arbaminch-Wezeka Road Segment approximately at 523 Km from Addis Ababa and at about Km 13+600 from Arbaminch in the South-West direction on the road to Jinka at UTM coordinates E-334,085 and N-652,342.

The bridge is designed by the Transport Construction Design Enterprise (TCDE) and built by Sur Construction a local Contractor in 1991 with good workmanship.

1.2.1. Observed Hydraulic Conditions

Sile Bridge has 20.00 m span and clear height of about 8.00 m. The existing bridge is located at sharp river bend. The location of the bridge is at the meandering section of the river which might be responsible for high head loss at the bridge inlet. The head loss increases the water stage on the upstream side of the bridge and results in high backwater at the inlet. At about 20-25m downstream of the bridge from the main road/bridge, there is a Bialy Bridge with a clear height of less than the existing bridge and which creates the back water that could affect the flow in the main bridge. According to the information obtained from the site and observed existing condition, the bialy bridge is frequently overtopped.

Photo 1-1: Bialy Bridge Downstream of the Sile River Bridge (Source: ERA, BMS-2012)

1.2.2. Structural Investigation

The Sile River Bridge is a Single Span Reinforced Concrete Deck Girder Bridge. From actual measurement of the existing superstructure, it is observed that, this bridge is a two lane two-way bridge having 7.32m carriage way width and 1.50m walkway at both side of the superstructure. The deck slab is spanned on 2.09m spaced four girders supported on two RC cantilever abutment which further rests on 15.00m long RC friction piles at both side of the road. Both reinforced concrete abutments and wing walls are supported on 1.00m pile-cup which is further rests on 15.00m long 12 reinforced concrete frictionless piles under both abutments.

Table 1-1: Dimension of Components of the Bridge

No.	Component	Dimension
1.	Clear Span	20.00m
2.	Bridge Location Co-ordinate	Easting = 334,088 Northing= 652,338
3.	Clear Height of First Abutment	3.40m
4.	Clear Height of Second Abutment	3.40m
5.	Wing wall Length of First Abutment	3.50m
6.	Wing wall Length of Second Abutment	4.60m
7.	Clear Road way Width	7.32m
8.	Side Walk Width	1.50m
9.	Total width (carriage and walk way)	10.32m

Concerning the Superstructure of the Bridge, it is in good condition and no defect is observed. There is steel railing on top both left and right walkway and placed with good conditions. No pavement weaving and displacement is observed on Asphalt Pavement Structure.

Severe foundation scouring, embankment depression and erosion, damaged and failed masonry and gabion embankment protection structure, displacement and missing are among the major observed defects on the substructure of the bridge. The observed major defects on reinforced concrete substructure components and channel bed of this bridge briefly discussed below.

During the site visit, it was observed also that, RC pile cap and some of the channel side pile foundation are exposed due to scour especially on the Arbaminch side. The substructure is severely scoured because it is continuously flashed and seriously affected by the October 2012 flood.

Photo1-2: Exposed Pile and Pile Cap due to Scour (Source: ERA, BMS-October 2012)

The road around the Bridge is severely damaged. According to the information gathered from peoples residing around the Bridge, the problem is more pronounced in the 2012 flood season. The flood has washed away all the river training work and erodes part of the road embankment.

Photo1-3: Eroded Embankment on the Left Side of River Bank on Arbaminch Side
(Source: ERA-BMS, October-2012)

1.2.3. Countermeasures

Protection works were implemented on the upstream side as well as under the Bridge to minimize the risk of total collapse of the Bridge.

According to the information obtained from the Ethiopian Roads Authority's Bridge Management System, a number of protection measures were implemented by to stop propagation of scour around the structures. Nevertheless, the protection measures were failed. The following photos describe the current condition.

Photo1-4: Collapsed Protection work at the upstream Inlet Upstream

(Source: ERA-BMS, October-2012)

Protection measures were failed from the bank into the river bed as shown in the above figure. The fallen material creates flow turbulence at the bridge inlet, increases the water stage at the inlet and aggravates the prevailing problem especially by eroding the bank. The change/ the failure rate are rapid as it is observed. As an example, the rate could be illustrated using the picture taken before and after the rainy season of 2012.

Photo1-5: Left Bank with Embankment Protection (Source: ERA-BMS, August 2012)

Photo1-6: Damaged Left Bank (Source: ERA-BMS, October 2012)

Photo1-7: Right Bank with Protection Work (Source: ERA-BMS, August 2012)

Photo1-8: Failed Right Bank Protection Work (Source: ERA-BMS, October 2012)

1.3. Statement of the Problem

It is known that, Highway hydraulic structures perform the vital function of conveying, diverting, or removing surface water from the road right-of-way. In this regard, various types of drainage facilities are required to protect the roads against surface and subsurface water. Therefore, highway drainage facilities must be designed to convey the water across, along, or away from the highway in the most economical, efficient, and safe manner without damaging the road or adjacent property.

Though Bridges are the most important and expensive highway hydraulic structures, frequently they are vulnerable to failure from flood related causes.

An investigation of the Sile River Bridge at existing conditions produced the following observations:

- Severe scour, cracks and failure of pile, pile cap and erosion of Abutment Foundation.
- Flooding around the Bridge location and debris on the downstream Bialy Bridge.
- Severe Erosion on the embankment (collapse of the back fill) and
- Collapse of wing wall and displaced Gabions and other countermeasures.

Based on the observed condition as well as the information obtained from the site, the following are expected causes for the Bridge failure.

- Under estimation of the design flood which makes the Bridge inadequate to pass the design flood.
- The Bridge is located at meandering section of the river (located on sharp river bend).
- Masonry Embankment and pile protection structure were constructed around both banks of upstream channel bed of the river. These protection structures might be aggravated scouring by increasing the velocity of flow during rainy season by constricting the natural flow width. Due to the obstruction effect, the channel is scoured severely increased and created instability on the protection structures. (i.e. Gabion and masonry wall).

As it is mentioned in the previous section, different types of countermeasures without conducting an investigation on the causes of the problem were implemented.

Nowadays, though various design alternatives, construction, inspection and maintenance practices exist; it is difficult to minimize such kinds of existing problem, because each intervention has its own drawback which is entirely dependent on cost, and limited effectiveness. Therefore, this study evaluates common bridge scour problems and causes of failure and recommends improvements in considering the hydraulic and hydrologic design parameters during design, construction, inspection and maintenance.

Generally, this research deeply investigated the major causes of failure of the Sile River Bridge which are mainly related to hydrologic and hydraulic factors and proposed recommendations which can help to minimize the current problems and to be further applied in the subsequent design and construction interventions in particular and research studies in general.

1.4. Research Questions

The following are the research questions in which this study tries to investigate and to respond.

- **i.** What are some of the Hydrological and Hydraulic factors that are not properly considered during design of the Sile River Bridge and that occurred between the year 1991 and 2012 that would cause failure of Bridge substructure components (Piles, Pile Caps, Abutments) and Countermeasures? and
- **ii.** Why Proper Design of Countermeasures is so important? and how does it expose Bridge Substructure Components to concentrated hydraulic loading?

1.5. General Objectives

The overall objectives of this research were:

- to investigate bridge failure causes due to hydrologic and hydraulic problems and

- to propose proper countermeasures, recommendations and conclusions for design, construction, and maintenance that will reduce this costly problem.

1.5.1. Specific Objectives

In this regard this research tries:

- to assess and analyze the different hydrological and hydraulic causes of failure of the existing Sile River Bridge.
- to interpret factors responsible for the problem and causes of failure of countermeasures taken and the necessary corrective measures.
- to provide recommendations to counter balance the problem and for adoption of specific research results and,
- to suggest future research needs.

1.6. Significance of the Research

Bridges form an essential part of a highway infrastructure. The fact is that closure of a bridge may result more severe and long lasting negative effect on traffic flow than closure of any other section of a high way makes. Therefore, Bridges are the most important component of a highway infrastructure. The construction cost of a bridge is also more expensive than other components of a highway if comparison is made based on linear measurement.

In spite of the above facts, it is only very limited action in terms of having data base on the failure causes, inspection efforts made towards maintaining of bridges found in the country. Many of the bridges have been deteriorated significantly over the past decades due to inadequate consideration of hydrologic and hydraulic parameters during design, construction, inspection, maintenance and other factors. Among these, Bridge Scour is one of the major causes of bridge failures in Ethiopia.

The output of this research work believed to greatly assist bridge designers in introducing the causes of failure of cross drainage structures as well as application of the required level of Hydrological and Hydraulic considerations during design, construction and also implementation of scour countermeasures.

1.7. Scope and Limitations of the Research

This study is conducted to determine the causes of failure of the bridge under consideration by conducting detail investigation to hydrologic, hydraulic causes and scour problems affecting bridge substructure components namely piles, pile caps, abutments and protection structures. Hence, the study does not consider the change in river morphology around the bridge opening and the land use change as a factor.

1.8. Structure of the Thesis

This Thesis consists of Six Chapters. The First Chapter deals about the overall background which deals about importance of roads and component drainage structures particularly Bridges, Bridge Scour, common hydrologic and hydraulic problems, general and specific objectives of the Thesis, brief description about the Sile River Bridge, statement of the problem, significance of the research and finally the scope and Limitations of the study.

The Second Chapter of the Thesis is the Literature Review which deals about definition and basic concepts of scour, types of scour, pier and abutment scour equations, factors affecting scour and scour modeling tools.

The Third Chapter is Methods and Materials which give emphasis on the type of data collected and methods used to analyze the problem such as hydrological, meteorological data and hydrological and hydraulic models.

The Fourth Chapter is results and discussion. In this section, using collected primary and secondary data all the hydrologic and hydraulic problems are analyzed and results are presented sequentially and discussed in detail. The Bridge watershed is delineated, soil and land use maps are produced, using SCS unit hydrograph model, the design flood is estimated, water surface profiles both upstream and downstream of the bridge under consideration are analyzed, bridge opening area adequacy is checked and scour is analyzed using HEC-RAS and checked using HEC-18 contraction and abutment scour equations and finally the results are discussed.

The Fifth Chapter addresses the proposed countermeasures to minimize the existing scour problem and replacement of the existing Sile River Bridge.

The Last Chapter of this Thesis is made to contain the conclusions drawn from the outputs and existing conditions of the Sile River Bridge and the proposed recommendations.

2. LITERATURE REVIEW

2.1. Introduction

Long roadway approach sections and narrow bridge openings force floodplain waters to re-enter the main channel at the bridge, causing a severe contraction in flow area that results in both contraction and local scour. This severe contraction in flow area produces a mixed flow pattern under the bridge, with increased velocities, shear stresses, and turbulence around the bridge pier. As a result, it is difficult to separate contraction scour and local scour processes. However, current scour practice assumes that contraction and local scour processes are independent and thus are determined separately and summed for total scour depth (Richardson and Davis, 2001). Furthermore, existing contraction scour prediction equations are based on theories of flow continuity and sediment transport in an idealized long contraction, while existing local scour prediction equations are based primarily on laboratory data, making many of the existing contraction and local scour prediction equations unsuitable with respect to field conditions. Idealized laboratory experiments which often employ rectangular channels and uniform sediment while ignoring effects of some important dimensionless parameters may limit the accuracy of scour depth estimate when applied to actual field conditions.

The depth of scour below the river bed level around the bridge piers and abutments in alluvial stream varies depending on the depth of flow, shape and size of the pier and abutment, angle of attack of flow and sediment characteristics. It has been found that it depends on various factors such as properties of flow, the bed material in the stream and at bridge crossing (grading, layering, particle shape and size etc.) bridge location and foundation geometry.

2.2. Types of Scour

The total scour at a river crossing consists of three components that, in general, can be added together (Richardson and Davies 1995). Cheremisinoff et al. (1987) on the other hand divided scour in to three. These include general scour, contraction scour, and local scour. Total scour divided into two major types, namely general scour and localized scour. General scour involves the removal of materials from the bed and bank across all or most of the width of a channel. It occurs irrespective of the existence of the bridge and can be either long-term or short-term.

In contrast to general scour, contraction scour and local scour are directly attributed to the existence of the bridge. Contraction scour results from acceleration of hydraulic flow due to a contraction caused by objects, such as bridges or revetments. According to (Fischenich and Landers 2000), contraction scour is generally limited to the length of the contraction or a short distance up and downstream.

Whereas Local scour usually occurs at a pier, abutment, erosion control devices, or other structures obstructing flow. The obstructions cause flow acceleration and create vortexes that remove surrounding sediments. Local scour can affect the stability of structures, such as riprap revetments, and lead to failures if measures are not taken to address the scour. Generally, depths of local scour are much larger than those of general and contraction scour, often by a factor of ten.

2.2.1. Degradation

Degradation is long-term streambed elevation changes due to natural or human-induced causes within the reach of the river on which the bridge is located. Degradation involves the lowering or scouring of the streambed over relatively long reaches due to a deficit in sediment supply from upstream and contributes to total scour.

Degradation usually appears as a general lowering of bed levels along a reach of river, and is caused by the reach seeking to adjust its longitudinal gradient to match the requirements of the flows and sediment loads that it carries. If the sediment load entering the reach is lower than the actual transport capacity within the reach, degradation starts at the upstream end and works its way downstream, so as to reduce the overall longitudinal gradient. However, if the channel downstream of the reach in question has greater sediment transport capacity, degradation starts at the downstream end of the reach and works its way upstream, leading to an overall increase in the longitudinal gradient. In the case of aggradation, the above causes and effects are reversed. Clearly, channel degradation is the more critical condition when considering scour at structures.

According to Pemberton and Lara (1984), Breusers and Raudkivi (1991), HEC18 (Richardson and Davis, 1995) and Hoffinans and Verheij (1997) in many rivers there is an approximate equilibrium or "regime" (with no continuing degradation or aggradation). However, the stable regime conditions to which the river has become adjusted may be disturbed by changes resulting from natural processes and/or human interference. These changes may include catchment changes, river channel changes and the influence of other structures.

2.2.2. Contraction Scour

Contraction scour involves the removal of material from the bed and banks across all or most of the width of the channel. This scour can result from a contraction of the flow by the approach embankments to the bridge encroaching onto the floodplain and/or into the main channel, from a change in downstream control of the water surface elevation, or from the location of the bridge in relation to a bend. In each case, scour is caused by an increase in transport of bed material in the bridge cross section.

Contraction scour is a sediment imbalance process that occurs during floods when the sediment supply from upstream is less than the sediment transport capacity in the bridge opening. (Hydraulic Design of Safe Bridges, US Department of Transportation, 2012).

At a bridge crossing, many factors can contribute to the occurrence of contraction scour. These; factors may include; the main channel naturally contracts as it approaches the bridge opening; the road embankments at the approach to the bridge cause all or a portion of the overbank flow to be forced in to the main channel; the bridge abutments are projecting in to the main channel; the bridge piers are blocking a significant portion of the flow area; and a drop in the downstream tail water which causes increased velocities inside the bridge. (Hydraulic Engineering Circular No.18, FHWA, 2012)

There are two forms of contraction scour that can occur depending on how much bed material is already being transported upstream of the bridge contraction reach. The two types of contraction scour are:

- **i.** Live-Bed contraction and
- **ii.** Clear-Water Contraction Scour.

To determine whether the flow upstream of the bridge is transporting bed material, the critical velocity V_c of the D_{50} should be considered and it should be compared with the mean velocity of the flow in the main channel or over bank area upstream of the bridge opening.

According to (FHWA, HEC-18 Publication, 2003), if the critical velocity of the bed material is larger than the mean velocity ($V_c > V$), this implies that, Clear-water contraction scour will exist. If the critical velocity is less than the mean velocity ($V_c < V$), live-bed contraction scour will exist and critical velocity can be calculated using the following equation.

$$V_{C} = K_u\, y^{1/6} D^{1/3} \qquad \text{……………………Equation (2.1)}$$

Where:

V_c = critical velocity above which bed material of size D smaller be transported (m/s)

y = average depth of flow upstream of the bridge (m)

D = particle size for V_c (m)

D_{50} = particle size in a mixture of which 50% are smaller, (m)

K_u = 6.19 (SI Units)

2.2.2.1. Live-Bed Contraction Scour

Live–bed contraction scour occurs when bed material is already being transported in to the contracted bridge section from upstream of the approach section (before the contraction reach).

This condition occurs when there is sufficient flow velocity to transport bed material upstream of the bridge. Very fine sediment (clay and silt) is often not found in channel beds in significant amounts and does not generally play a role in either clear-water or live-bed contraction scour. The water may be turbid due to suspended transport of silt and clay, but is still considered as clear-water from the standpoint of bed material transport.

A modified version of Laursen's 1960 equation for live-bed scour at a long contraction is recommended to predict the depth of scour in a contracted section (Laursen, 1960). The modification is to eliminate the ratio of Manning (n). The equation assumes that bed material is being transported from the upstream section.

$$\frac{y_2}{y_1} = \left[\frac{Q_1}{Q_2}\right]^{6/7} \left[\frac{W_1}{W_2}\right]^{K_1} \quad \text{.......................Equation (2.2)}$$

$$y_s = y_2 - y_0 \text{ (average contraction scour depth)}$$

Where:

y_1 = Average depth in the upstream main channel, (m)
y_2 = Average depth in the contracted section, (m)
y_0 = Existing depth in the contracted section before scour, (m)
Q_1 = Flow in the upstream channel transporting sediment, (m^3/s)
Q_2 = Flow in the contracted channel, (m^3/s)
W_1 = Bottom width of the upstream main channel that is transporting bed material, (m)
W_2 = Bottom width of main channel in contracted section less pier width(s)
k_1 = Exponent determined below

V_*/T	k_1	Mode of Bed Material Transport
<0.50	0.59	Mostly contact bed material discharge
0.50 to 2.0	0.64	Some suspended bed material discharge
>2.0	0.69	Mostly suspended bed material discharge

V_* = $(gy_1S_1)^{1/2}$, shear velocity in the upstream section, (m/s)

T = fall velocity of bed material based on the D_{50}, m/s for all velocity in English units, multiply in m/s by 3.28

g = acceleration of gravity (m/s^2)

S_1 = slope of energy grade line of main channel, (m/m)

2.2.2.2. Clear-Water Contraction Scour

Clear-water conditions occur for fine sediment sizes (sands and fine gravel) only when flow velocity is small and for coarse sediment sizes (coarse gravel and cobbles) even for relatively high velocity.

The following is the recommended clear-water contraction equation is based on a development suggested by Laursen (1963).

$$y_2 = \left[\frac{K_u Q^2}{D_m^{2/3} W^2}\right]^{3/7} \quad \text{....................... Equation (2.3)}$$

$$y_s = y_2 - y_0 \text{ (average contraction scour depth)}$$

Where:

y_2 = Average equilibrium depth in the contracted section after contraction scour, (m)

Q = Discharge through the bridge or on the set-back overbank area at the bridge associated with the width W, (m^3/s)

D_m = Diameter of the smallest non-transportable particle in the bed material

($1.25\ D_{50}$) in the contracted section, (m)

D_{50} = Median diameter of the bed material, (m)

W = Bottom width of the contracted section less pier width, (m)

y_0 = Average existing depth in the contracted section, (m)

K_u = 0.0025

2.2.3. Local Scour

Local scour occurs where the flow field is disrupted by an obstruction. The term "local" is used because scour is in the vicinity of the obstruction, not across the entire channel or bridge section. The flow is redirected and accelerates, vortexes form, and there is increased turbulence. The two most common types of local scour at bridges are pier scour and abutment scour.

2.2.3.1. Pier Scour and Its Mechanism

Local scour is the engineering term for the erosion of the soil surrounding a bridge foundation (piers and abutments), which is the result of the erosive action of the flowing water, excavating and carrying away material from around the piers and abutments of bridges (Hoffmans and Verheij, 1997; Melville and Coleman, 2000; Richardson and Davis, 1991). The process combines the complexities of a three-dimensional flow pattern (characterized by different vortex systems around the structure) with suspended and bed sediment transport. The phenomenon has attracted the interest of many researchers and, because of its complexity; an experimental approach is the usual practice (Melville and Coleman, 2000).

The basic mechanism causing local scour at piers is the down-flow at the upstream face of the pier and formation of vortices at the base (Heidarpour et al. 2003; Muzzammil et al. 2004). The flow decelerates as it approaches the pier coming to rest at the face of the pier. The approach flow velocity, therefore, at the stagnation point on the upstream side of the pier is reduced to zero, which results in a pressure increase at the pier face. The associated stagnation pressures are highest near the surface, where the deceleration is greatest, and decrease downwards (Melville and Raudkivi 1977). In other words, as the velocity is decreasing from the surface to the bed, the stagnation pressure on the face of the pier also decreases accordingly i.e. a downward pressure gradient. The pressure gradient arising from the decreased pressure forces the flow down the face of the pier, resembling that of a vertical jet. The resulting down-flow impinges on the streambed and creates a hole in the vicinity of the pier base. The strength of the down-flow reaches a maximum just below the bed level. The down flow impinging on the bed is the main scouring agent (Melville and Raudkivi 1977).

According to (Breusers et al. 1977) the down flow rolls up as it continues to create a hole and, through interaction with the oncoming flow, develops into a complex vortex system. The vortex then extends downstream along the sides of the pier. This vortex is often referred to as horseshoe vortex because of its great similarity to a horseshoe. Thus the horseshoe vortex developed as a result of separation of flow at the upstream face of the scour hole excavated by the down-flow. The horseshoe vortex itself is a lee eddy similar to the eddy or ground roller downstream of a dune crest. (Breusers and Raudkivi, 1991). The horseshoe vortex is very effective at transporting the dislodged particles away past the pier. The horseshoe vortex is as a result of scour but is not the cause of scour (Breusers and Raudkivi 1991). As the scour depth increases, the horseshoe vortex strength diminishes, which automatically leads to a reduction in the sediment transport rate from the base of the pier (Lagasse et al. 2001).

As shown in the Figure below, besides the horseshoe vortex in the vicinity of the pier base, there are also the vertical vortices downstream of the pier referred to as wake vortices (Dargahi, 1990). The separation of the flow at the sides of the pier produces the so called wake vortices. These wake vortices are not stable and shed alternately from one side of the pier and then the other. It should be noted, however, that both the horseshoe and wake vortices erode material from the base region of the pier. The intensity of the wake vortices is drastically reduced with distance downstream, such that sediment deposition is common immediately downstream of the pier (Richardson and Davies1995).

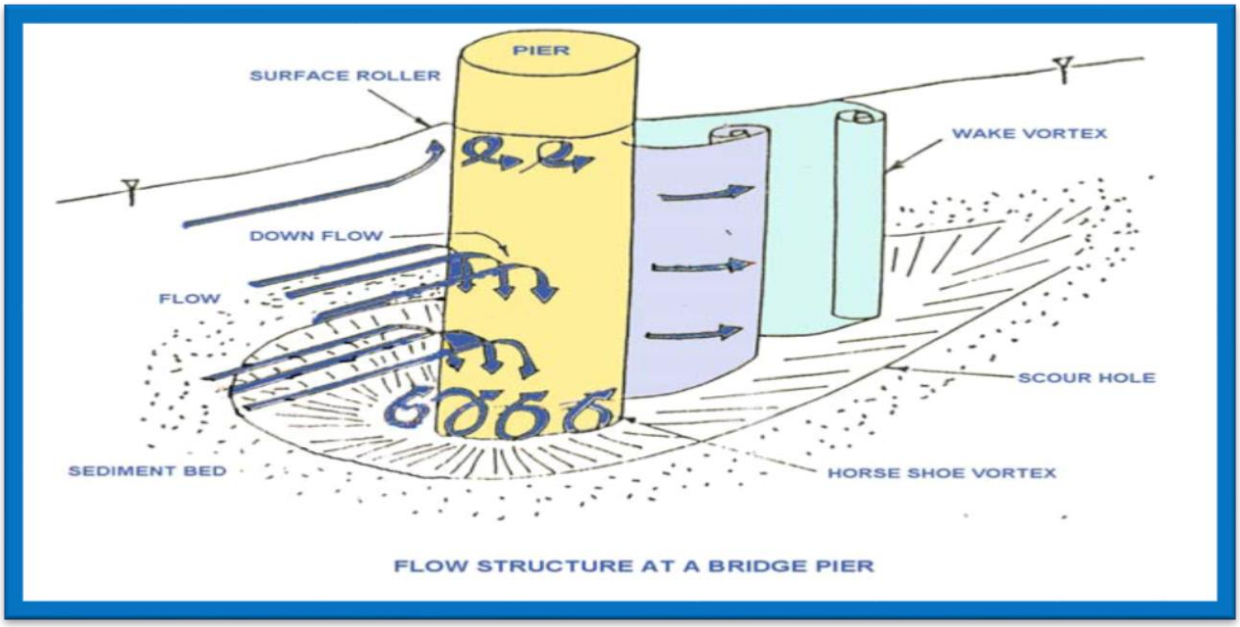

Figure2-1: Flow and Scour Pattern at a Circular Pier (Melville & Coleman, 2000)

2.2.3.2. Abutment Scour

The two principal types of bridge abutment forms are wing-wall abutments and spill-through abutments. These abutment forms may be supported on piled or slab footings.

Wing-wall abutments have vertical walls that retain the earth fill material comprising the embankment approach to the abutment. The walls can be angled from about 45to 90 degrees. The abutment face is vertical as well. The overall form of the abutment is quite bluff, and causes large-scale turbulence structures to develop in the flow around the abutment. Wing-wall abutments are commonly used for small bridges with one to three spans, as the abutment form lends itself to placement on the banks of streams and creeks, or small rivers that do not have a pronounced floodplain.

Abutment scour occurs when the abutment and roadway embankment obstruct the flow. The following are the major causes of abutment failure and damage caused by a combination of these factors.

- **i.** Overtopping of abutments or approach embankments
- **ii.** Lateral channel migration or stream widening process

iii. Contraction scour and

iv. Local scour at one or both abutments.

The flow obstructed by the abutment and approach highway embankment accelerates and often forms a vortex starting at the upstream end of the abutment and running along the toe of the abutment. Generally a wake vortex forms at the downstream end of the abutment.

Recent studies of abutment scour by Wong (1982), Tey (1984), Kwan (1984, 1988), Kandasamy (1985, 1989), Dongol (1994) and many others have shown that the scour mechanism at abutments is very similar to the scour mechanism at piers. The down flow and the principal vortex at the upstream corner of the abutment, together with the secondary vortices and wake vortices at the middle part and the downstream corner of the abutment, cause complex interactions between the fluids and the bed material and are mainly responsible for the scour at abutments. Observations of flow patterns around abutments derived from flow visualization techniques using dye injection, dye crystals strategically placed on the sand bed, paper floats, and smoke tunnel experiments by various researchers including Liu (1961), and Gill (1970) are summarized in the figure below.

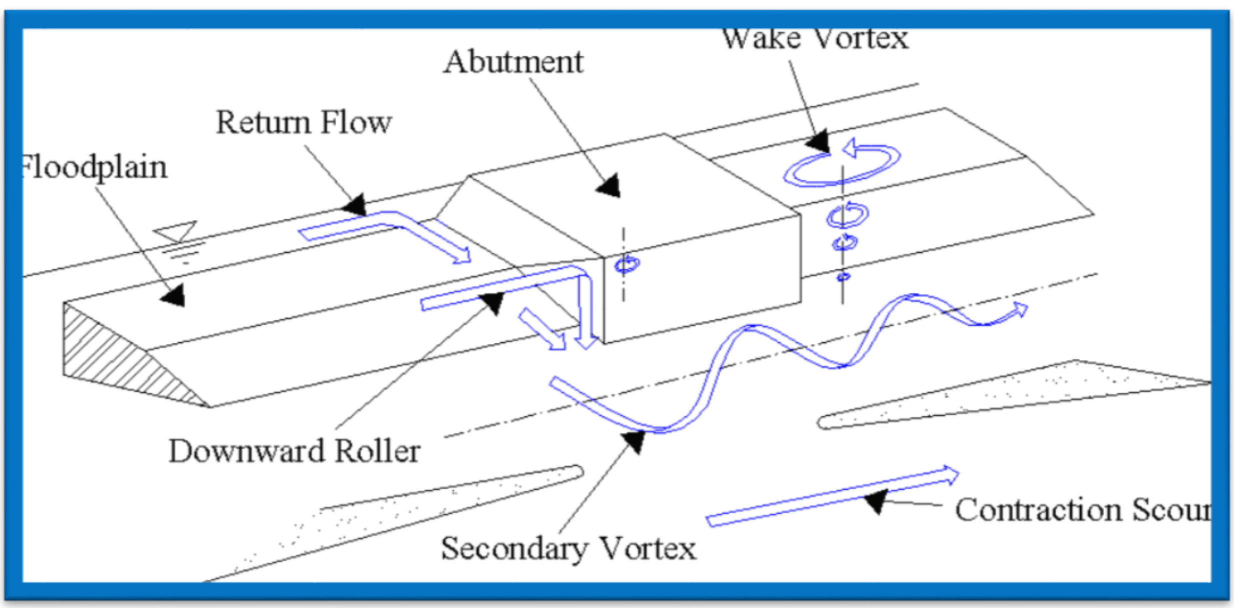

Figure 2-2: Flow patterns around a wing-wall abutment (Hua Li, Roger A. Kuhnle & Brian D. Barkdoll, 2006)

The flow field around abutments embedded vertically in a sediment-bed is complex in detail, involving separation of flow to develop three-dimensional vortex flow; and the complexity increases with the development of the scour hole. The flow field around piers has been well researched by Hjorth (1975), Melville (1975), Melville and Raudkivi (1977), Dey (1995), Dey et al. (1995) and Graf and Istiaro (2002). But, research on the flow field around abutments has been very limited. Using hydrogen bubble technique, Kwan (1989) and Kwan and Melville (1994) detected the three-dimensional flow field in a scour hole around a wing-wall abutment. They concluded that a primary vortex, being similar to the horseshoe vortex around piers, along with the down flow is the primary cause of scouring at abutments. Rajaratnam and Nwachukwu (1983), and Ahmed and Rajaratnam (2000) also investigated the flow fields at groyne and abutment, respectively, placed on a planar or un scoured bed. But, no attempt has so far been made to study the three-dimensional flow field around a vertical-wall and semicircular abutments.

2.3. Pier Scour Equation

The leading method for design estimation of pier scour is the method herein termed the Richardson and Davis (2001) method. It often is colloquially called the CSU method, because it stems from extensive research conducted at Colorado State University. This method currently is in FHWA’s design guide HEC-18, and is recommended by AASHTO.

Other methods may be used in conjunction with the HEC-18 method; e.g., the method developed by Wilson (1995) who uses extensive field data from bridges in Mississippi. A method proposed by Sheppard and Miller (2006) is being used increasingly, notably in Florida (FDOT 2010).

The method developed by Melville 1997, (also in Melville and Coleman 2000) is used in conjunction with the Richardson et al. method, though is not formally recommended by HEC-18 or AASHTO. It is used quite extensively in other countries besides the U.S.

Melville's method merged with that by Sheppard and Miller (2006) has evolved into the Sheppard-Melville method, consequent to NCHRP Project 24-32 (Sheppard et al. 2011).

Local scour at piers is a function of bed material size, flow characteristics, fluid properties and the geometry of the pier. The subject has been studied extensively in the laboratory, but there is limited field data. As a result of the many studies, there are many equations. In general, the equations, which give similar results, are for live-bed scour in cohesion less sand-bed streams.

The HEC-18 pier scour equation (based on the CSU equation) is recommended for both live-bed and clear-water pier scour. The equation predicts maximum pier scour depths. Basic applications include simple pier substructure configurations and riverine flow situations in alluvial sand-bed channels. The equation can be adapted for wide pier applications, more complex (3-element) substructure configurations, multiple columns skewed to the flow, estimating scour from debris on piers, and scour in tidal waterways. An alternative approach that represents the complexity of the bridge pier scour flow field and the full range of pier geometries the equation is:

$$\frac{y_s}{y_1} = 2.0\, K_1 K_2 K_3 \left[\frac{a}{y_1}\right]^{0.65} Fr_1^{\ 0.43} \quad \text{…………………Equation (2.4)}$$

As a Rule of Thumb, the maximum scour depth for round nose piers aligned with the flow is:

$y_s \le 2.4$ times the pier width (a) for $Fr \le 0.8$
$y_s \le 3.0$ times the pier width (a) for $Fr > 0.8$

In terms of y_s/a, Equation (2.1)

$$\frac{y_s}{a} = 2.0\, K_1\, K_2\, K_3 \left[\frac{y_1}{a}\right]^{0.35} Fr_1^{\ 0.43} \quad \text{…….......Equation (2.5)}$$

Where:

y_s = Scour depth,(m)

y_1 = Flow depth directly upstream of the pier, (m)

K_1 = Correction factor for pier nose shape

K_2 = Correction factor for angle of attack of flow from table

K_3 = Correction factor for bed condition from table

a = Pier width, (m)

L = Length of pier, (m)

Fr_1 = Froude number upstream of the pier=$V_1/(gy_1)^{1/2}$

V_1 = Mean velocity of flow directly upstream of the pier, (m/s)

g = Acceleration due to gravity 9.81m/s^2

The correction factor, K_2, for angle of attack of the flow, 2, is calculated using the following equation:

$$K_2 = \left[\cos\theta + \frac{L}{a}\sin\theta\right]^{0.65}$$ ………………..Equation (2.6)

If L/a is larger than 12, use L/a = 12 as a maximum in Equation 2.3 and Table 2.2 Table 2.2 illustrates the magnitude of the effect of the angle of attack on local pier scour.

Table 2-1: Correction Factor, K_1, for Pier Nose Shape

No.	Shape of Pier Nose	K_1
1.	Square nose	1.1
2.	Round nose	1.0
3.	Circular Cylinder	1.0
4.	Group of cylinders	1.0
5	Sharp nose	0.9

Source: Hydraulic Engineering Circular No. 18, Publication No. FHWA 12-003, 2012

Table 2-2: correction factor, K_2, for angle of attack, 2, of flow

Angle	L/a=4	L/a=8	L/a=12
0	1.0	1.0	1.0
15	1.5	2.0	2.5
30	2.0	2.75	3.5
45	2.3	3.3	4.3
90	2.5	3.9	5.0
Angle =skew angle of flow			
L=length of Pier			

Source: Hydraulic Engineering Circular No. 18, Publication No. FHWA 12-003, 2012

Table 2-3: Increase in equilibrium pier scour depths, K_3, for bed condition

Bed condition	Dune Height in (ft)	K_3
Clear-water scour	N/A	1.1
Plane bed and Anti-dune	N/A	1.1
Small dunes	$10>H\geq 2$	1.1
Medium dunes	$30>H\geq 10$	1.2 to 1.1
Large dunes	$H\geq 30$	1.3

Source: Hydraulic Engineering Circular No. 18, Publication No. FHWA 12-003, 2012

2.4. Abutment Scour Equations

Equations for predicting abutment scour depths such as Liu et al. (1961), Laursen (1980), Froehlich (TRB 1989), and Melville (1992) are based entirely on laboratory data. The problem is that little field data on abutment scour exist. Liu et al.'s equations were developed by dimensional analysis of the variables with a best-fit line drawn through the laboratory data. Laursen's equations are based on inductive reasoning of the change in transport relations due to the acceleration of the flow caused by the abutment. Froehlich's equations were derived from dimensional analysis and regression analysis of the available laboratory data.

Melville's equations were derived from dimensional analysis and development of relations between dimensionless parameters using best-fit lines through laboratory data.

Until recently, the equations in the literature were developed using the abutment and roadway approach length as one of the variables. This approach results in excessively conservative estimates of scour depth. Richardson and Richardson pointed this out in a discussion of Melville's (1992) paper: (73, 72)

The reason the equations in the literature predict excessively a conservative abutment scour depth for the field situation is that, in the laboratory flume, the discharge intercepted by the abutment is directly related to the abutment length; whereas, in the field, this is rarely the case.

Many of the abutments scour prediction equations presented in the literature use the length of an abutment (embankment) projected normal to flow as an independent variable. In practice, the length of embankment projected normal to flow that is used in these relationships is determined from the results of 1-dimensional hydraulic models such as HEC-RAS (USACE 2010a) which assume an average velocity over the entire cross section . In reality, conveyance and associated velocity and flow depth at the outer extremes of a floodplain are much less, particularly in wide and shallow heavily vegetated floodplains. This flow is typically referred to as "ineffective" flow. When applying abutment scour equations that use the length of embankment projected normal to flow, it is imperative that the length used be the length of embankment blocking "live" flow.

Two equations for the computation of live-bed abutment scour are recommended. When the wetted embankment length is divided by the approach flow depth is less than or equal to 25, the FHWA’s design guide and HEC No.18 recommend using an equation by Froehlich (Froehlich, 1989) and when the wetted embankment length (L) divided by the approach flow depth (y_1) is greater than 25 using the HIRE equation (Richardson 1990) is recommended.

i. Froehlich's Abutment Scour Equation

Froehlich (TRB 1989) analyzed 170 live-bed scour measurements in laboratory flumes by regression analysis to obtain the following equation:

$$\frac{y_s}{y_a} = 2.27\, K_1\, K_2 \left[\frac{L'}{a}\right] Fr^{\,0.61} + 1 \qquad \text{..............Equation (2.7)}$$

Where:

K_1 = Coefficient of Abutment Shape

K_2 = Coefficient for angle of embankment to flow

K_2 = $(\theta/90)^{0.13}$

$\theta < 90^0$ if embankments points downward, $\theta > 90^0$ if embankment points upstream

L' = Length of active flow obstructed by the embankment, (m)

A_e = Flow area of approach cross section obstructed by the embankment, (m^2)

F_r = Froude number of approach flow upstream of the abutment $V_e\ (g_a)^{1/2}$

V_e = Q_e/A_e, (m/s)

Q_e = Flow obstructed by the abutment and approach embankment, (m^3/s)

y_a = Average depth of flow on the flood plain (A_e/L), (m)

L = Length of embankment projected normal to the flow,(m)

y_s = Scour depth (m)

ii. The HIRE Equation

The HIRE equation is developed by the USACE which is based on field data of scour at the end of spurs in the Mississippi River .The Equation is:

$$\frac{y_s}{y_1} = 4Fr^{\,0.33}\, \frac{K_1}{0.55}\, K_2 \qquad \text{.............Equation (2.8)}$$

Where:

y_s = scour depth in, (m)

y_1 = Depth of flow at the toe of the abutment on the overbank or in the main channel, (m), taken at the cross section just upstream of the bridge.

K_1 = Correction factor for abutment shape.

K_2 = Correction factor for angle of attack θ) of flow with abutment. θ =90^0 when abutments are perpendicular to the flow, θ <90^0 if embankments points downward, and

F_{r1} = Froude number based on velocity and depth adjacent and just upstream of the abutment toe.

Table 2-4: Correction factor for Abutment shape, K_1

Description	K_1
Vertical-wall Abutment	1.00
Vertical wall Abutment with wing walls	0.82
Spill-through Abutment	0.55

Source: Hydraulic Engineering Circular No. 18, Publication No. FHWA 12-003, 2012

2.5. Factors Affecting Scour

Abutment scour depends on the interaction of the flow obstructed by the abutment and roadway approach and the flow in the main channel at the abutment. The discharge returned to the main channel at the abutment is not simply a function of the abutment and roadway length in the field case. Abutment scour depth depends also on the following factors.

2.5.1. Soil-Size and Gradation of Sediments

The type of soil supporting a bridge foundation governs erosion potential and the long term behavior of a foundation. Likewise, geotechnical conditions affect footing designs.

Characteristics of the bed sediments are derived from particle size distribution curves. The two most commonly used parameters are median sediment diameter $d_{50}$and geometric standard deviation Sg= $[(d_{84}/d_{16})^{0.5}]$ of particle size distribution, which is a measure of uniformity of the bed sediments.

Blench (1957), Garde *et al* (1961) and Gill (1972) reported that sediment size has an influence on the maximum scour depth. Laursen (1960) found that maximum scour depth is affected by sediment size under clear-water scour but not under live-bed scour.

Ahmad (1953), Izzard & Bradley (1958), Garde *et al* (1961) and Gill (1972) found that the rate of scour is different for different bed sediments. According to them, fine sediments are scoured at a faster rate than course sediments. Ramu (1964) observed that for the same sediment size, a change in sediment gradation Sg affects the equilibrium scour depth. Ahmad (1953) asserted that equilibrium scour depth depends on the sediment gradation Sg. Ettema (1980) and Raudkivi & Ettema (1983) found that the maximum clear-water equilibrium scour depth ds at a bridge pier depend on the sediment grading Sg.

The percentage of soil types with scour problems are listed in the Table below. It is seen that sand foundations have 48% of scour problems while silt foundations do not display any scour problem. (Handbook of Scour Countermeasures Designs, FHWA-NJ-2005-027, 2007).

Table 2-5: Soil Types with Scour Problems

Sediment Type	Percent (%)
Sand	48
Cohesive	19
Mixed	13
Gravel	10
Bedrock	5
Uncertain	5
Silt	0
Total	**100**

Source: Handbook of Scour Countermeasures Designs, FHWA-NJ-2005-027, 2007

2.5.2. Approaching Flow

According to Laursen (1952), the approaching flow depth (y) is an important factor to determine scour depth. Experimental results of Gill (1972), Wong (1982), Tey (1984) and Kandasamy (1989) indicate that for constant value of the shear velocity ratio v_*/v_{*c}, the maximum scour depth increases with increase in approaching flow depth. It is also observed that the maximum scour depth increases at a decreasing rate with increase in approaching flow depth. After Kandasamy (1989), for shallow flow depths, the scour depth increases proportionally with y, but is independent of L. On the other hand, for intermediate flow depths, the scour depth depends on both y and L. However, Melville (1992) distinguished short and long abutments. He concluded that for short abutments $L/y \geq 1$, the scour depth is independent of flow depth; and for long abutments. $L/y \geq 25$, the scour depth is dependent on flow depth. However, most abutments are neither long nor short, as a result of which the scour depth is influenced by both y and L. Dey & Barbhuiya (2004a) reported that for smaller flow depths, the equilibrium scour depth increases significantly with increase in y; whereas for higher flow depths, equilibrium scour depth is independent of flow depth.

2.5.3. Type and Shape of the Structure

The shape of the abutment plays an important role on equilibrium scour depth. Streamlined bodies, such as semicircular (SC), spill-through (ST) and wing-wall (WW) abutments, produce vortice of feeble strength; while blunt obstructions, for example vertical-wall abutments, are capable of producing strong turbulent vortices (Robert Ettema, Tatsuaki Nakato, and Marian Muste, 2010). Consequently, a relatively large scour depth is observed at a blunt obstruction. From laboratory experimental data, Laursen & Toch (1956), Liu *et al* (1961), Garde *et al* (1961) and Wong (1982) concluded that vertical wall abutments produce greater scour depth in comparison with spill-through and wing-wall abutments. Scour at vertical wall abutments with wing walls is reduced to 82 percent of the scour of vertical wall abutments without wing walls. However, Melville (1992) asserted that, the importance of abutment shape diminishes when the abutment becomes longer.

2.5.4. Location/Orientation

As a general rule, the abutments most vulnerable to damage are those located at or near the channel banks. Where abutments are set back from the channel, especially on wide floodplains, large local scour holes are developed with scour depths of as four times the approach flow depth on the floodplain. (Hydraulic Engineering Circular No. 18, Publication No FHWA-HIF-12-003).

The angle of approaching flow with respect to the abutment alignment, termed angle of attack, significantly influences scour depth. It was experimentally studied by Laursen &Toch (1956), Garde *et al* (1961), Zaghloul (1983) and Kwan (1984). Garde *et al* (1961) reported that for the same flow, sediment and abutment conditions, the maximum scour depth is greatest for a spur dike with an inclination of 90.

Concerning the skew angle, for an abutment angled downstream, the scour depth is decreased, whereas the scour depth is increased for an abutment angled upstream.(HEC-18, FHWA,-HIF-12-003).

According to the NCHRP Report No. 587, due to the abutment layout, the flow field, and the erodibility of sediment and soil at bridge sites cause the deepest scour to occur at any, or all, of three locations near an abutment, these are in the main channel near the abutment, a short distance downstream of the abutment and at the abutment itself.

2.6. Scour Modeling Tools

It is known that, the HEC-18 pier-scour equation is not the only common empirical equation (Mueller & Wagner, 2002). Other notable examples include Jain & Fischer (1979), Laursen & Toch (1956), Sheppard (2006), and Melville (1988, 1997). These equations were developed with data from laboratory experiments. Hence, they have inherent errors due to scaling and/or unrealistic representation of field conditions. As such, these equations are prone to gross over estimates of scour depth prediction (Wagner et al, 2006, Benedict & Caldwell, 2005; Mueller & Wagner, 2002).

Errors in predicting scour primarily stem from one of the three sources: estimation of hydraulic parameters, determination of scour-prediction variables, and application of scour prediction equations (Wagner et al, 2006). Hydraulic parameters are commonly estimated from simplified hydraulic models that distribute flow across the approach section and do not accurately capture complex velocity patterns found in the field. Commonly used scour prediction variables include bridge geometry, channel geometry, hydraulic characteristics and sediment properties, but their individual contributions to scour are not always accurately captured. Regarding scour-prediction equations, simplifications made to estimate scour based on laboratory measurements have made scour prediction less accurate when applied in field settings. Finally, uncertainty stems from the fact that the ranges of the various parameters over which the equations are valid are typically unknown (Johnson, 1995).

This literature search address only the more commonly available/popular models (i.e., non-proprietary) employed for this specific application (for scour analysis specifically contraction and local scour at piers and abutments). The models addressed herein include HEC-RAS and HEC-18. A brief description of HEC-RAS and HEC-18 is presented below.

HEC-RAS is a computer program that models the hydraulics of water flow through natural rivers and other channels. The program is one-dimensional, meaning that there is no direct modeling of the hydraulic effect of cross section shape changes, bends, and other two- and three-dimensional aspects of flow. The program was developed by the US Department of Defense, Army Corps of Engineers in order to manage the rivers, harbors, and other public works under their jurisdiction; it has found wide acceptance by many others since its public release in 1995(NCHRP, Criteria for Selecting Hydraulic Models,2006).

The Hydrologic Engineering Center (HEC) in Davis, California developed the River Analysis System (RAS) to aid hydraulic engineers in channel flow analysis and floodplain determination. It includes numerous data entry capabilities, hydraulic analysis components, data storage and management capabilities, and graphing and reporting capabilities.

HEC-RAS has merits, notably its support by the US Army Corps of Engineers, the future enhancements in progress, and its acceptance by many government agencies and private firms. It is in the public domain and peer-reviewed and available to download free of charge from HEC's web site. Various private companies are registered as official "vendors" and offer consulting support and add on software. Some also distribute the software in countries that are not permitted to access US Army web sites. However, the direct download from HEC includes extensive documentation, and scientists and engineers versed in hydraulic analysis should have little difficulty utilizing the software.

Concerning the disadvantages of HEC-RAS, numerical instability problems might be happened during unsteady analyses, especially in steep and/or highly dynamic rivers and streams. It is often possible to use HEC-RAS to overcome instability issues on river problems. The other limitation of HEC-RAS is, since it is a 1-dimensional hydrodynamic model and will therefore not work well in environments that require multi-dimensional modeling. However, there are built-in features that can be used to approximate multi-dimensional hydraulics.

HEC-RAS has been applied extensively for examining bridge crossings. Mohammad, et al., 1998 applied HEC-RAS to examine design scour and flows around new piers associated with the retrofit of a bridge in Mendocino County, CA. They also examined the scour and flows associated with cofferdams to be installed during construction of the new piers. This application makes use of the capabilities outlined in Brunner, 1999. Brunner describes the integration of the bridge scour equations, as outlined in HEC-18 (Richardson, et al., 2001), into the HEC-RAS modeling system. The program has the capability of calculating contraction scour, pier scour, and abutment scour at bridge crossings with minimal additional input during model creation.

3. METHODS and MATERIALS

3.1. Brief Description of the Study Area

The Sile River Bridge is found in the South-West part of Ethiopia, near Arbaminch town. The Bridge can be accessed using Addis Ababa-Hosainna-Sodo-Arbaminch-Konso Road or Addis Ababa-Shashemene-Alaba-Kulito-Sodo-Arbaminch-Konso Road. The former is the shortest route with relatively less traffic when compared to the later. The Sile River is perennial, un gauged and covered with alluvial deposits (Silt, Sand and Gravel).

3.1.1. Climate and Topography

Climate in the area is categorized as semi-arid and the temperature ranges from 31^0c to 38^0c. The area gets rain fall twice in a year peak in October and April. The study area has a flat to rolling topography. The elevation is 1123m above sea level. The elevation lowers gradually when going from Arbaminch down to Konso and further to Jinka.

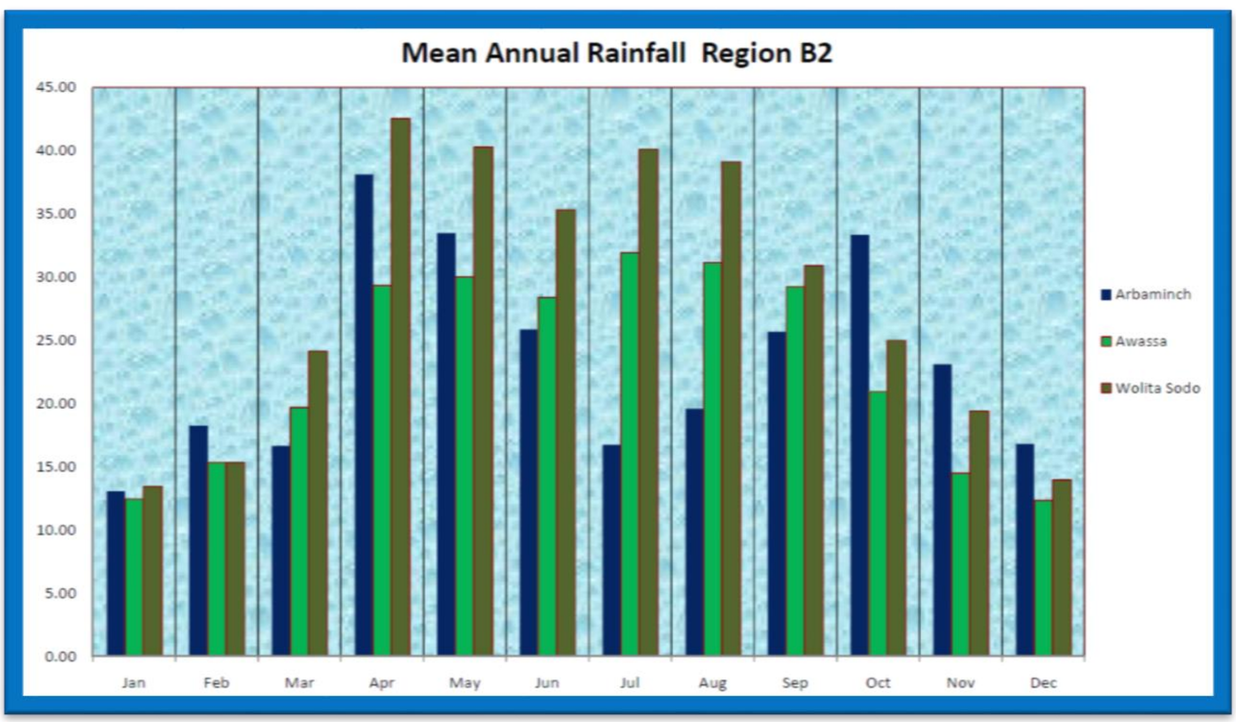

Figure 3-1: Mean Annual Rainfall of Region B2 (Source: ERA-DDM, 2013)

3.1.2. Location

The Bridge is located along the Arbaminch-Konso Road at about Km 13.6 from Arbaminch town at UTM coordinate E-334,085 and N-652,342. It is located at meandering section of the River at a sharp bend of the river where the change in the morphology is dynamic. The geometry of the river is almost U-shaped with embankments on both abutments. The study area is found in the Rift Valley River Basin.

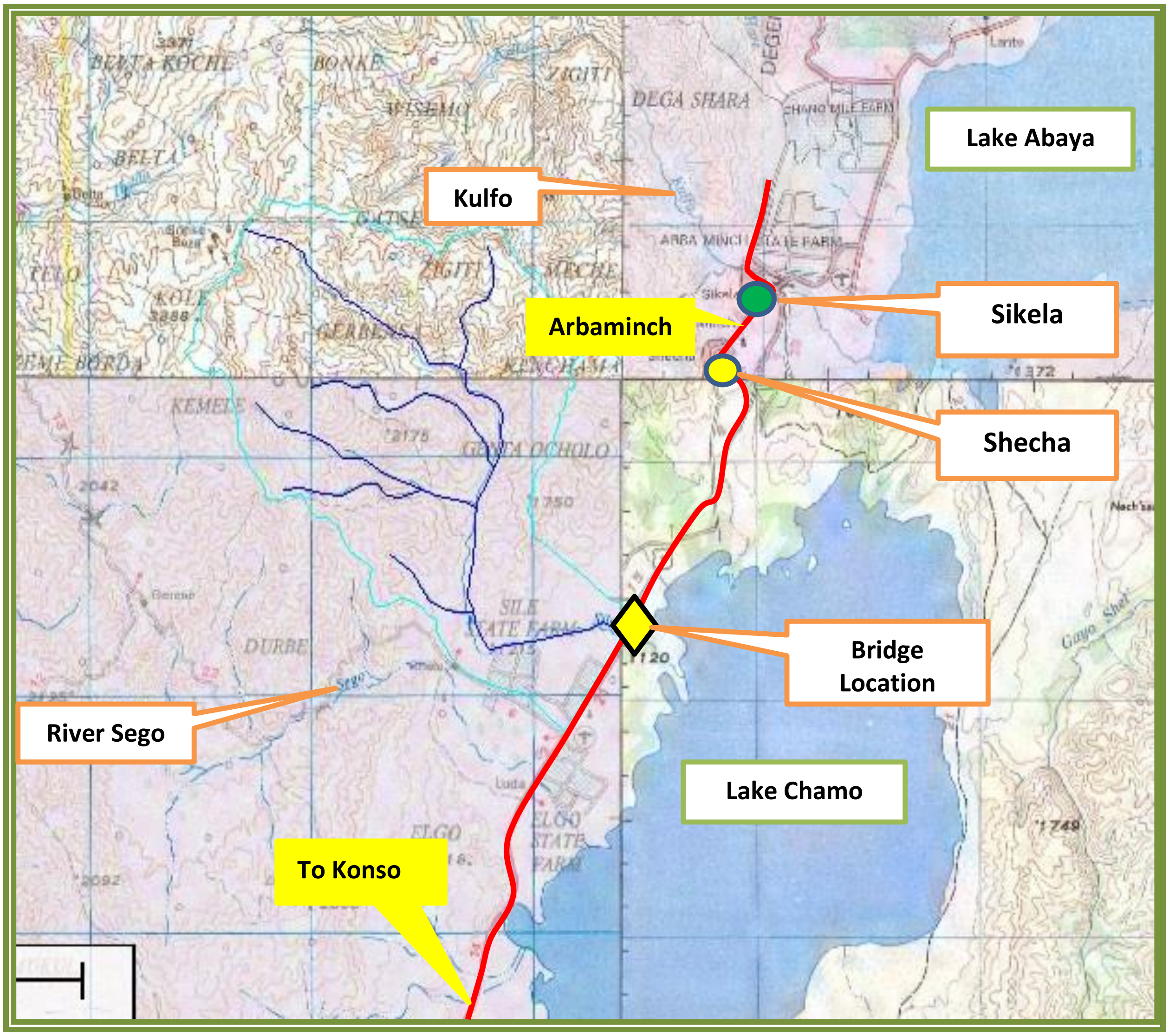

Figure 3-2: Location Map of the Sile River Bridge

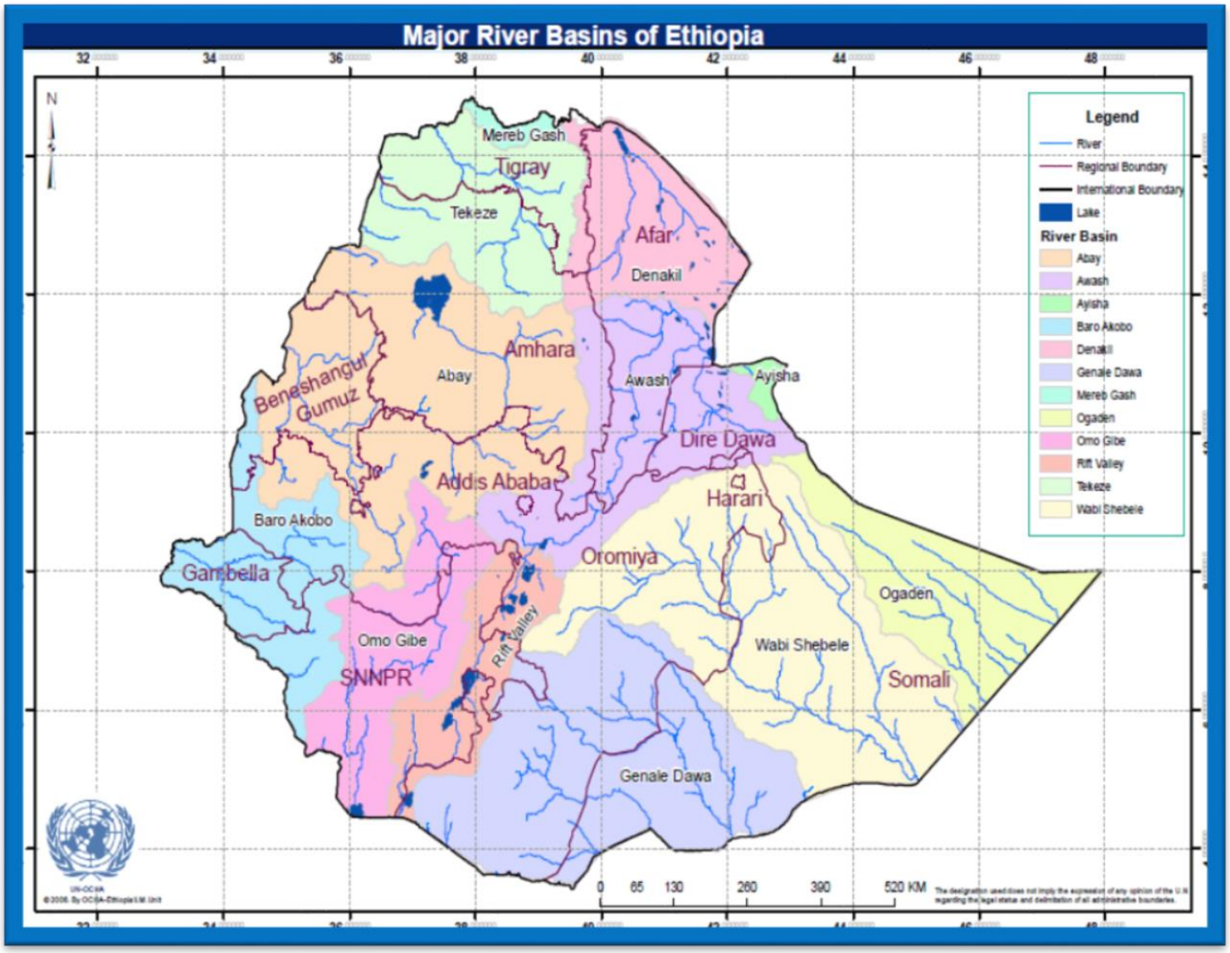

Figure3-3: Major River Basins of Ethiopia (Source: MoWIE**)**

3.2. Collection & Development of Data

Both primary and secondary data pertinent to the study were collected from different institutions. Concerning Secondary Data, I have collected it from Ministry of Water, Irrigation and Energy, Ethiopian Roads Authority-Bridge Management Team, the Ethiopian Meteorological Agency, Water Works Design and Supervision Enterprise, Transport Construction and Design Enterprise, Ethiopian Roads Construction Corporation (ERCC) and Primary Data from the site and key informants.

All are presented in the following sections and used as an input for analysis of key Hydrological, Hydraulic and Scour parameters.

3.2.1. Hydrological Data

This is the major problem. I have tried to collect recorded stream flow data but like most rivers in Ethiopia, the Sile River is un gauged and the peak flood discharge used to check the adequacy of the bridge opening cannot be estimated from recorded stream flow data. The rivers which are gauged in the area are river Kulfo which is about 20Km from Sile at the upstream side and river Gato and Woito which are found at the downstream side of Sile at 57Km and 157.2Km respectively from Arbaminch. Though river Sego is at about 7Km downstream of the Sile River which is more or less with in similar catchment characteristics, hence the river is un gauged. The peak stream flow data of Kulfo which is found around Sikela for the years from 1991 to 2013 is attached as Appendix-II on page 96.

With regard to previous hydrological studies, I have reviewed the Rift Valley River Basin Master Plan of 2008 which is developed by MoWIE. Hence, this study does not include a regional model for hydrological analysis for different return periods which can be applied to determine design discharges with in the basin like the Omo-Gibe River Basin Master Plan developed in 1995.

3.2.2. Meteorological Data

I have found maximum daily highest rainfall records and rainfall intensity records of one hour and 24 hour for 18 years from 1987 to 2004 from Arbaminch Meteorological Station and also the National Meteorological Agency in Addis Ababa as presented in Appendix-II.

According to ERA's Drainage Design Manual 2002, ten years of continuous or synthesized records, Gumbel Method is adopted to estimate the design rainfall of the study area and it is determined by using the following Equation.

$$X_T = X_M + K_T S_x \quad \text{..........................Equation (3.1)}$$

Where:

X_T = Design Rainfall for the Return Period –T

X_M = Mean Daily Highest Rainfall (mm)

K_T = Frequency Factor

S_X = Standard Deviation

3.2.3. Maps

Concerning Maps the following are used:

- Topographic Map of the study area (Scale of 1:250,000 and 1:50,000).
- Geological Map of Ethiopia (Scale 1: 250,000).
- Soil Map of Ethiopia (Scale 1: 100,000) and
- Land use/ land cover Map of Ethiopia (Scale 1: 100,000)

3.2.4. Surveying Data

I have collected survey data and Digital Terrain (surface) Model of the study area which were collected at different times by the ERA, Sodo District DED, ERA-BMS and from Net Consulting Engineers PLC. All these data are used for the hydraulic analysis and adequacy check of the existing bridge using HEC-RAS 4.0 Beta and Eagle Point AutoCAD, 2007.

3.2.5. Soil and Geology

Disturbed Soil samples from the Bridge approach area are collected. To conduct laboratory tests a total of six (6) samples from the upstream, downstream side of the bridge and from the river channel, right and left river banks were collected mixed and representative soil sample is taken for laboratory analysis. ASTM D 422 - Standard Test Method is used.

The dry sieve analysis is applied. In order to conduct the analysis equipment like Balance, Set of Sieves, Cleaning Brush, Sieve Shaker, and Timing Device were used. The Unified Soil Classification System (USCS) is used for Classification.

The Unified Soil Classification System (USCS) is a rapid method for identifying and grouping soils, originally developed by Casagrande for military construction purposes. The USCS is based on grain size and plasticity. In this system, soils are first divided in to one of the two classes: coarse-grained (more than 50% of the particles by weight are larger than 0.074mm or the ≠ 200 sieve), or fine-grained (more than 50% of the particles are finer than this size).

Coarse grained soils are then identified by a letter designation “G” if more than half of the coarse fraction is greater than 4.76mm (≠ 4 sieve), or “S” if more than half are finer. The G and S are followed by a second letter. W-if the soil is well graded, P- if the soil is poorly graded, M- if the soil contains appreciable amounts of silt and C- if the soil contains appreciable amounts of clay. Concerning the Geology of the study area it is analyzed using the geological map of Ethiopia.

Table 3:1 Unified Soil Classification System (USCS)

General Classification	Major Division	Minor Division	Soil Classification Group Symbol	Soil Classification Group Name
GRAVELS More than 50% of coarse fraction retained on No.4	CLEAN GRAVELS <5%	Cu≥4, and 1≤Cc≤3	GW	Well-graded gravel
		Cu<4,and 1>Cc>3	GP	Poorly-graded gravel
	GRAVELS WITH FINES >12%	Fines classify as ML or MH	GM	Silty gravel
		Fines Classify as CL or CH	GC	Clayey gravel
SANDS More than 50% of coarse fraction passes No.4	CLEAN SANDS< 5% fines	Cu≥6,and 1≤Cc≤3	SW	Well-graded sand
		Cu<6,and 1>Cc>3	SP	Poorly graded sand
	SANDS WITH FINES>12% fines	Fines classify as ML or MH	SM	Silty sand
		Fines Classify as CL or CH	SC	Clayey sand
SILTS AND CLAYS Liquid limit less than 50	Inorganic	PI>7 and plots on or above “A” line	CL	Lean clay
		PI<4 or plots below “A” line	ML	Silt
	Organic	Liquid limit-over dried / Liquid limit-not dried<0.75	OL	Organic clay, Organic silt
SILTS AND CLAYS Liquid limit 50 or more	Inorganic	PI plots on or above “A” line	CH	Fat clay
		PI plots below “A” line	MH	Elastic silt
	Organic	Liquid limit-over dried / Liquid limit-not dried<0.75	OH	Organic clay, Organic silt
Highly fibrous organic soils	Primarily organic matter, dark in color, and organic color		Pt	peat

Source: Evaluating Scour at Bridges (FHWA), 2001

3.3. Brief Description about the Models

Many comprehensive hydrologic models have been developed in the past decades due to advances in hydrologic sciences and Geographical information system (GIS). Among them the SCS (Soil Conservation Service) method of peak discharge estimation (Runoff estimation), developed by the U.S soil conservation service (1972), has been used for computing the peak discharge.

Concerning the Hydraulic Models and Scour analysis, the HEC-RAS 4.0 Beta, HEC-18 and Eagle Point Auto CAD 2007 are used. HEC-RAS is an integrated system of software, designed for interactive use in a multi-tasking, multi-user network environment. The system is comprised of a graphical user interface (GUI), separate hydraulic analysis components, data storage and management capabilities, graphics and reporting facilities. It is also used to analyze scour by exporting data used for hydrologic and hydraulic analysis.

An overview of how the data flow throughout the hydrologic and hydraulic analysis is presented below.

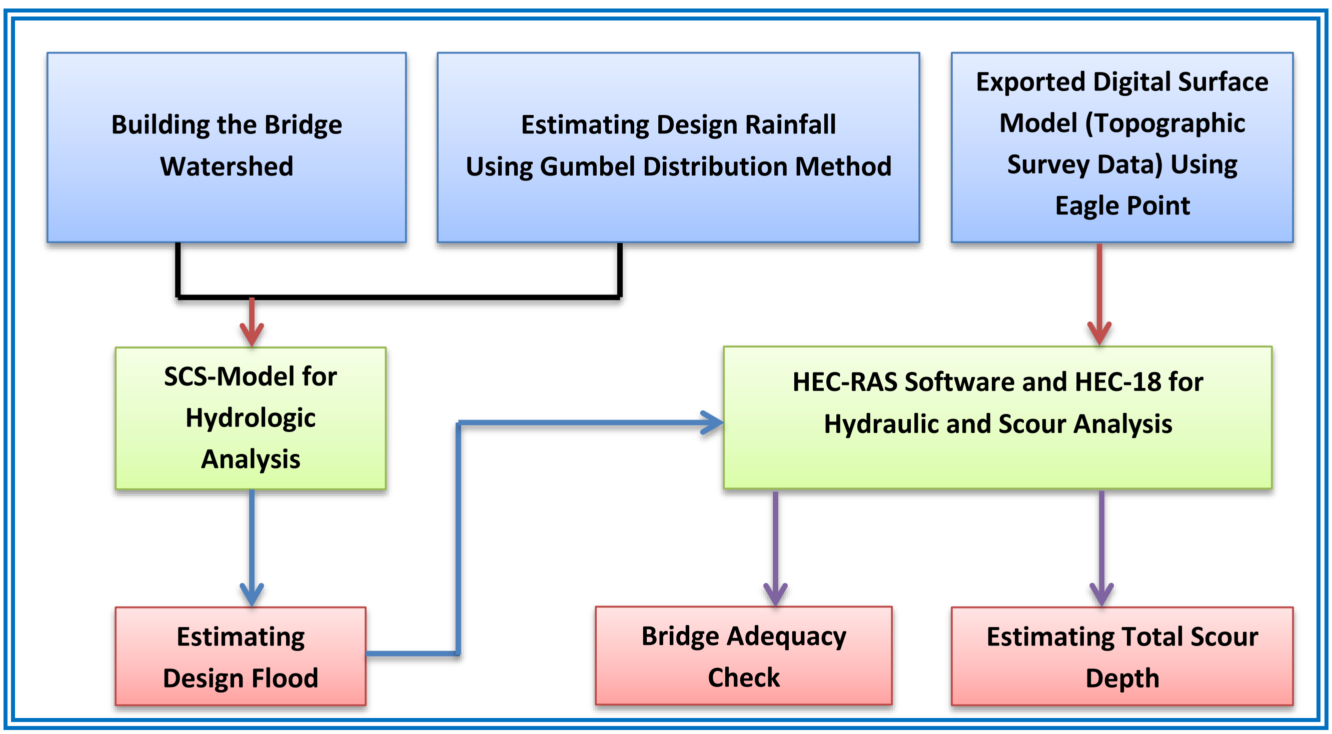

Figure 3-4: Overview of the Flow of Hydrologic and Hydraulic Analysis

3.4. The SCS Unit Hydrograph Model

The SCS require basic data like: catchment area, a runoff factor, time of concentration, and rainfall. The SCS approach, however, is more sophisticated in that it considers also the time distribution of the rainfall, the initial rainfall losses to interception and depression storage, and an infiltration rate that decreases during the course of a storm. With the SCS method, the direct runoff can be calculated for any storm, either real or fabricated, by subtracting infiltration and other losses from the rainfall to obtain the precipitation excess.

According to the ERA's drainage design manual 2002, of all possible hydrologic methods, the SCS is the most applicable in all parts of the country.

3.4.1. Catchment Area

A catchment area is determined from topographic maps and field surveys. For large catchment areas it might be necessary to divide the area into sub-catchment areas to account for major land use changes, obtain analysis results at different points within the catchment area, or locate storm water drainage structures and assess their effects on the flood flows. A field inspection of existing or proposed drainage systems shall be made to determine if the natural drainage divides have been altered. These alterations could make significant changes in the size and slope of the sub catchment areas.

3.4.2. Rainfall

The SCS method is based on a 24-hour storm event which has a Type-II time distribution. The Type-II storm distribution is a 'typical" time distribution which the SCS has prepared from rainfall records. It is applicable for interior rather than the coastal regions and should be appropriate for Ethiopia. The Type-II rainfall distribution will usually give a higher runoff than a Type-I distribution. To use this distribution it is necessary for the user to obtain the 24-hour rainfall value for the frequency of the design storm desired, and then multiply this value by 24 to obtain the total 24-hour storm volume in millimeters.

3.4.3. Rainfall-Runoff Equation

A relationship between accumulated rainfall and accumulated runoff was derived by SCS from experimental plots for numerous hydrologic and vegetative cover conditions. Data for land-treatment measures, such as contouring and terracing, from experimental catchment areas were included. The equation was developed mainly for small catchment areas for which daily rainfall and catchment area data are ordinarily available. It was developed from recorded storm data that included total amount of rainfall in a calendar day but not its distribution with respect to time. The SCS runoff equation is therefore a method of estimating direct runoff from 24-hour or 1-day storm rainfall. The equation is:

$$Q = (P- I_a)^2 / (P - I_a) + S \qquad \text{………………….Equation (3.2)}$$

Where:

Q = accumulated Direct Runoff (mm)

P = accumulated rainfall potential maximum runoff (mm)

I_a = initial abstraction including surface storage ,interception & infiltration prior to run off (mm)

S = potential maximum retention (mm)

The relationship between I_a and S was developed from experimental catchment area data. It removes the necessity for estimating I_a for common usage. The empirical relationship used in the SCS runoff equation is:

$$I_a = 0.2S \qquad \text{…………………..Equation (3.3)}$$

Substituting 0.2S for I_a in equation (3.1), the SC rainfall-runoff equation becomes:

$$Q_u = \frac{\left[P-0.2S\right]^2}{P+0.8S} \qquad \text{…………..Equation (3.4)}$$

S is related to the soil and cover conditions of the catchment area through the CN. CN has a range of 0 to 100, and S is related to CN by:

$$S = \frac{25400}{CN} - 254 \quad \text{.......... Equation (3.5)}$$

The peak discharge is determined by using 24-hrs return period rainfall (P) and the direct runoff (Q) using the figure below.

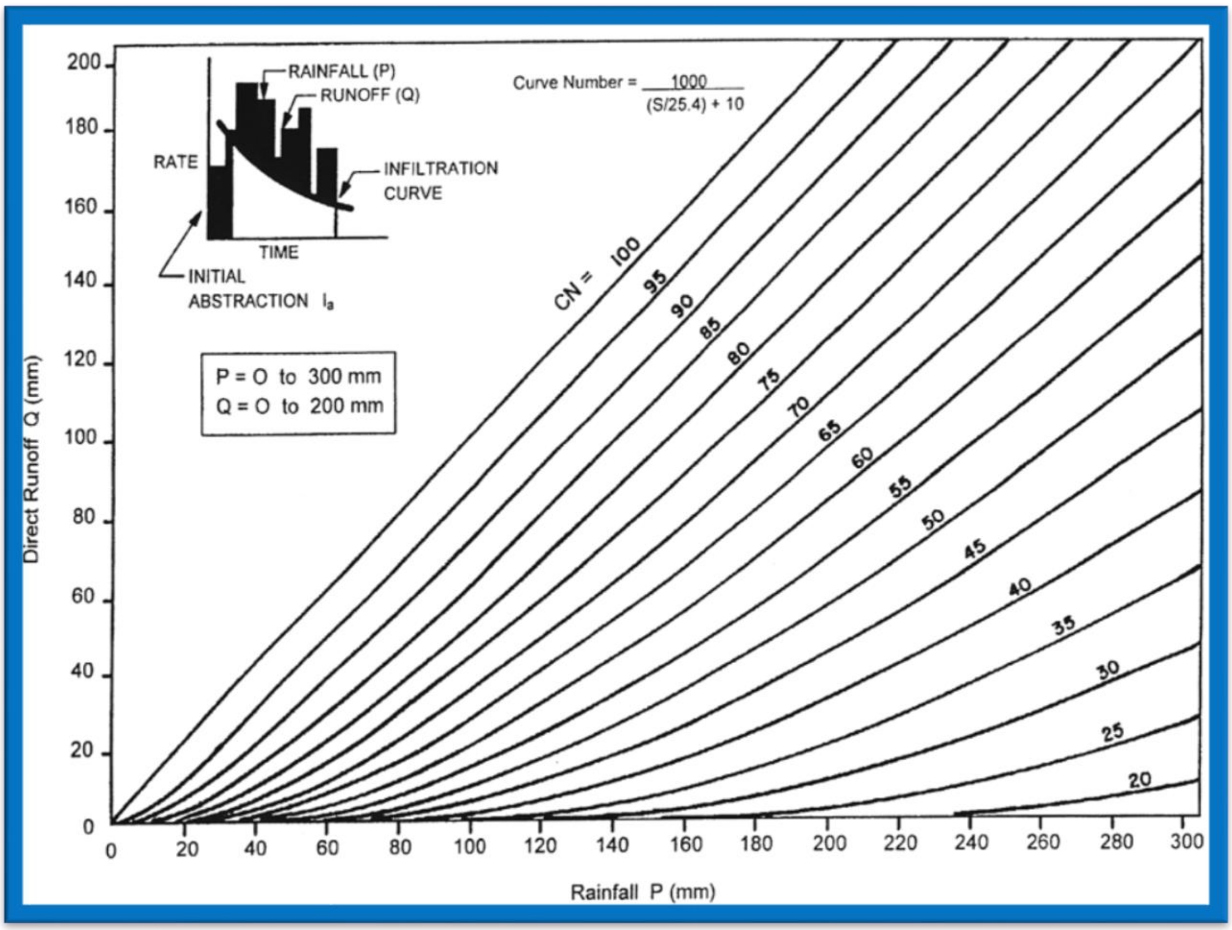

Figure 3-5: SCS Relation between Direct Runoff, Curve Number & Precipitation

(Source: ERA, Drainage Design Manual, 2002)

Table 3-2: Rainfall Regions of Ethiopia

Mean Monthly & Annual Rainfall Region	Station
A1	Axum, Mekele, & Maichew
A2	Gondar, Debre Tabor, Bahir Dar, Debre Markos, Fitche, Addis Ababa
A3	Nazareth, Kulumsa, Robe
A4	Metehara, Dire Dawa, Mieso
B1	Jimma, Bedele, Gore, Nekempte
B2	Arba Minch, Soddo, Awasa
C	Kombolcha, Woldiya, Sirinka
D1	Gode, Kebri Dihar
D1	Kibre Mingist, Negele, Moyale, Yabelo

Source: ERA-DDM, 2002

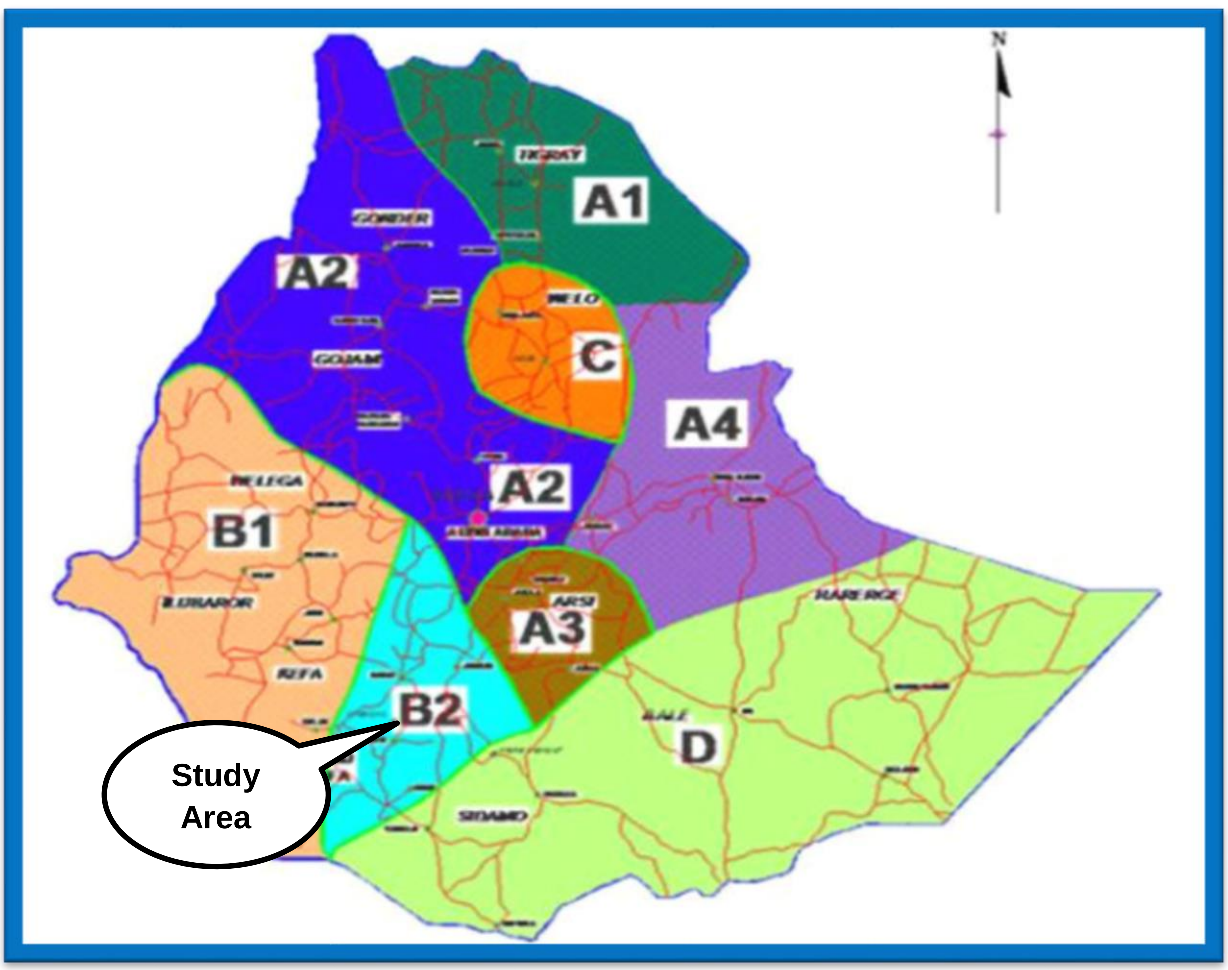

Figure 3-6: Rain fall Regions of Ethiopia (Source: ERA-DDM, 2013)

3.4.4. Run-off Factors

Runoff is rainfall excess or effective rainfall - the amount by which rainfall exceeds the capability of the land to infiltrate or otherwise retain the rainwater. The principal physical catchment area characteristics affecting the relationship between rainfall and runoff are land use, land treatment, soil types, and land slope.

3.4.4.1. Land Use

Land use is the catchment area cover, and it includes both agricultural and non-agricultural uses. Items such as type of vegetation, water surfaces, roads, roofs, etc. are all part of the land use.

3.4.4.2. Land Treatment

Land treatment applies mainly to agricultural land use, and it includes mechanical practices such as contouring or terracing and management practices such as rotation of crops.

The SCS uses a combination of soil conditions and land-use (ground cover) to assign a runoff factor to an area. These runoff factors, called runoff Curve Numbers (CN), indicate the runoff potential of an area. The higher the CN, the higher is the runoff potential.

3.4.5. Hydrological Soil Groups

Soil properties influence the relationship between runoff and rainfall since soils have differing rates of infiltration. Permeability and infiltration are the principal data required to classify soils into Hydrologic Soils Groups (HSG). Based on infiltration rates, the Soil Conservation Service (SCS) has divided soils into four hydrologic soil groups as follows:

Group A: Sand, loamy sand or sandy loam. Soils having a low runoff potential due to high infiltration rates. These soils primarily consist of deep, well-drained sands and gravels.

Group B: Silt loam, or loam. Soils having a moderately low runoff potential due to moderate infiltration rates. These soils primarily consist of moderately deep to deep, moderately well to well drained soils with moderately fine to moderately coarse textures.

Group C: Sandy clay loam. Soils having a moderately high runoff potential due to slow infiltration rates. These soils primarily consist of soils in which a layer exists near the surface that impedes the downward movement of water or soils with moderately fine to fine texture.

Group D: Clay loam, Silty clay loam, sandy clay, Silty clay or clay. Soils having a high runoff potential due to very slow infiltration rates. These soils primarily consist of clays with high swelling potential, soils with permanently-high water tables, soils with a clay pan or clay layer at or near the surface, and shallow soils over nearly impervious parent material.

3.4.6. Runoff Curve Numbers

The ERA's Drainage Design Manual 2002 gives a series of tables related to runoff factors. The tables are based on an average antecedent moisture condition, i.e., soils that are neither very wet nor very dry when the design storm begins. Curve numbers has to be selected only after a field inspection of the catchment area and a review of cover type and soil maps. Care has to been taken in the selection of curve numbers (CNs). Use a representative average curve number, CN, for the catchment area. Selection of overly 31 conservative CNs will result in the estimation of excessively high runoff and consequently excessively costly drainage structures. Selection of conservatively high values for all runoff variables results in compounding the runoff estimation. It is better to use average values and design for a longer storm frequency.

3.4.7. Time of Concentration

Time of concentration is the time required for water to flow from hydraulically remote point of catchments area to the point under investigation. The most intense rainfall that contributes at drainage structures crossing will be that the duration equal to the time of concentration. The time of concentration is estimated using Kirpich's equation. Depending on the slope of the river, the time of concentration is computed on reach bases and summed up.

$$T_C = \sum_{i=1}^{i=n} \frac{0.00032\, L_i^{\,0.77}}{S_i^{\,0.385}} \qquad \text{…………Equation (3.5)}$$

Where:

T_c = Time of Concentration (hr)

L_i = Length of Stream Segment (m)

S_i = Slope equal to H/L, where H is the difference in elevation between the reach (m)

3.4.8. I_a/p-Parameter

I_a/p is a parameter that is necessary to estimate peak discharge rates. I_a- denotes initial abstraction and p-is the 24 hour rainfall depth for a selected return period. The 24 hour rainfall depth is taken from ERA drainage design manual for rainfall region B2. For a given 24 hour rainfall distribution I_a/P represents the fraction of rainfall that must occur before runoff begins.

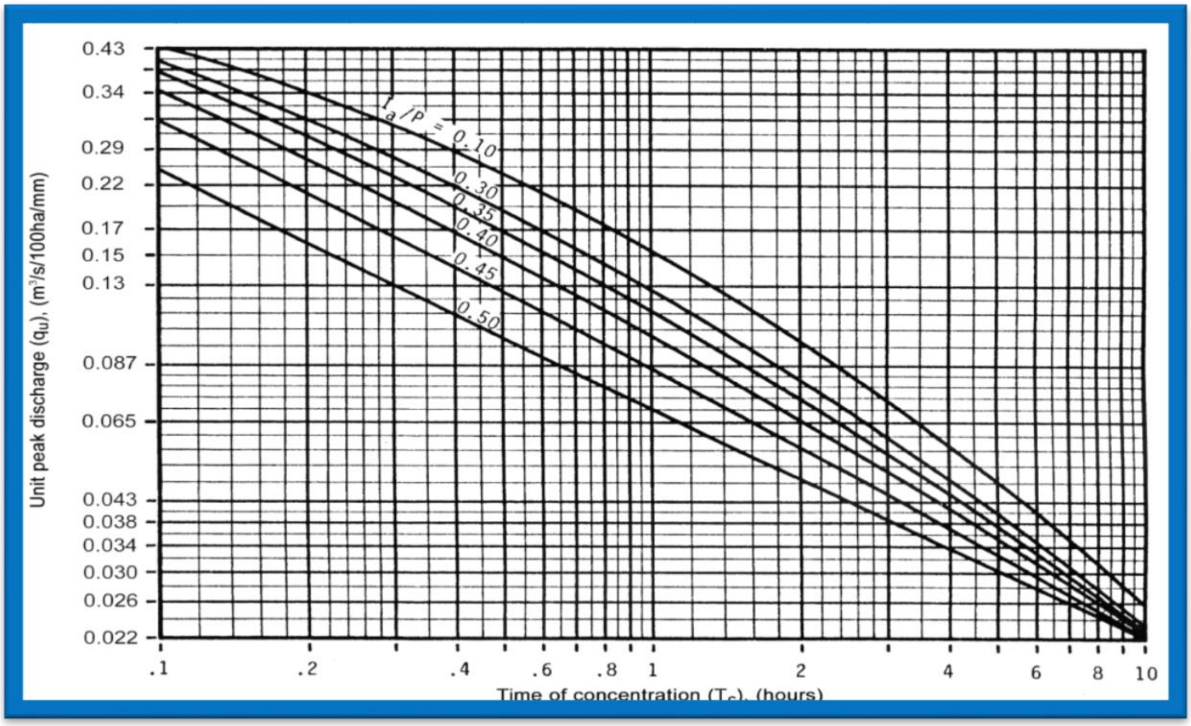

Figure 3-7: Unit Peak Discharge, Type II Rainfall

Table 3-3: I_a - Values for Runoff Curve Numbers (CN)

CN	I_a (mm)	CN	I_a (mm)	CN	I_a (mm)
40	76.2	60	33.9	80	12.7
41	73.1	61	32.5	81	11.9
42	70.2	62	31.1	82	11.2
43	67.3	63	29.8	83	10.4
44	64.6	64	28.6	84	9.7
45	62.1	65	27.4	85	9.0
46	59.6	66	26.2	86	8.3
47	57.3	67	25.0	87	7.6
48	55.0	68	23.9	88	6.9
49	52.9	69	22.8	89	6.3
50	50.8	70	21.8	90	5.6
51	48.8	71	20.6	91	5.0
52	46.9	72	19.8	92	4.4
53	45.1	73	18.8	93	3.8
54	43.3	74	17.9	94	3.3
55	41.6	75	16.9	95	2.7
56	39.9	76	16.1	96	2.1
57	38.3	77	15.2	97	1.6
58	36.8	78	14.3	98	1.0
59	35.3	79	13.5	99	0.4

Source: ERA-DDM, 2002

3.4.9. Peak Discharge Estimation

The peak discharge is estimated from the following equation.

$$Q_p = q_u \, A \, Q_u \qquad \text{……………Equation (3.6)}$$

Where:

Q_p = Peak Discharge (m^3/s)

q_u = Unit peak Discharge ($m^3/s/km^2/mm$)

A = Drainage Area (Km^2)

Q_u = Accumulated Run off (mm)

3.5. Hydraulic Models

Any hydraulic model, whether it is numerical or physical, has assumptions and requirements. It is important to be aware of and understand the assumptions because they form the limitations of that approach. It is the goal of any hydraulic model study to accurately simulate the actual flow condition. Violating the assumptions and ignoring the limitations will result in a poor representation of the actual hydraulic condition. Treating the model as a black box will often produce inaccurate results. Therefore, the approach should be selected based primarily on its advantages and limitations, though also considering the importance of the structure, potential project impacts, cost, schedule and its applicability.

3.5.1. HEC-RAS Model

The main objective of the HEC-RAS program is quite simple to compute water surface elevations at all locations of interest for either a given set of flow data (steady flow simulation) or by routing hydrographs through the system (unsteady flow simulation).

The data needed to perform these computations are divided in to the following categories: geometric data; steady flow data; unsteady flow data; and sediment data. Geometric data are required for any of the analyses performed within HEC-RAS. Other data types are only required depending on the specific type analysis.

3.5.1.1. Geometric Data

The basic geometric data consists of establishing the connectivity of the river system; cross section data, reach lengths, energy loss coefficients (friction losses, contraction and expansion losses) and stream junction information. Hydraulic structure data's (bridge, culverts, weirs etc.) which are also considered geometric data's.

a. River System Schematic

It is required for any geometric data set with in the HEC–RAS system. The schematic defines how the various river reaches are connected, as well as establishing a naming convention for referencing all the other data.

b. Cross Section Geometry

Boundary geometry for the analysis of flow in natural stream is specified in terms of ground surface profiles (cross section) and the measured distance between them (reach lengths). Cross sections are located at intervals along a stream to characterize the flow carrying capability of the stream and its adjacent floodplain. Other data that are required for each cross section consists of: downstream reach length, roughness coefficients, and contraction and expansion coefficient.

c. Reach Length

The measured distances b/n cross sections are referred to as reach lengths. The reach lengths for the left overbank, right over bank and channel are specified on the cross section data.

d. Energy Loss Coefficients

Several types loss coefficients are utilized by the program to evaluate energy loses; (1) Manning's n values or equivalent roughness "K" values for friction loss, (2) contraction and expansion coefficients to evaluate transition losses and (3) Bridge and culvert loss coefficients to evaluate losses related to weir shape, pier configuration, pressure flow and entrance and exit conditions. Manning' n selection of an appropriate value for Manning's n is very significant to the accuracy of the computed water surface profiles.

The value of manning's n is highly variable and depends on a number of factors including: surface roughness; vegetation; channel irregularities; channel alignment; scour and deposition; obstructions; size and shape of the channel; stage and discharge; seasonal changes; temperature; and suspended material and bed load.

3.5.1.2. Steady Flow Data

Steady flow data are required in order to perform a steady water surface profile calculation steady flow data consists of flow regime, boundary conditions and peak discharge information.

3.6. Evaluating Scour at Bridges and Scour Equations

The computation of scour at the Bridge can be conducted using different models based upon the methods outlined in Hydraulic Engineering Circular No. 18 (HEC-18, FHWA, 2001).

Section 3.5.1 presents the methods and equations for computing contraction scour and local scour at piers and abutments. Most of the material in this section is taken directly from the HEC-18 publication (FHWA, 2001).

HEC-18 is used to determine the overall depth of scour and should be referenced for a thorough discussion. Hence, the critical velocity V_C for beginning of motion has to be calculated in order to determine the flow upstream of the bridge is transporting material or not. To calculate the critical velocity, the following equation, Laursen (1963) is used:

$$V_C = K_u\, y^{1/6}\, D^{1/3} \qquad \text{Equation (3.7)}$$

Where:

V_c = critical velocity above which bed material of size D smaller be transported (m/s)

y = average depth of flow upstream of the bridge (m)

D = particle size for V_c (m)

D_{50} = particle size in a mixture of which 50% are smaller, (m)

K_u = 6.19 (S.I. Units)

3.6.1. Live-Bed Contraction Scour Equation

In order to estimate the live-bed contraction scour, the following Laursen's (1960) live-bed scour equation is used.

$$\frac{y_2}{y_1} = \left[\frac{Q_2}{Q_1}\right]^{6/7} \left[\frac{W_1}{W_2}\right]^{K_1} \quad \text{……….Equation (3.8)}$$

$y_S = y_2 - y_0$ (average contraction scour depth)

Where:

y_2 = Average depth after scour in the contracted section, (m).

y_1 = Average depth in the main channel or floodplain at the approach section, (m).

y_o = Average depth in the main channel or flood plain at the contracted section before scour,(m).

Q_1 = Flow in the main channel or floodplain at the approach section, which is transporting sediment, (m^3/s).

Q_2 = Flow in the main channel or floodplain at the contracted section, which is transporting sediment, (m^3/s)

W_1 = Bottom width in the main channel or floodplain at the approach section, (m). This is approximated as the top width of the active flow area in HEC-RAS.

W_2 = Bottom width of the main channel or floodplain at the contacted section less pier widths, (m). This is approximated as the top width of the active flow area.

K_1 = Exponent for mode of bed material transport.

V*/ω	K1	Mode of Bed Material Transport
<0.50	0.59	Mostly Contact Bed Material Discharge
0.50 to 2.0	0.64	Some Suspended Bed Material Discharge
>2.0	0.69	Mostly Suspended Bed Material Discharge

Where:

V* = $(gy_1S_1)^{1/2}$, shear velocity in the main channel or floodplain at the approach section, (m/s).

ω = Fall velocity of bed material based on D_{50}, (m/s).

g = Acceleration of gravity, (m/s²).

S_1 = Slope of the energy grade line at the approach section, (m/m).

3.6.2. Clear-Water Contraction Scour Equation

The following clear-water contraction scour equation is used since it is recommended by HEC No.18 publication based on a research conducted by Laursen (1963):

$$y_2 = \left[\frac{K_U Q_2}{D_m^{2/3} W^2}\right]^{3/7} \quad \text{……..…...Equation (3.9)}$$

$y_S = y_2 - y_0$ (average contraction scour depth)

Where:

y_2 = Average equilibrium depth in the contracted section after contraction scour, (m)

Q = Discharge through the bridge or on the set-back overbank area at the bridge associated with the width W, (m^3/s)

D_m = Diameter of the smallest non-transportable particle in the bed material (1.25 D_{50}) in the contracted section, (m)

D_{50} = Median diameter of the bed material, (m)

W = Bottom width of the contracted section less pier width,(m)

y_0 = Average existing depth in the contracted section,(m)

K_u = 0.0025

3.6.3. Abutment Scour Equations

As it is described in the previous section the HEC No.18, two equations for the computation of live-bed abutment scour are recommended. These are:

3.6.3.1. Froehlich's Abutment Scour Equation

The following Froehlich (1989) equation is used.

$$\frac{y_s}{y_a} = 2.27\, K_1 K_2 \left[\frac{L'}{y_a}\right]^{0.43} Fr^{\,0.61} + 1 \qquad \text{.....Equation (3.10)}$$

Where:

K_1 = Coefficient of Abutment Shape

K_2 = Coefficient for angle of embankment to flow

K_2 = $(\theta/90)^{0.13}$, **$\theta < 90^0$** if embankments points downward, **$\theta > 90^0$** if embankment points upstream

L' = Length of active flow obstructed by the embankment, (m)

A_e = Flow area of approach cross section obstructed by the embankment, (m^2)

F_r = Froude number of approach flow upstream of the abutment, $V_e\,(g\,y_a)^{1/2}$

V_e = Q_e/A_e (m/s)

Q_e = Flow obstructed by the abutment and approach embankment, (m^3/s)

y_a = Average depth of flow on the flood plain (A_e/L), (m)

L = Length of embankment projected normal to the flow, (m)

y_s = Scour depth, (m)

3.6.3.2. The HIRE Equation

The HIRE equation is:

$$\frac{y_s}{y_1} = 4Fr^{\,0.33} \frac{K_1}{0.55} K_2 \qquad \text{.......Equation (3.11)}$$

Where:

y_s = Scour depth in, (m)

y_1 = Depth of flow at the toe of the abutment on the overbank or in the main channel, (m), taken at the cross section just upstream of the bridge.

K_1 = Correction factor for abutment shape.

K_2 = Correction factor for angle of attack θ of flow with abutment.

θ = 90^0 when abutments are perpendicular to the flow, θ $<90^0$ if embankments points downward, and $K_2 = (\theta/90^0)^{0.13}$

F_{r1} = Froude number based on velocity and depth adjacent and just upstream of the abutment toe.

Table 3-4: Correction factor for Abutment shape, K_1

Description	K_1
Vertical-wall Abutment	1.00
Vertical wall Abutment with wing walls	0.82
Spill-through Abutment	0.55

4. RESULTS and DISCUSSION

4.1. Results

Using the methods described in Chapter-3 and the following procedures, all Hydrological, Hydraulic and Scour parameters pertinent to the study are determined and presented sequentially as follows.

4.1.1 Land Use

The area is mostly covered with vegetables, fruit trees like Banana, Mango and Crops (93% cultivated land and only 7% of lower part is open shrub land).

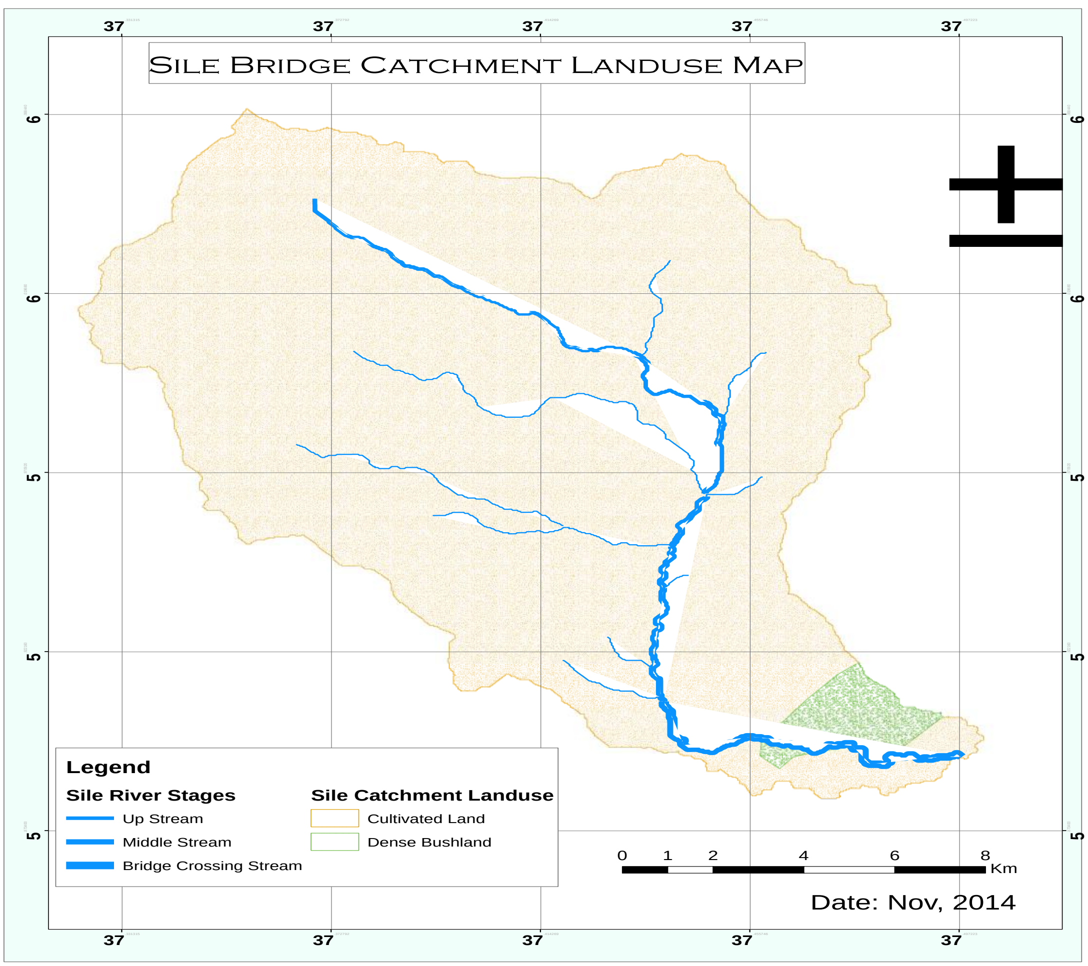

Figure 4-1: Land use Map of the Sile River Catchment

4.1.2. Hydrology

The seasonal variation in climate is associated with the oscillation of the Inter-Tropical Convergence Zone (ITCZ), a low-pressure area of convergence. It is known that, between June and September the ITCZ is located at the Northern part of Ethiopia and the ITCZ shifts to Southern Ethiopia from September to November and April causing a major rainy season in the area.

According to the Ethiopian Meteorological Agency and Ministry of Water Irrigation and Energy, there are few meteorological stations along the road Arbaminch-Konso alignment and only two rivers are gauged along the road (Rivers Gato and Weito). Both rivers are gagged manually two times a day. Hence this road crosses a number of rivers, streams of perennial and intermittent in nature.

As the name *Arbaminch* (40 springs) implies that, the area is known by its appreciable surface and ground water potential.

4.1.3. Geology and Soil

According to the Geological Map of Ethiopia by Mengesha Tefera et.al 1999 (scale of 1:2,000,000), the geology of the research area can be classified in the following manner.

- Alluvial and Lacustrine deposit (Q): Sand, Silt, Clay, Diatomite, Limestone and Beach Sand.
- Awata Group (ARa): Biotite, Hornblende, Siliminite, Garnet, Calc-silicate, and Quartezofeldspatic Gneisses, Marble and Granulite.
- Jimma Volcanics (Pjr): Upper part Rhyolite and Trachyte flows and Tuff with minor Basalt.
- Jimma Volcanics (Pjr): Lower flood Basalt with minor Salic flows.

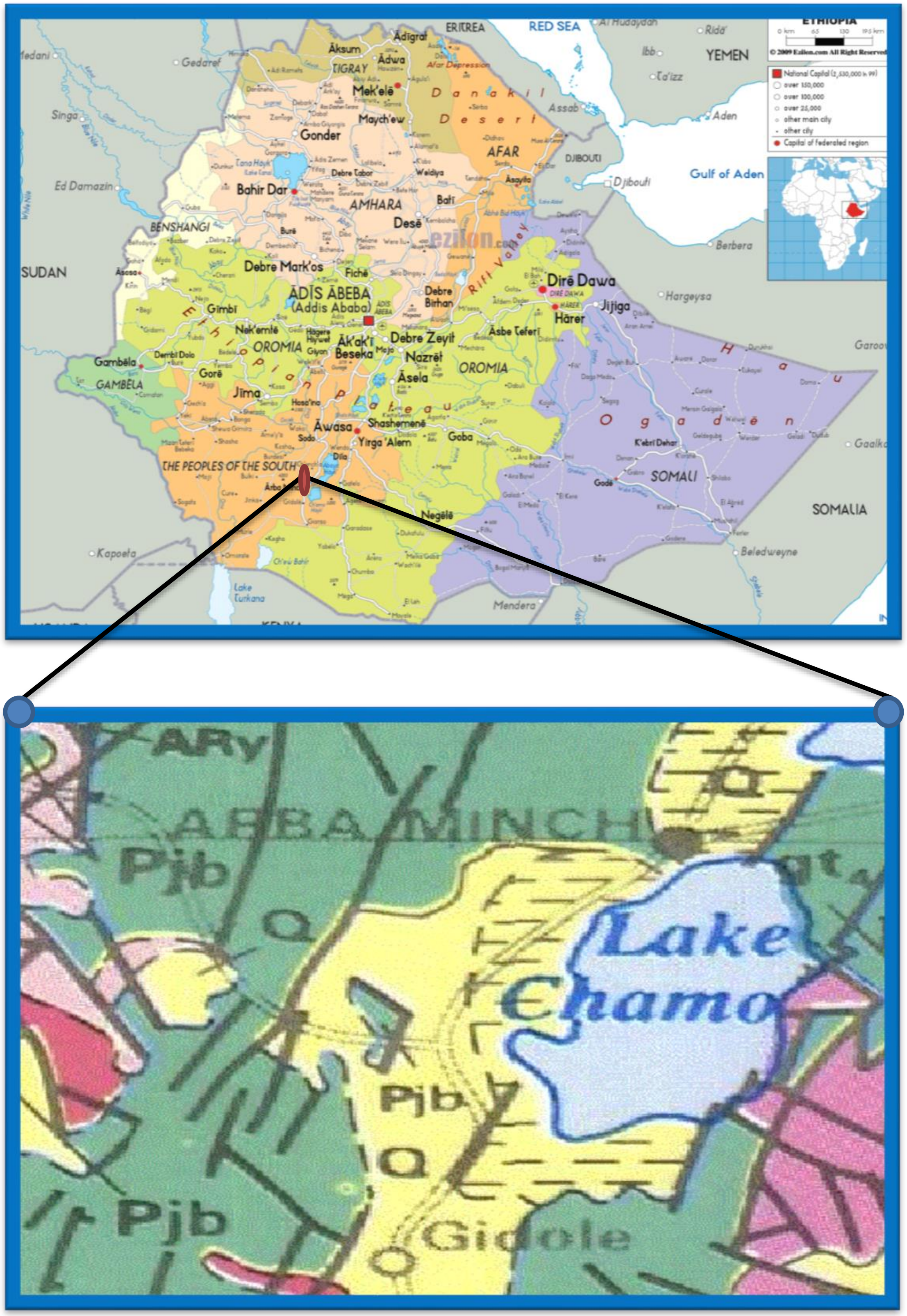

Figure 4-2: Geology of the Study Area (Source: Mengesha Tefera et.al, 1999)

According to the field survey, geological map of the study area, ERA's drainage design manual 2002, the hydrologic soil group of the research area is categorized under hydrologic soil group-B.

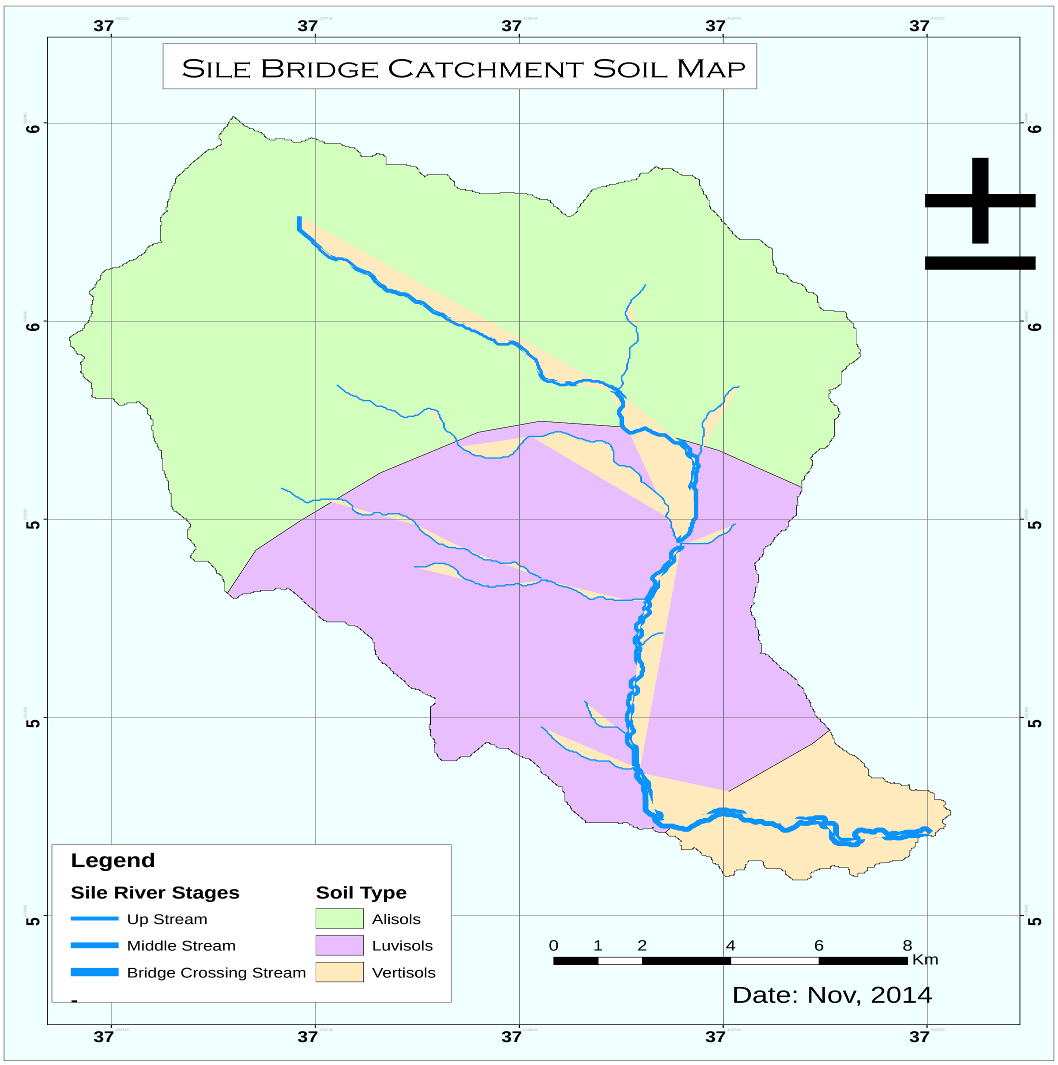

Figure 4-3: Soil Map of the Sile River Bridge Catchment

4.1.4. Hydrological Design Criteria

The hydrological parameters are determined as per the methods stated in Chapter-3, such as for flood Estimation, the SCS has been adopted and for return periods; the design flood is estimated based on ERA-DDM, 2002.

.

Table 4-1: Design Storm Frequency by Geometric Criteria

Structure Type	Geometric Design Standard			
	DS1/DS2	DS3/DS4	DS5/6/7	DS8/9/10
Gutters and Inlets	10/5	2	2	-
Side Ditches	10	10	5	5
Ford/Low-Water Bridge	-	-	-	5
Culvert, pipe (see Note) Span<2m	25	10	5	5
Culvert, 2m<span <6m	50	25	10	10
Short span Bridges 6m<Span<15m	50	50	25	25
Medium Span Bridges 15m<Span<50m	100	50	50	50
Long Span Bridges Spans>50m	100	100	100	100
Check/Review Flood	200	200	100	100

Source: ERA-DDM, 2002

4.1.5. Building the Bridge Watershed

The catchment delineation is performed in ArcGIS 10.2 of hydrology analysis extension. SRTM 30 meter resolution DEM data, which is the most widely used, recommended and is used to delineate the accurate catchment area. The DEM data was checked and Geo-referenced using large scale (1:50,000 scale) Topographic Map of the study area. Generally from the GIS analysis the Sile river catchment covers 229.36 Km^2 of area and its elevation varies from 3380 masl at the highest point and 1117 masl at the crossing.

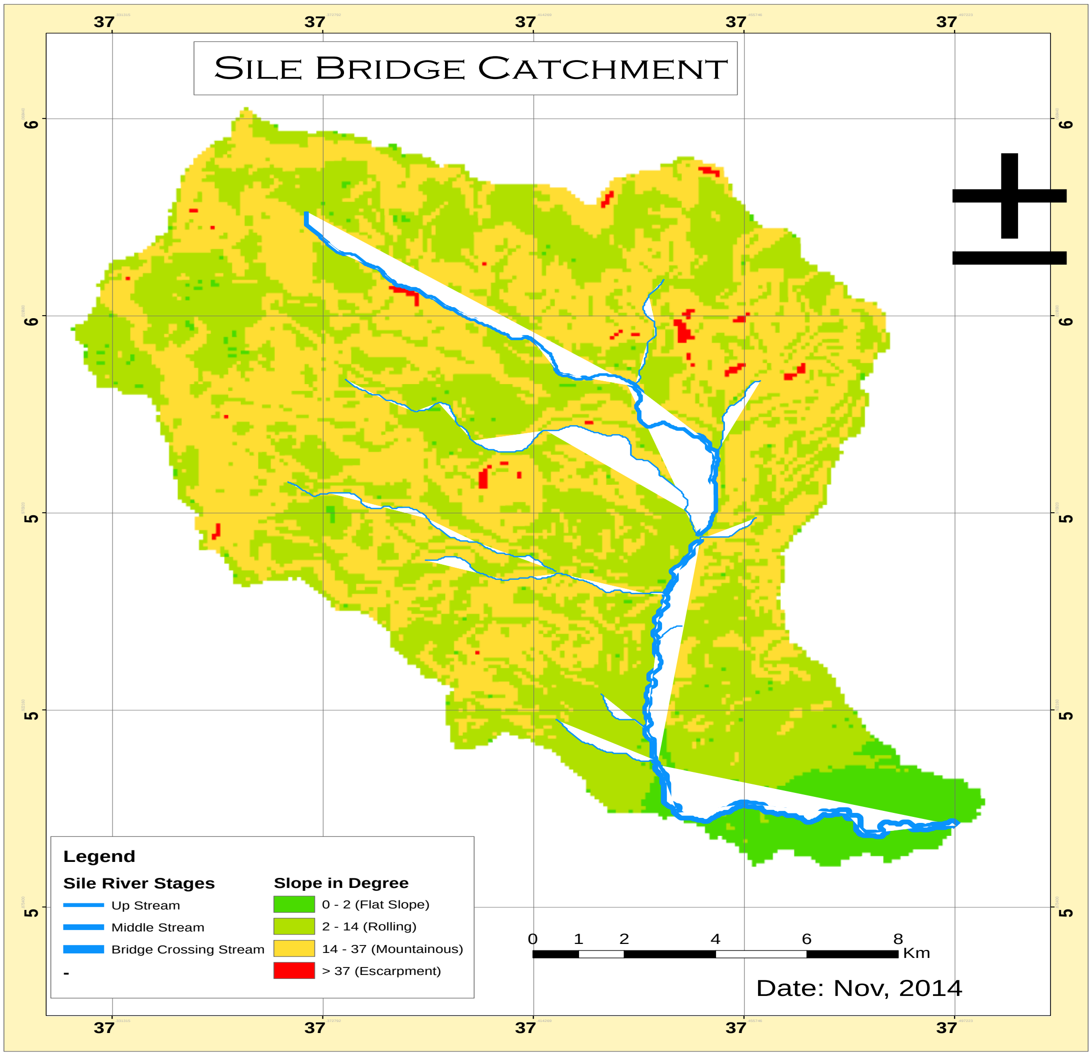

Figure 4-4: Sile River Bridge Catchment

4.1.6. Design Flood Estimation Using SCS Unit Hydrograph

The design flood is estimated at the bridge crossing for 25, 50 and 100 years return periods using the SCS unit hydrograph method.

The design rainfall, the curve number and time of concentration are the parameters which are required to determine the design flood. The parameters are determined as described in the subsequent section.

Analysis is performed using the collected annual maximum 24 hour rainfall data set, the frequency analysis was followed (annexed on page 96) and the SPELL Stat. program was used to identify the fittest distribution for the data set. The result of the analysis shows that the data set fitted with the Extreme Value Distribution Type III and Gumbel distribution. Hence the point rain fall determined by Gumbel is a little bit higher than the one which is determined by the Extreme Value Type III and acceptable to the one which is collected from the site and key informants.

Table 4-2: Daily Highest Rainfall of Arbaminch Rainfall Station

Year	Daily Highest Rainfall (mm)	Year	Daily Highest Rainfall (mm)
1987	**39.0**	1996	**66.8**
1988	**46.9**	1997	**68.2**
1989	**72.1**	1998	**46.6**
1990	**39.3**	1999	**75.3**
1991	**54.0**	2000	**54.3**
1992	**71.2**	2001	**48.0**
1993	**70.0**	2002	**40.6**
1994	**38.0**	2003	**46.8**
1995	**40.7**	2004	**38.8**
X_M = **53.15** S_X = **13.26**			

The table below shows the computed design rainfall values using equation 3.1 and interpolated Frequency factor (K_T) Gumbel Distribution from standard table. (Appendix-III) on page 96.

Table 4-3: Design Rainfall Using Gumbel Extreme Distribution

No. of Samples(n)	Return Period (Years)	Frequency Factor K_T	Design Rainfall (mm)
18	25	2.5857	87.44
	50	3.2639	96.43
	100	3.9372	105.36

The result from the Gumbel Method is taken for further analysis (P_{25}=87.44mm, P_{50}=96.43mm and P_{100}=105.36mm) i.e. design discharge estimation using SCS method.

i. Time of Concentration

The time of concentration is estimated using Equation (3.5) which is Kirpich's equation. Depending on the slope of the river, the time of concentration is computed on reach bases and summed up and summarized in table 4-4.

ii. The Curve Number

The potential maximum soil water retention, S, is related to hydrologic soil properties, land cover and management conditions as well as, the soil moisture status of the Catchment prior to rainfall event and expressed by a dimensionless response index termed the catchment curve number (CN).

The CN number is selected according to soil type, moisture condition and land cover/use of the watershed area. The weighted curve number of the drainage basin is 75 for Sile river drainage basin.

iii. Rainfall Runoff Equation

The direct runoff from 24-hour or 1-day storm rainfall is determined using equation 3.3. After determination of the various input parameters as discussed above, the peak unit discharge, q_u read from figure 3-5 as function of ratio of I_a & P and T_c. I_a= initial abstraction including surface storage, interception, and infiltration prior to runoff in (mm) and P is design point rainfall. Then the peak discharge is computed using equation 3.6.

The result of hydrological design/peak flood computation using SCS method is summarized and presented in the table below. The design floods at the bridge crossing are 348m^3/s, 397.4m^3/s and 512m^3/s for 25, 50 and 100 years return periods respectively.

Table 4-4: Sile River Bridge Crossing Design Discharge Estimated using SCS Method

RIVER	Cat. A	Stream Length	Highest Elev.	Cros. Elev.	River Slope	Tc	CN	S	24HOUR DESIGN POINT RAIN FALL(mm)			DIRECT RUN OFF (mm)			PEAK DISCHARGE (m^3/s)		
Sile	Km^2	m	m	m	m/m	hr			P_{25}	P_{50}	P_{100}	Q_{u} 25	Q_{u} 50	Q_{u} 100	Q_{p} 25	Q_{p} 50	Q_{p} 100
	229.36	9564	3380	1635	0.183	0.71	75	84.7	87.44	96.43	105.36	32	38.5	45	348	397.4	512
		13375	1635	1195	0.033	1.78											
		9421	1195	1117	0.0083	2.29											
						4.78											

Notice:

- Total length of the Sile River Channel is 32,360m
- Direction of flow is from Right to Left
- Average River Channel Slope is 7.48 % and
- Terrain classification according to the ERA's Route Selection Manual is, Rolling.

4.1.7. Soil Sieve Analysis

The results are presented as follows.

- Visual Classification of the Soil: Dark Brown to Black Fine Sand to Gravel
- Wt. of Dry Sample: 502.23

Table 4-5: Sieve Analysis using ASTM D 422 - Standard Test Method

Sieve Number	Particle Diameter (mm)	Mass of Soil Retained (g)	Percent Retained (%)	Cumulative Retained (%)	Percent Fine (%)
4	4.750	22.79	4.54	4.54	95.46
10	2.000	34.18	6.80	11.34	88.66
20	0.850	39.07	7.78	19.12	80.88
40	0.425	95.97	19.11	38.23	61.77
60	0.250	129.67	25.82	64.05	35.95
100	0.150	166.94	33.24	97.29	9.71
200	0.075	9.69	1.93	99.22	0.78
Pan	-	3.87	0.77	99.99	0.01
	Total	**502.23**	**99.99**		

The analysis is conducted with 1% error which is within the acceptable range.

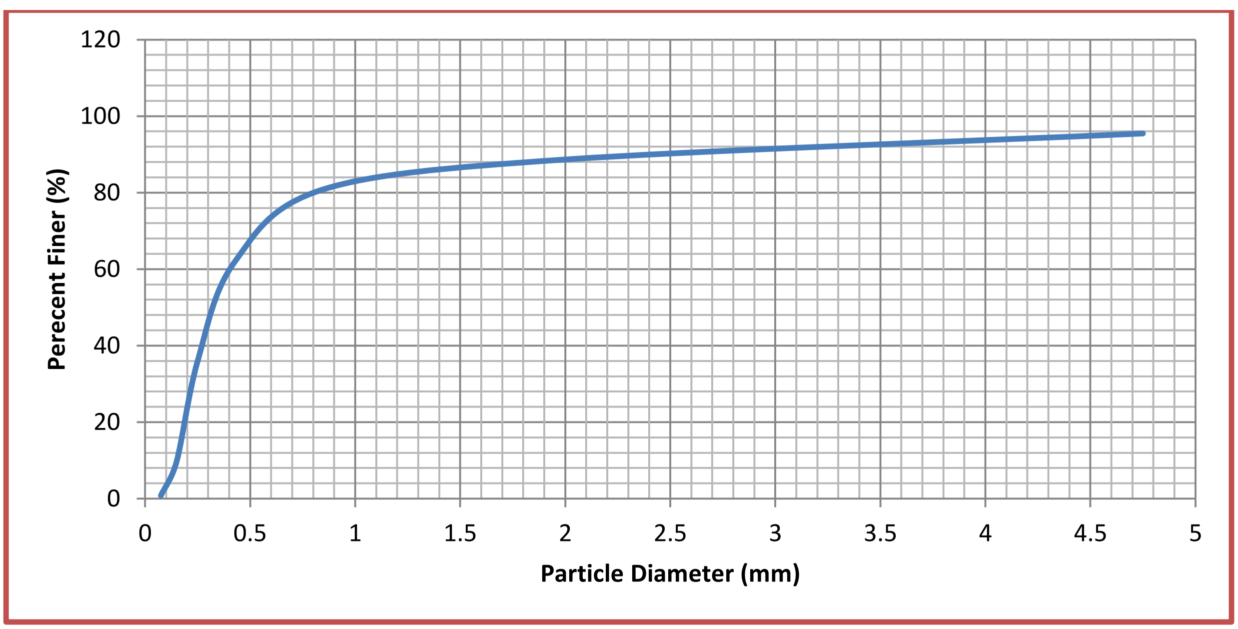

Figure 4-5: Grain Size Distribution Curve

From the above grain size distribution curve:

D_{10}=0.125mm (effective size)

D_{30}=0.21mm

D_{50}=0.31mm

D_{60}=0.40mm and

Uniformity Coefficient (C_U) and Coefficient of Gradation (C_C) are computed as follows.

$$C_U = \left[\frac{D_{60}}{D_{10}}\right] \quad \text{............Equation (4.6)}$$

$$C_C = \left[\frac{D_{30}^2}{D_{60}\times D_{10}}\right] \quad \text{.............Equation (4.7)}$$

From the above, Uniformity Coefficient is 3.2 whereas Coefficient of Gradation is 0.9. According to the USCS described in section 3.2.5 table 3.1, the soil of the bridge crossing area in both classifications is classified as a poorly graded gravel (GP) and poorly graded sand (SP) having more than 50% of the coarse fraction retained on ≠ 4 Sieve.

4.1.8. Determining the Water Surface Profile

Based on the Bridge Dimension, River Morphology around the crossing and the Estimated Design Flood, the water surface profile upstream and downstream of the bridge crossing is determined using HEC-RAS and the backwater/ water stage on the upstream side of the bridge is determined and the data collected from the site is verified.

The estimated design flood at the crossing is 397.4 m^3/s and 512 m^3/s for 50 and 100 years return period respectively. And the bridge dimension:

- Clear Span =20.0m
- Clear Height=8.0m and
- Contracted section=14.10m as shown in the figure below (the 20m span is constricted as result of protection work).

As clearly described under section 3.5.1.1., when the surface (digital terrain model for the analysis is exported using Eagle Point Auto CAD,2007 to HEC-RAS 4.0 Beta, other data that are required for each cross section consists of downstream reach length, roughness, contraction and expansion coefficients were properly used. For reference, the report generated by HEC-RAS is attached as Appendix-IV on page 103.

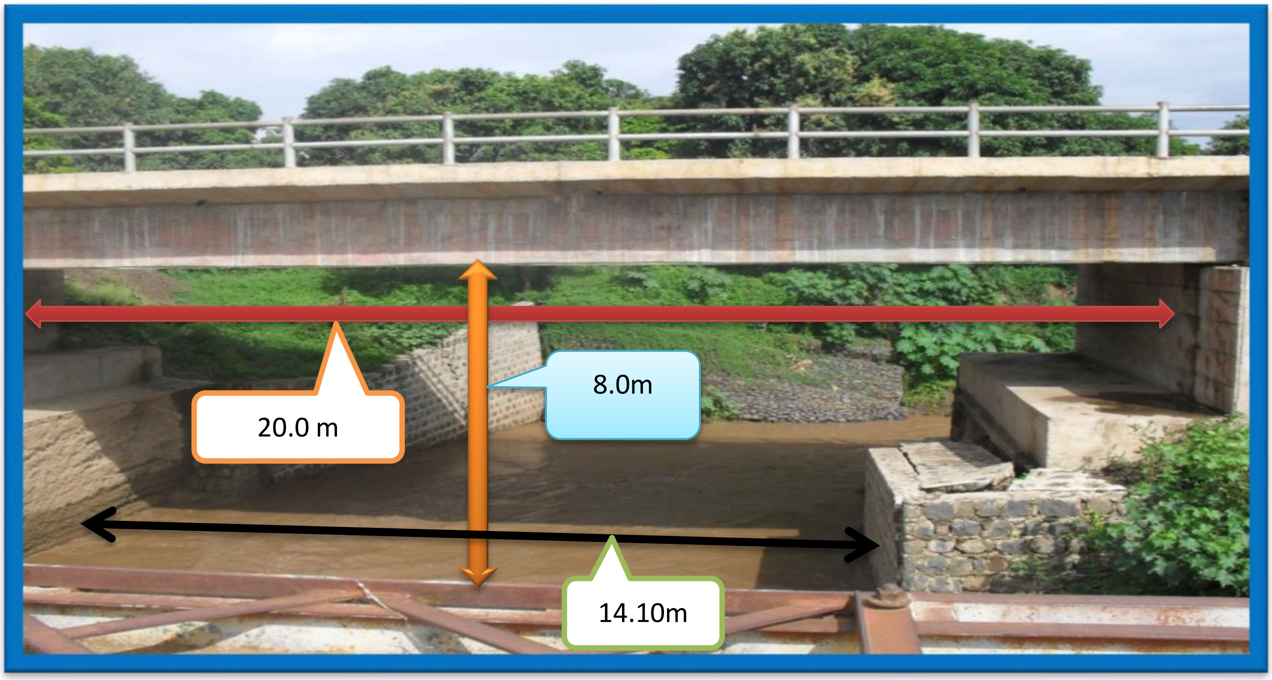

Figure 4-6: Bridge Opening Area

Input data for the existing bridge hydraulic analysis

- Design flood of 397.4m^3/s for 50 year return period.
- River topographic survey data which is analyzed using eagle point software to extract cross section and the plan of the river. The plan-profile data is exported to HEC-RAS for the hydraulic analysis.
- Existing bridge layout.

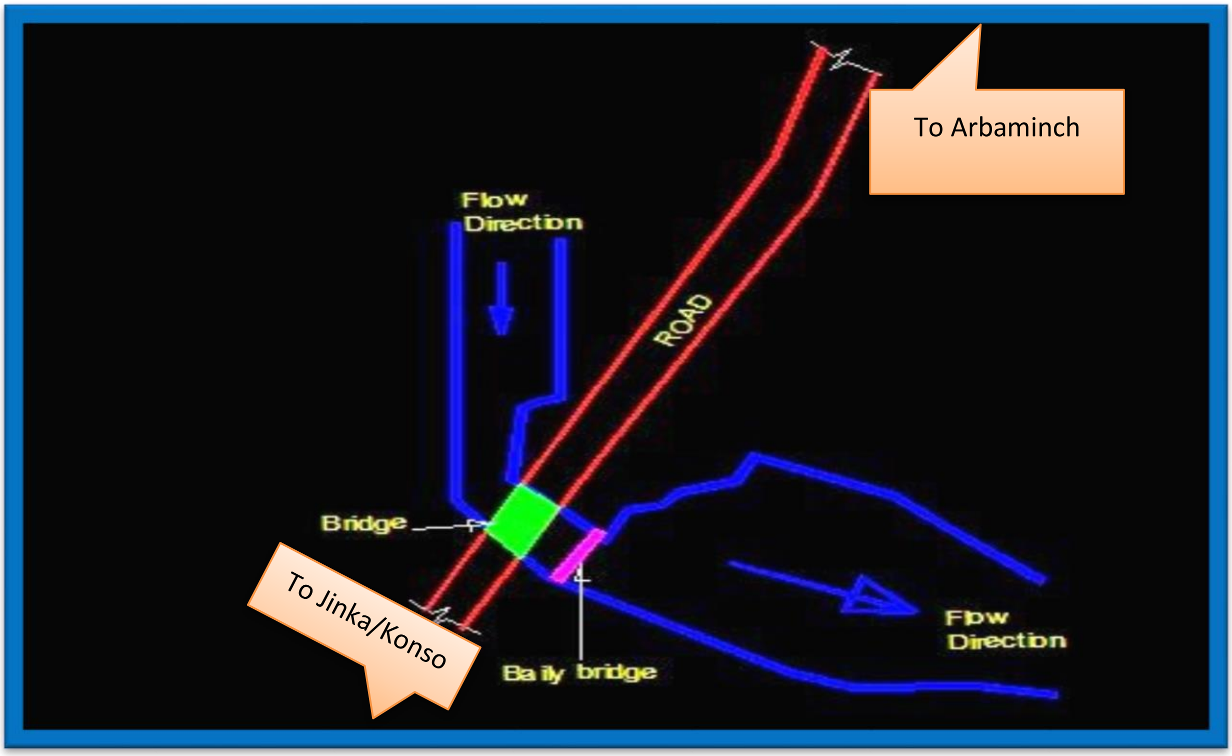

Figure 4-7: Sile River Lay Out With Respect to the Road/Bridge

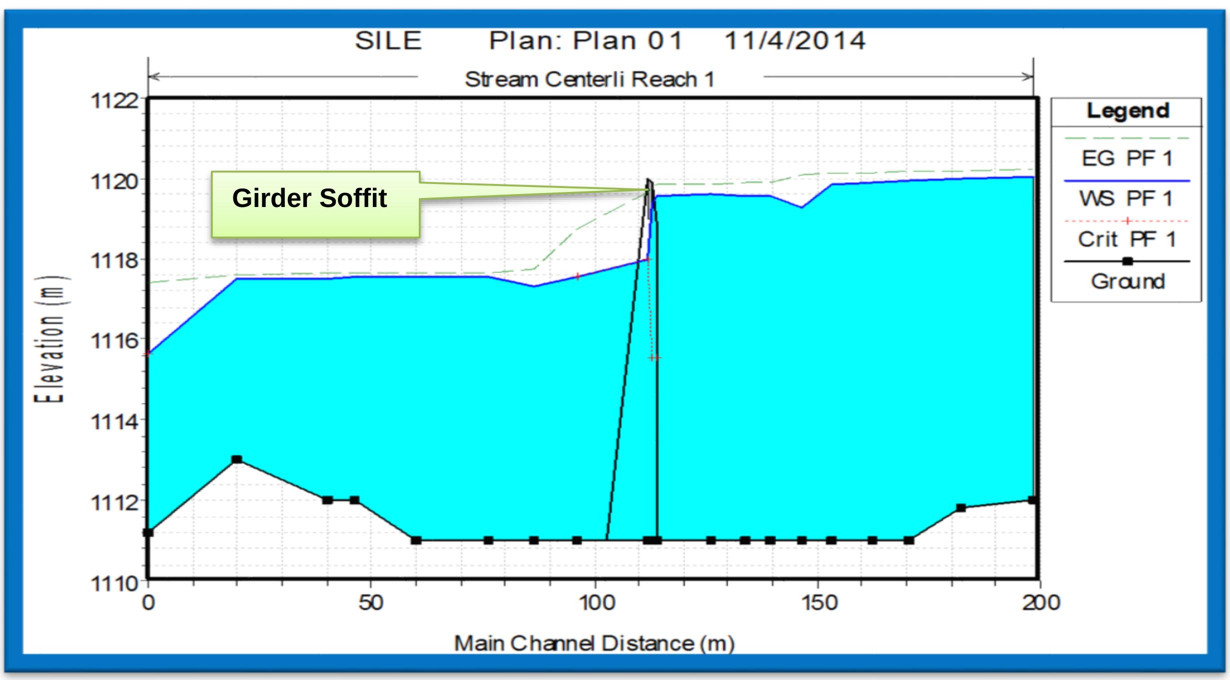

Figure 4-8: 50yr. Peak Flood Water Surface Profile Upstream & Downstream of the Bridge

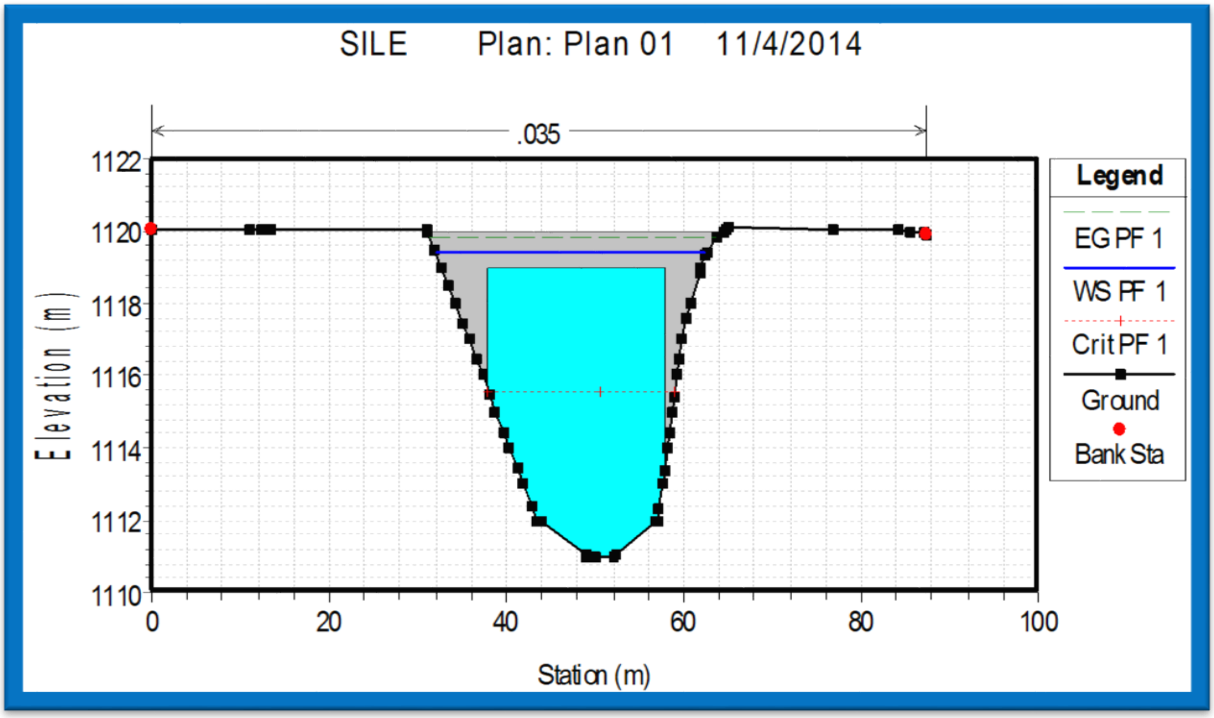

Figure 4-9: 50yr. Peak Flood River Cross Section and Flow Condition under the Bridge

4.1.9. Total Scour Depth

The computation of scour is done using HEC-RAS based on the methods outlined in Hydraulic Engineering Circular No.18 (FHWA, 2001).

As it is discussed in the previous section Contraction scour is computed using HEC-RAS and checked with Live-Bed contraction scour equation. All of the variables except K1 and D50 are obtained automatically from HEC-RAS output file. Hence, I have changed some variables to values what I think appropriate according to the existing condition on the ground and data collected from the site.

Concerning abutment scour like contraction scour, the program automatically selects values for all the other variables based on the hydraulic output and default settings. The only required is to enter the abutment type (vertical abutment with wing wall) and the result is checked with Froehlich Equation as suggested by the data output of HEC-RAS.

Based on the above, the contraction and abutment scour is computed and the result is summarized in the table below.

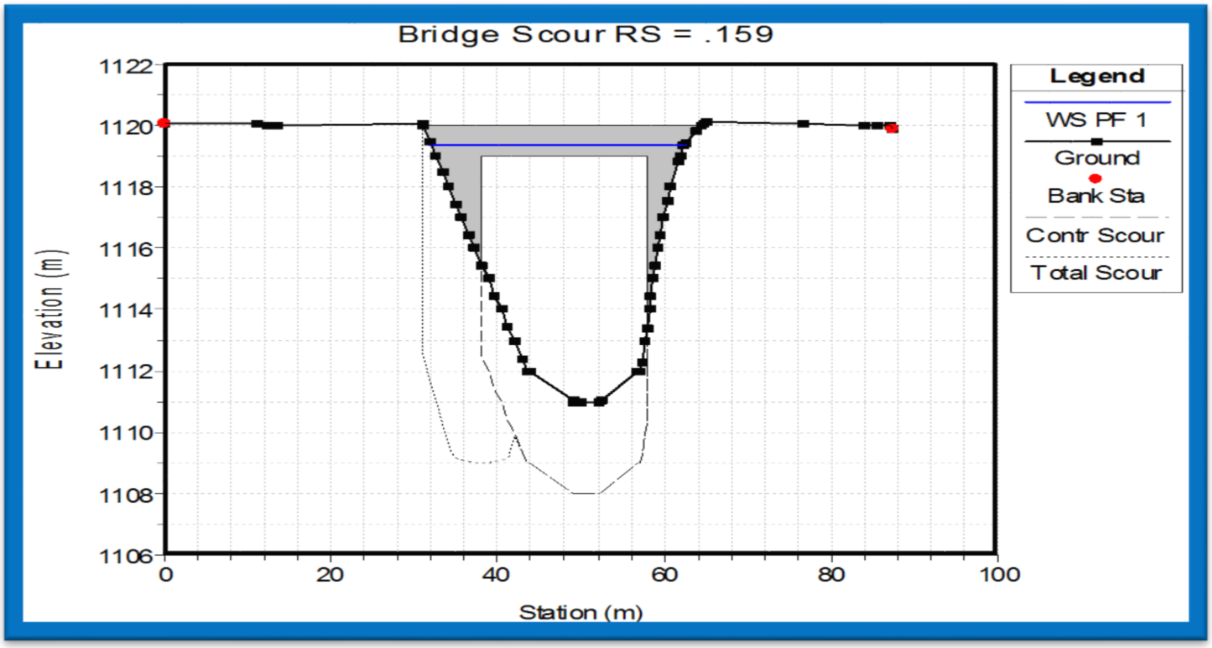

Figure 4-10: Contraction and Abutment Scour Analysed Using HEC-RAS

Table 4-6: Summary of Contraction Scour Depth

Contraction Scour			
Input Data	**LOB**	**Channel**	**ROB**
Average Depth (m)	5.00	7.54	5.00
Approach Velocity (m/s)	0.50	0.75	0.50
Br Average Depth (m)	5.00	5.00	5.00
BR Opening Flow (m3/s)	40.5	397.4	40.5
BR Top Width (m)	20.00		
Grain Size D50(mm)	0.31		
Approach Flow (m3/s)	512.00		
Approach Top Width (m)	30.00		
K1 Coefficient	0.69		
Result			
Scour Depth Ys (m)	3.03		
Critical Velocity (m/s)	0.58		
Equation	**Live**		

Table 4-7: Summary of Abutment Scour Depth

Abutment Scour		
Input Data	**Left**	**Right**
Station at Toe (m)	38.00	58.00
Toe Station at approach (m)	38.00	52.14
Abutment Length (m)	15.65	0.00
Depth at Toe (m)	4.04	5.87
Degree of Skew (degrees)	90.00	90.00
K1 Shape Coefficient	0.82 - Vert. with wing walls	
Degree of Skew (degrees)	90.00	90.00
K2 Skew Coefficient	1.00	1.00
Projected Length L' (m)	15.65	0.00
Average Depth Obstructed Ya (m)	1.10	
Flow Obstructed Qe (m3/s)	11.25	
Area Obstructed Ae (m2)	17.14	
Results		
Scour Depth Ys (m)	3.50	
Qe/Ae = Ve	0.66	
Froude #	0.20	
Equation	Froehlich	
Total Scour Depth		
Contraction Scour Depth(m)	3.03	
Abutment Scour Depth(m)	3.50	
Total Scour (m)	**6.53**	

4.2. Discussion

According to the hydrologic and hydraulic analysis (peak flood water surface profile upstream and downstream of the bridge), the existing Sile River Bridge is insufficient to pass the design flood. The water surface profile for the design flood shows that, the flood level upstream of the bridge is above the soffit level. The existing bridge could not satisfy the requirement for free board and could be overtopped from the design flood. In this regard, for design flood of 397.4m^3/s, about 1.20m clearance is required between the flood level for 50 years recurrence interval and Girder soffit as per the recommendation of ERA Bridge Design Manual, 2002.

Generally, the water surface level of the model output is slightly higher than above the water level which is acquired from the site. This could be as a result of flood recurrence interval. In both cases the bridge does not satisfy the requirements or inadequate to pass the design flood as per the required standard

Concerning the scour analysis, the total scour depth estimated is 6.53m. Hence, the actual scour depth measured at the site is about 5.80m. This is emanated from:

- Equations to estimate scour were developed using the abutment and roadway approach length as one of the variables. This approach results in excessively conservative estimates of scour depth.

- The other reason why the equations predict excessively a conservative abutment scour depth is that, in the laboratory flume, the discharge intercepted by the abutment is directly related to the abutment length; whereas, in the field, this is rarely the case.

- Many of the abutments scour prediction equations presented use the length of an abutment (embankment) projected normal to flow as an independent variable. In practice, the length of embankment projected normal to flow that is used in these relationships is determined from the results of 1-dimensional hydraulic models such as HEC-RAS which assume an average velocity over the entire cross section . In reality, conveyance and associated velocity and flow depth at the outer extremes of a floodplain are much less, particularly in wide and shallow heavily vegetated floodplains.

The actual bridge condition and scour depth at the site is presented graphically as follows.

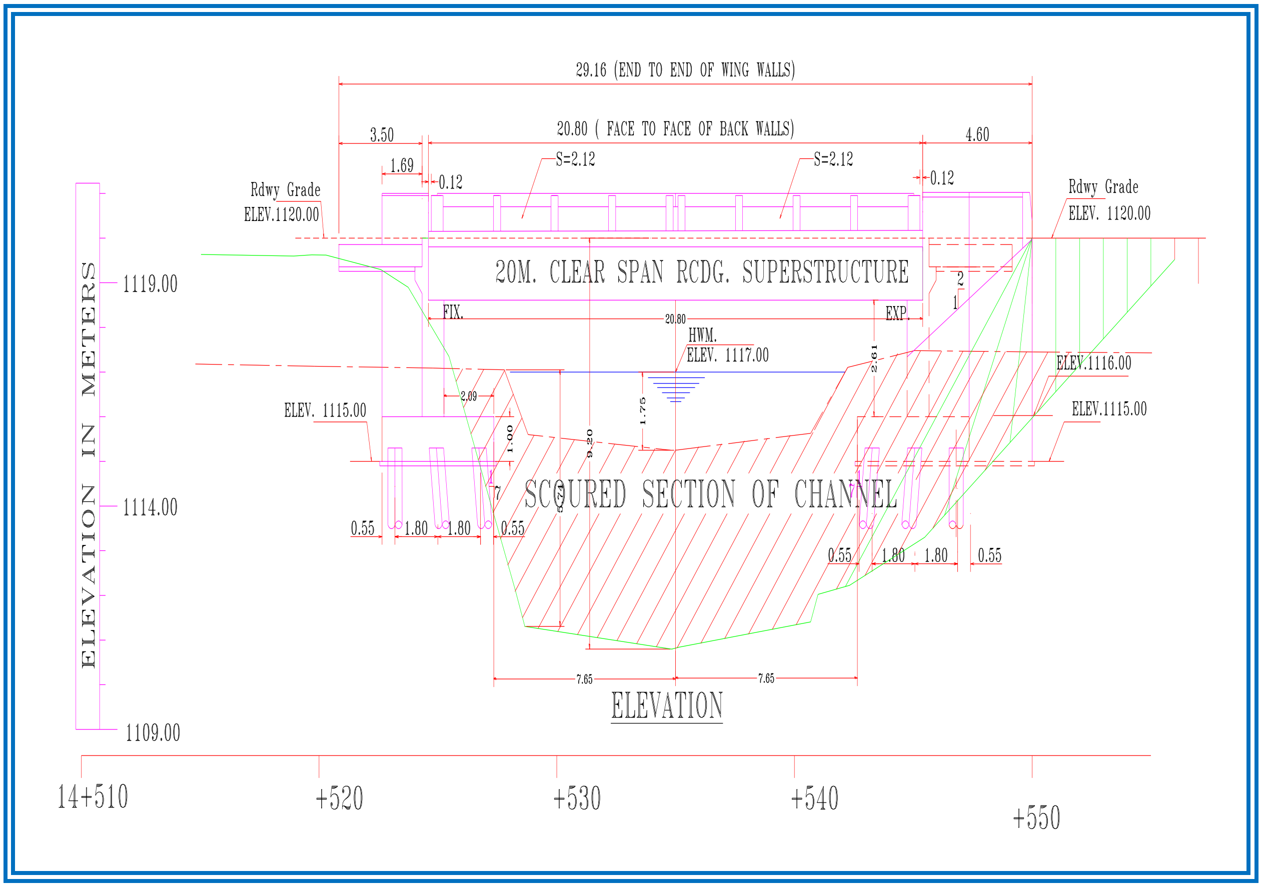

Figure 4-11: Actual Existing Bridge Condition and Scoured Section Using CAD

5. COUNTERMEASURES

5.1. Introduction

A wide variety of countermeasures have been used to control channel instability and scour at bridge foundations. Countermeasures can be grouped based on their functionality with respect to scour and stream instability. The three main groups of Countermeasures are:

- Hydraulic Countermeasures,
- Structural Countermeasures, and
- Monitoring.

Hydraulic countermeasures can be further classified as river training structures and armoring countermeasures.

Countermeasures for local scour at abutments consist of countermeasures that improve flow orientation at the bridge end and move local scour away from the abutment, as well as revetments and riprap placed on spill slopes to resist erosion.

Sile Bridge is under critical condition which requires immediate intervention. The scour under the structure is significant. Detailed hydraulic and structural analyses were performed to come up with comprehensive remedial measures. The following are proposed remedial measures.

5.2. Guide Banks

Guide Banks are highly recommended to improve the flow alignment and move the local scour away from the abutment. Guide Banks of rock embankments should be placed on both abutments. The major use of guide banks is to prevent erosion by eddy action at the bridge abutments where concentrated flood flow traveling along the upstream side of an approach embankment enters the main flow at the bridge.

The proposed Guide Banks can protect not only bridge abutments from local scour, but also the approach embankment because of the still water area behind it. When embankments span wide floodplains, the flows from high waters must be aligned to flow smoothly through the bridge opening. Overbank flows on the floodplain can severely erode the approach embankment and could increase the depth of the scour at the bridge abutment. Guide banks can be used to redirect the flow from the embankment and to transfer the scour away from the abutment. Moreover, Guide banks serve to reduce the separation of flow at the upstream abutment face and maximize the total bridge waterway area, and reduce the abutment scour by lessening the turbulence at the abutment face.

5.3. River Training & Erosion Protection

River training works and channelization are highly recommended to control and guide the flow within well-defined banks. The existing masonry embankment protection wall of Arbaminch side banks were collapsed and transported by the flood due to instability created by erosion of the channel bed. Accordingly, these dictate that provision of rigged Embankment Protection structure like Masonry Retaining wall is questionable due to highly erodible thick silty foundation material with poor bearing capacity. The rigged embankment protection structure might be safe if only if it rests on pile foundation material.

In order to protect the exposed parts of piles from further erosion, instability and damage due to collusion by transported debris, it is recommend to cast-in situ C-25 concrete around the exposed pile portion similar with previously constructed concrete protection around Jinka side abutment pile. This might be done either by short creating or by constructing proper formwork and concreting after that.

For stabilizing the channel bed from further scouring provide PVC coated gabion mattress on both upstream, channel bed and downstream channel of the river and provide 2.00m deep PVC coated Gabion cut-off wall.

Also widening of Jinka side banks by channel excavation might be one of the possible remedial measures in order to decrease the effect of scouring and flow discharge velocity at Jinka side foundation.

5.4. Diversion Channel and Provision of Double Cell Box Culvert

According to the analysis as well as observed site condition, the existing structure is inadequate to pass the design flood. Therefore, in addition to the above proposed protection measures , auxiliary opening is required to make the bridge adequate as well as to reduce stress on the protection structures which are proposed to make the bridge safe due to the bridge location.

The hydraulic design of the bridge is performed using HEC-RAS software. On the basis of the upstream channel assessment and detail field investigation, additional opening is proposed at about 40m on the left hand side of the river bank (on ArabaMinch Side). The layout of the proposed additional structure and diversion channel arrangement is shown in the figure below which is taken from the model based on the actual ground survey.

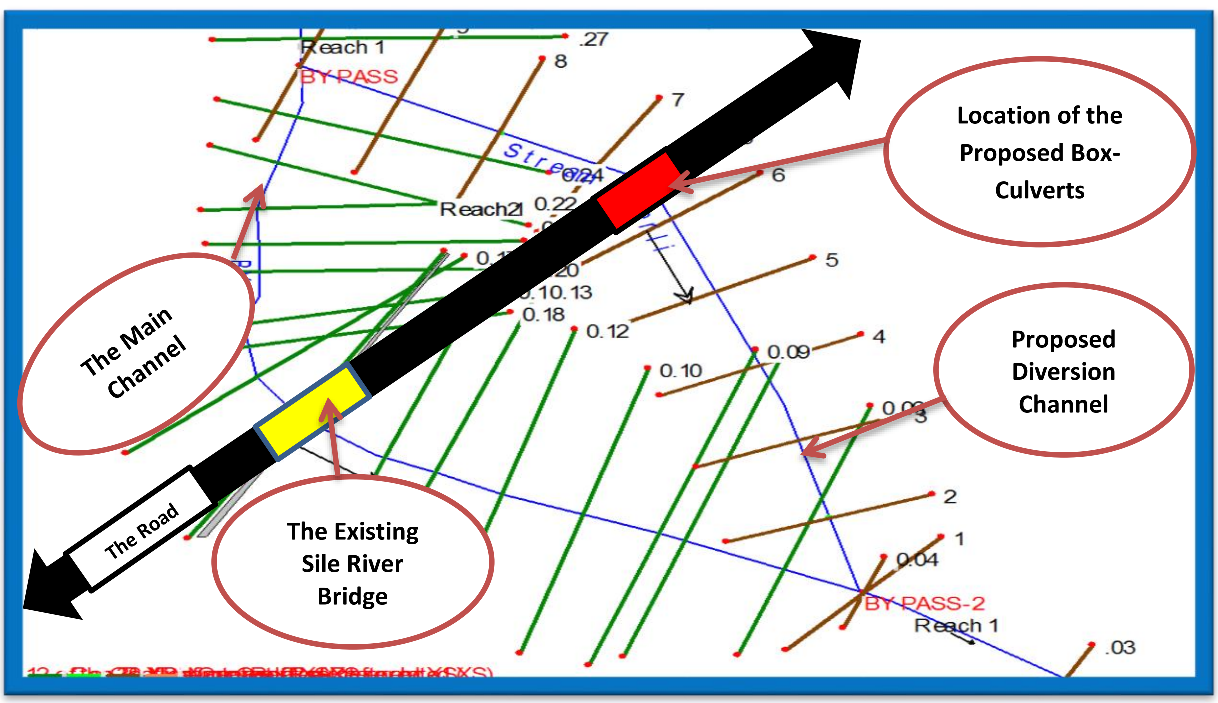

Figure 5-1: Schematic Layout of Structures and Diversion Channel of Sile River

Double cell box culvert with 5.0m by 5.0m is proposed to take some flow during high flood at location shown in the above figure. Under normal condition, the flow will pass through the main Sile River channel by raising the invert of the proposed culvert. The culvert invert will be raised by 2.0m from the existing river channel level. The model outputs of the bridge after the provision of the culvert are shown in the figure below.

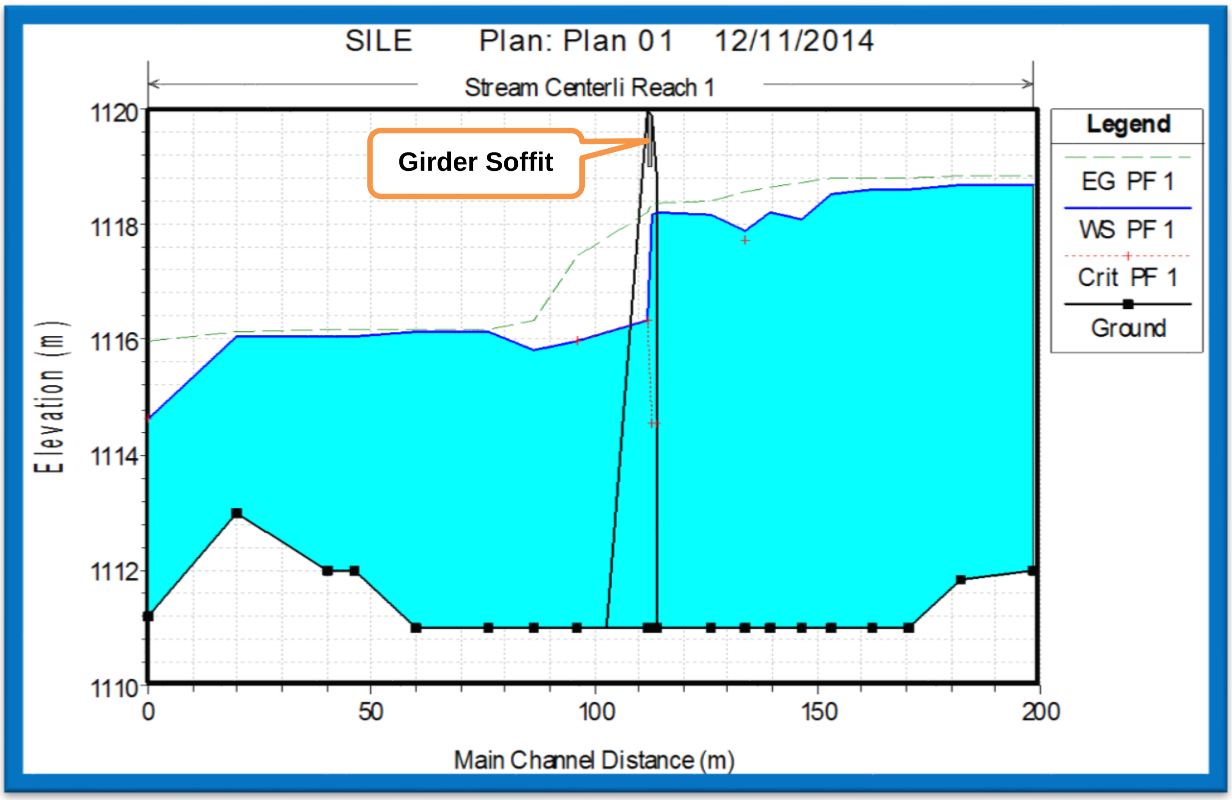

Figure 5-2: Water Surface Profile under Sile Bridge after the Provision of Box-Culvert

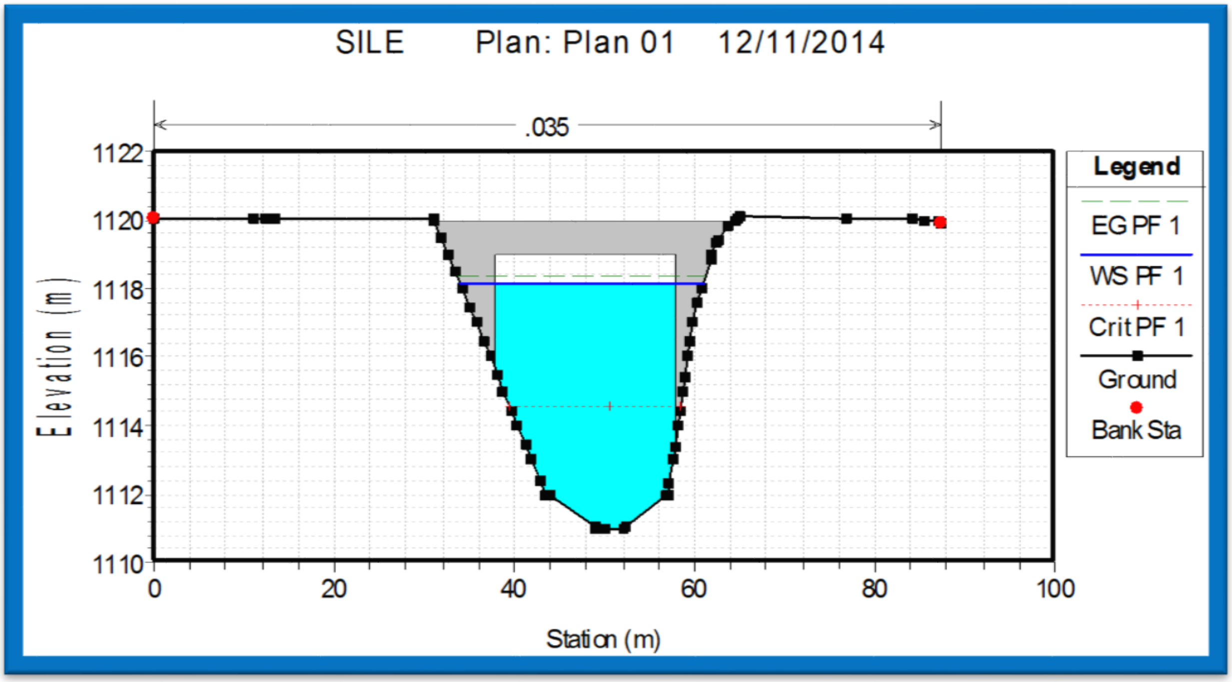

Figure 5-3: Cross section of Sile Bridge after the Provision of the Box-Culvert

The analysis shows that the proposed culvert can convey significant amount of discharge during high flood.

As shown in the above figures, the water surface is dropped and the required freeboard is achieved as discharge of at least $100m^3/s$ and above could pass through the new Box Culvert during high flood. To notice the change in the water surface profile with and without Culvert, compare figures: 5-2 and 5-3 with figure: 4-8 and 4-9. Moreover, the water surface profile in the diverted channel and in the box-culvert is presented as follows.

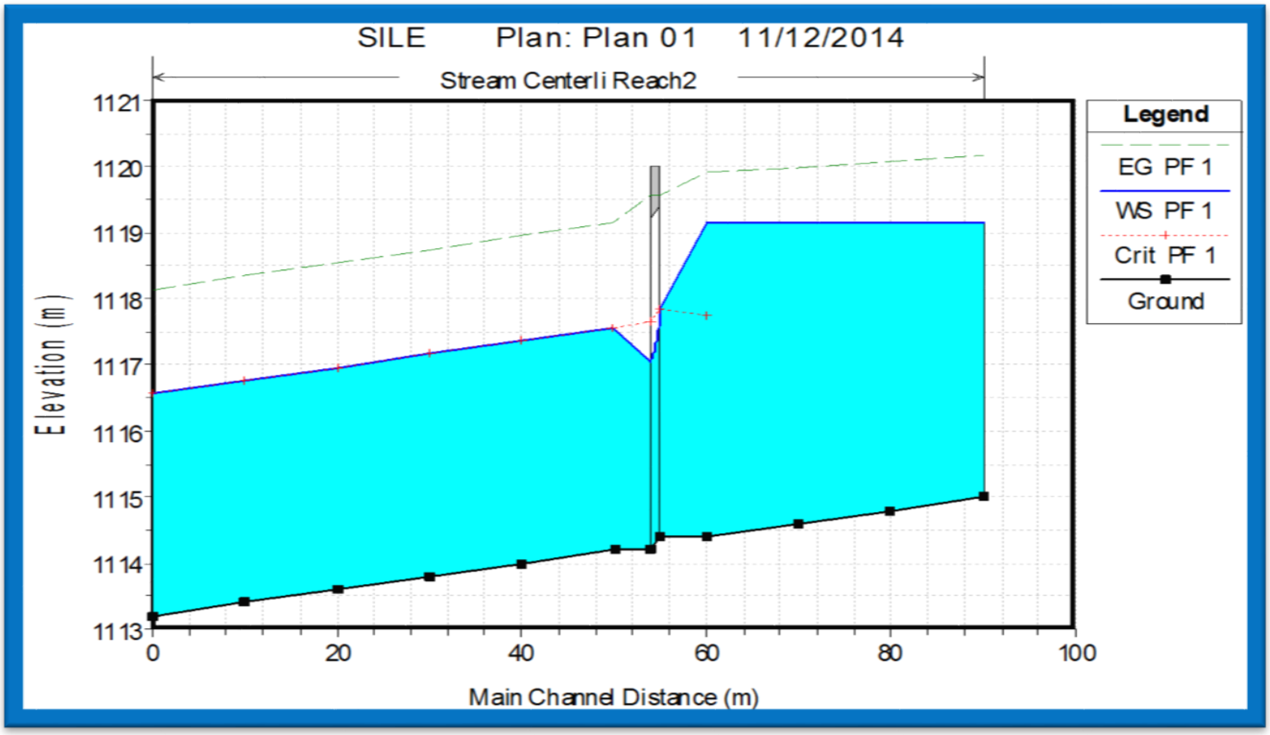

Figure 5-4: Water Surface Profile in the Diverted Channel Upstream & Down Stream of the Box Culvert

The provision of additional structure not only reduces the amount of flood that passes through under the bridge but also decreases the force that the water exerted on the masonry head wall especially due to bends just upstream of the bridge on the right bank and scour on the bridge substructure.

In order to avoid erosion /piping under the structure, the cut off wall shall be extended from the structure invert into the river bed by more than 2.0m.

5.5. New Bridge

The Existing Sile River Bridge is located at a sharp bend where the river morphology is dynamic. Hence, it should be located on a straight reach downstream with stable natural banks and to the channel having adequate opening area. From site investigation a 40m (double span) bridge having a pier at the middle is proposed this will avoid the problem though, it has its own cost implication and priority. The following figure indicates the location of the proposed bridge.

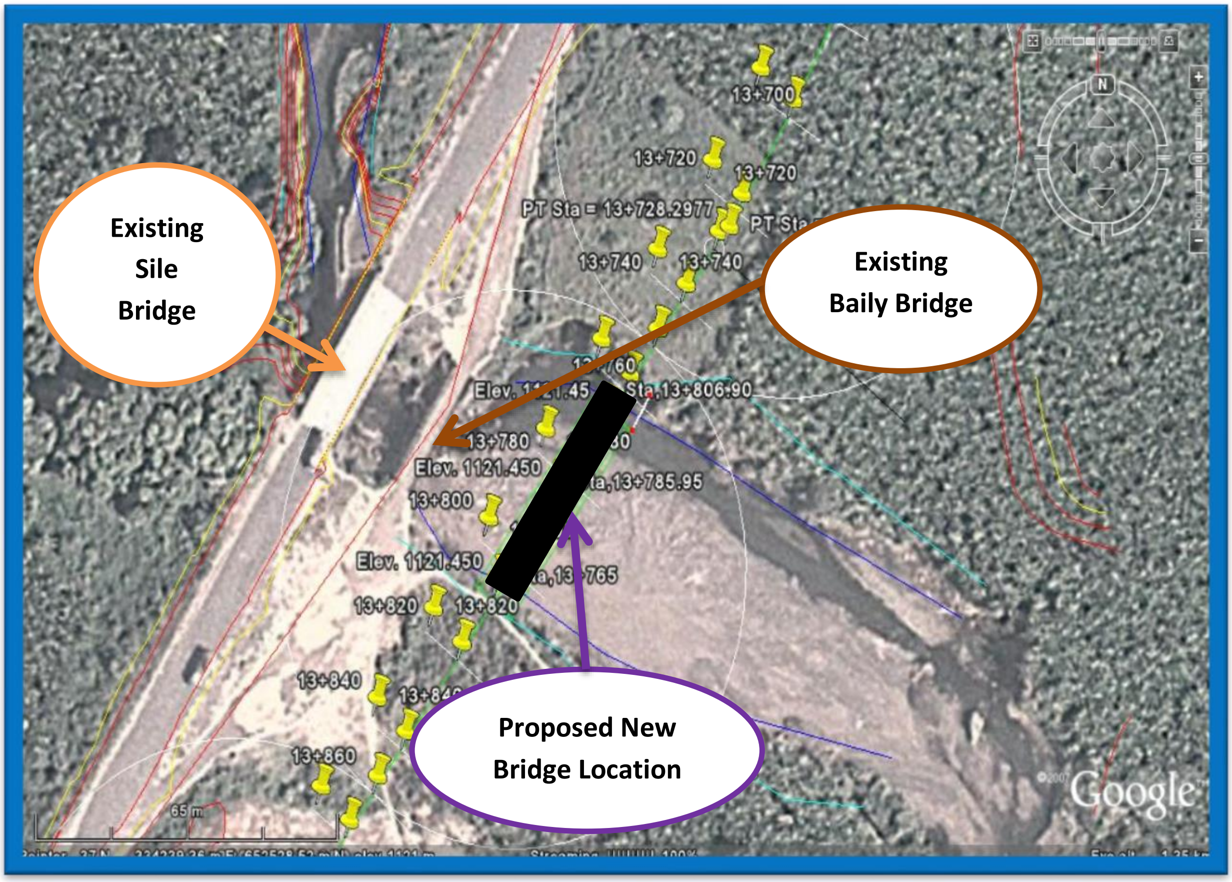

Figure 5-5: Proposed New Bridge site Using Google Earth

5.6. Periodic Inspection and Maintenance

Finally Periodic inspection of the existing condition of the Sile Bridge and maintenance of the mitigation measures is very important. This includes maintenance of all the above proposed channel, embankment and scour protection measures.

6. CONCLUSIONS and RECOMMENDATIONS

6.1. Conclusions

This study comprises an extensive assessment and analysis on the major causes of failure of the Sile River Bridge, the case under study and particularly the scour problem at the river channel at the Bridge Abutments. The analysis was conducted with the intent of providing recommendation. So this study presents the failure causes of Sile River Bridge, proposed Countermeasures and indicates clear direction as to further minimize the problem by supporting with further researches.

The following are the main causes for failure of the Sile River Bridge.

i. Under estimation of the design flood makes the bridge inadequate to pass the design flood. The existing single span 20m bridge is inadequate to pass the design flood. The span of the bridge becomes shorter and having a smaller opening area which create more backwater.

ii. Scour around the abutments and on the main channel which is estimated about 5.80m. The Bridge is failed due to a contraction scour in the main channel and local scour at the abutments since the flow area of the stream is reduced, both by a natural contraction (or constriction) of the stream channel and by countermeasures built at different times under the bridge.

iii. Positioning of the bridge is the other factor. In this regard, the Bridge is located at meandering section of the river and this exposed the substructures for a concentrated hydraulic loading.

iv. The different Countermeasures, Masonry Embankment and Pile Protection structures which are built at different times around both banks of upstream channel bed of the river, Instead of protecting the sub-structures of the bridge, these “protection structures” aggravate scouring by increasing the velocity of flow during rainy season by constricting the natural flow width. Due to the obstruction effect, the channel is scoured severely and created instability of the existing protection structure and

v. The soil material for both abutments and channel at the crossing are poor. The channel, floodplain, and embankment components of a bridge-waterway boundary usually comprise different zones of alluvial sediments and soil which is poorly graded. Abutments' foundation, piles and pile caps are severely scoured through different processes at varying rates of erosion.

6.2. Recommendations

i. In order to estimate the accurate design flood in the study area, the Sile River should be gagged and more meteorological stations should be established. There should be also proper recording and documentation of both hydrological and meteorological data.

ii. Research needs regarding scour processes concern better definition of abutment scour, how scour varies with the parameters determining the potential maximum scour depth, and what considerations limit scour depth at abutments is inevitable.

iii. Numerous scour-induced failures of bridge abutments often result as a consequence of inadequate monitoring and maintenance of approach channel features and concomitantly at times the deterioration of the abutment embankment. Therefore, an important group of research needs relates to improving ways to monitor and maintain bridge waterway conditions in order to avert abutment failure. Developments in monitoring techniques and maintenance methods can help to reduce abutment failure. Research is mandatory to improve implementation of monitoring and maintenance practices.

iv. Communications between Designers and Maintenance Personnel (crew) are essential. Design personnel are encouraged to contact maintenance personnel for their input on difficulties they identify in maintaining drainage structures. Reports by the maintenance forces of both effective and non-effective hydraulic installations aid designers in future work.

v. Development of instrumentation and techniques to better facilitate routine observation and recording bridge-waterway conditions, and to identify waterway and embankment deteriorations that may increase abutment susceptibility to scour failure is indispensable.

vi. Detail investigation is necessary on the newly proposed bridge location such as geo-technical.

REFERENCES

Ahmed, F. and Rajaratnam, N. (2000). “Observations on Flow around an Abutment.” J of Engineering Mechanics, ASCE, Vol. 125, No. 1, pp. 51-59.

Bridge Design Manual, Ethiopian Roads Authority, 2001.

Dey, S., Bose Sujit K. and Sastry, L. N. 1995. Clear Water Scour at Circular Piers: A Model, Journal of Hydraulic Engineering, 121(12), 869-876.

Dey, S. 1997, Local Scour at Piers, part 1: A Review of Development of Research. Int. J. Sediment Res., Vol. 12, No. 2, pp. 23-44.

Dey, S. 1995, Three-Dimensional Vortex Flow Field Around a Circular Cylinder in a quasi-equilibrium scour hole. Sadhana, Proc. Indian Acad. Sci., Vol. 20, No. December, pp. 771-785.

Drainage Design Manual, Ethiopian Roads Authority, 2002.

FDOT (2010), “Bridge Scour Manual,” Florida Department of Transportation, Tallahassee, FL.

Fischenich, J.C., and Landers, M. (2000). Computing Scour. Technical Note EMRRPSR-05, http://el.erdc.usace.army.mil/elpubs/pdf/sr05.pdf.

Graf, W. H. and Istiarto, I. 2002, Flow Pattern in the Scour hole Around Cylinder. J. Hydr. Res., Vol. 40, No. 1, pp. 13-20.

HEC-18, Evaluating Scour at Bridges, Federal Highway Administration (FHWA) publication, Hydraulic Engineering Circular No.18, 1993.

Hoffmans GJCM and Verheij HJ (1997) Scour Manual. AA Balkema, Rotterdam, The Netherlands.

Hydraulic Design of Safe Bridges, US Department of Transportation, 2012.

Kwan, T. F. 1989, A Study of Abutment Scour. Report No. 451, School of Engineering, University of Auckland, Auckland, New Zealand.

Kwan, T. F. and Melville, B. W. 1994, Local Scour and Flow Measurements at Bridge Abutments. J. Hydr. Res., Vol. 32, No. 5, pp. 661-673.

Lauchlan, C.S. and Melville, B.W. (2001) "Riprap Protection at Bridge Piers," Journal of Hydraulic Engineering, v 127, n 5, May, 2001, p 412-418

Manual for Concrete Bridge Maintenance, Ethiopian Roads Authority, 2010.

Melville, B. W. 1975, Scour at Bridge Sites. Report No. 117, School of Engineering, University of Auckland, Auckland, New Zealand.

Melville, B. W. and Raudkivi, R. J. 1977, Flow Characteristics in Local Scour at Bridge Piers. J. Hydr. Res., Vol. 15, No. 4, pp. 373-380.

Melville BW and Coleman SE (2000) Bridge Scour. Water Resources Publications, LLC, Colorado, USA.

NCHRP, Criteria for Selecting Hydraulic Models,2006.

Rajaratnam, N. and Nwachukwu, B. A. 1983, Flow Near Groyne-like Structures. J. Hydraulic Eng., ASCE, Vol. 109, No. 3, pp. 463-480.

Richardson E and Davis S (2001) Evaluating Scour at Bridges. Federal Highway Administration (FHWA), Washington, D.C., USA

Robert Ettema, Tatsuaki Nakato, and Marian Muste, Estimation of Bride Scour at Bridge Abutments NCHRP 24-20 , Transportation Research Board, Washington DC,2010.

Robert Ettema, George Constantinescu and Bruce Melville, Evaluation of Bridge Scour Research: Pier Scour Processes and Predictions, National Cooperative Highway Research Program, 2011.

Sheppard, D. M., and Miller, W. (2006), "Live-bed Local Pier Scour Experiments," Journal of Hydraulic Engineering-ASCE, Vol. 132, No. 7, 635-642.

Sheppard, M., Demir, H. and Melville, B.W. (2011). "Scour at Wide Piers and Long Skewed Piers," NCHRP Report 682, Transportation Research Board of the National Academies, Washington D.C.

Tey, C. B. (1984). "Local Scour at Bridge Abutments." Report No. 329, University of Auckland, School of T. Engineering, Department of Civil Engineering Private Bag, Auckland, New Zealand.

Wilson, K. V., (1995), "Scour at Selected Bridge sites in Mississippi," US Geological Survey Water-Resources Investigations Report 94.4241, Reston, VA.

APPENDIX- I

Topographic Survey Data of Sile River Bridge

Topographic Survey Data of Sile River Bridge

Pt.No	Northing	Easting	Elevation	Remark
1.	652324.1	334088.3	1120.344	BM 153
2.	652358	334097	1120	BM 152
3.	652362.6	334110.4	1119.988	BM 150
4.	652358	334097	1120.009	BM 152
5.	652477.7	334160.3	1119.796	cl
6.	652476	334163.5	1119.979	eg
7.	652475	334165.7	1119.745	s
8.	652474.7	334167	1119.091	l
9.	652478.7	334156.9	1119.556	r
10.	652479.8	334155.1	1119.374	rs
11.	652479.3	334153.4	1118.718	rstrctop
12.	652480.6	334151.9	1118.796	rstbott
13.	652481.6	334142.7	1118.268	r
14.	652457.8	334153.1	1119.906	cl
15.	652456.2	334156	1120.121	ls
16.	652455.6	334157.6	1120.039	lsh
17.	652454.5	334161.3	1118.787	l
18.	652458.9	334149.5	1119.674	re
19.	652459.8	334147.6	1119.51	rs
20.	652460.7	334143.4	1118.136	rb
21.	652462.8	334137.5	1117.483	r
22.	652462.8	334137.6	1117.483	r
23.	652439	334145.1	1120.052	cl
24.	652437.5	334148.4	1120.194	le
25.	652437.2	334149.6	1120.119	ls
26.	652435.5	334152.8	1119.026	lb
27.	652441	334142	1118.095	re
28.	652441	334142	1119.795	re
29.	652441.6	334140.7	1119.718	rs
30.	652445	334133.6	1117.738	rb
31.	652447.4	334129.9	1117.505	r
32.	652421.8	334136.7	1120.077	cl
33.	652419.4	334141	1120.245	le
34.	652418.5	334142.6	1119.833	ls
35.	652418.1	334143.8	1119.215	lb
36.	652423.2	334133.8	1119.896	re
37.	652424.2	334132	1119.713	rs

Pt. No	Northing	Easting	Elevation	Remark
38.	652427.1	334125.8	1117.828	rb
39.	652403.7	334127.6	1120.068	cl
40.	652401.4	334131.6	1120.166	le
41.	652401	334133.9	1119.752	ls
42.	652394.5	334145.2	1116.869	l
43.	652376.7	334178.2	1116.694	l
44.	652405.2	334124.2	1119.912	re
45.	652405.7	334123	1119.822	rs
46.	652409.1	334117.1	1117.773	rb
47.	652414.6	334106.5	1117.576	rb
48.	652418.3	334099.6	1117.461	rb
49.	652386.6	334118.9	1120.088	cr
50.	652385.6	334121.6	1120.116	le
51.	652384.8	334123.1	1120.079	ls
52.	652383.8	334126.8	1119.704	ls
53.	652379.8	334134.8	1117.032	lb
54.	652374.2	334153.4	1116.789	lb
55.	652365	334175.1	1116.744	lb
56.	652388.4	334115.4	1119.948	re
57.	652389.7	334113.4	1119.733	rs
58.	652392.7	334108.1	1118.114	rb
59.	652401.2	334095.5	1117.354	rb
60.	652368.5	334108.6	1120.054	cl
61.	652367	334111.5	1120.03	le
62.	652365.8	334113.1	1119.977	ls
63.	652363.3	334118.1	1118.058	ls
64.	652361	334125.5	1117.735	lb
65.	652355.7	334143.4	1116.972	lb
66.	652347.1	334168.1	1116.807	lb
67.	652371	334105.9	1119.997	re
68.	652371.7	334104	1119.882	rs
69.	652375.9	334099.8	1118.184	rb
70.	652374.3	334091.7	1118.952	rb
71.	652352.5	334099.8	1120.084	cl
72.	652350.2	334102.3	1120.063	le
73.	652349.5	334103.7	1119.937	ls
74.	652345.7	334111.1	1117.839	lb
75.	652340.2	334121.9	1117.775	lb
76.	652312.7	334148.1	1111.365	lb

Pt. No	Northing	Easting	Elevation	Remark
77.	652281.4	334181.4	1111.197	lb
78.	652343	334125.5	1117.205	lb
79.	652348.7	334138.8	1117.015	Lb
80.	652353.9	334096.7	1120.04	re
81.	652354.5	334095.5	1119.98	rs
82.	652356.5	334088	1116.506	rb
83.	652351	334093.8	1119.291	barge
84.	652351	334093.8	1119.293	b1barg
85.	652351	334093.8	1119.293	b1
86.	652351	334093.8	1120.293	b1
87.	652346.6	334101.5	1120.293	b2
88.	652335.8	334090.5	1120.125	brgt-cl
89.	652334.2	334093.7	1120.098	bl
90.	652337.6	334087.6	1120.113	bl
91.	652322.6	334083.5	1120.109	cl
92.	652320	334086.9	1119.971	le
93.	652313.8	334095.4	1117.359	lb
94.	652309.8	334103.9	1117.208	lb
95.	652302.3	334113.3	1117.302	lb
96.	652296.7	334124.4	1117.165	lb
97.	652286.2	334141.3	1117.069	lb
98.	652277.1	334160.3	1116.849	lb
99.	652273.8	334178.2	1117.068	lb
100.	652277.9	334193.5	1111.254	lmerat
101.	652278	334167.5	1111.112	lmerat
102.	652287.1	334148.2	1111.273	lmerat
103.	652300.1	334127	1111.183	lmerat
104.	652324.2	334079.2	1120.158	re
105.	652339.5	334073.2	1116.508	rb
106.	652343.4	334074.5	1117.448	rb
107.	652350.5	334074.4	1117.527	rb
108.	652361.6	334074.9	1117.478	rb
109.	652372.3	334074.6	1117.108	rb
110.	652384	334072.6	1117.546	rb
111.	652398.7	334072.7	1117.553	rb
112.	652427.2	334074.6	1117.489	rb
113.	652437.6	334074.3	1117.459	rb
114.	652305.4	334074.5	1120.088	cl
115.	652304	334077.1	1120.004	le

Pt. No	Northing	Easting	Elevation	Remark
116.	652302.2	334079.4	1119.744	ls
117.	652298.4	334084.9	1117.127	lb
118.	652286.4	334104.9	1117.338	lb
119.	652276.6	334126.4	1117.227	lb
120.	652263.7	334117.4	1117.276	lb
121.	652330.3	334066.4	1116.859	rb
122.	652335.1	334054.5	1116.666	rb
123.	652304.7	334069.5	1119.972	re
124.	652305.9	334067.7	1119.834	rs
125.	652308	334065.1	1118.905	rb
126.	652337.1	334113.3	1117.301	barge2
127.	652327.2	334109.4	1117.263	barge2
128.	652373.7	334091.8	1118.995	rb
129.	652349.2	334088.1	1115.776	rb
130.	652361.6	334088.1	1116.592	gabiw
131.	652373.2	334090.5	1117.066	gabiw
132.	652398.7	334095.1	1117.527	rb
133.	652428.4	334097.4	1117.542	rb
134.	652308.8	334146.8	1110.306	rb
135.	652308.7	334146.8	1110.3	tp
136.	652308.8	334146.8	1110.305	tp
137.	652308.8	334146.8	1111.911	tp
138.	652289.1	334151.7	1111.654	tp
139.	652289.2	334151.6	1111.648	tp..
140.	652289.2	334151.6	1111.648	tp..
141.	652335.3	334125.2	1110.389	merat
142.	652343.8	334140	1110.769	merat
143.	652316.2	334128.5	1111.285	cl-m
144.	652306.3	334157.6	1111.432	cl-m
145.	652324.7	334166	1110.458	mart
146.	652288.9	334201.6	1111.835	cl-m
147.	652310.7	334212.2	1110.662	m
148.	652269.4	334233.8	1110.218	cl-m
149.	652276.9	334246.2	1109.834	m
150.	652318.2	334101.9	1111.983	bb
151.	652325.3	334106.7	1110.774	bbc
152.	652334.5	334112.8	1112.872	bb
153.	652329.8	334087	1111.357	bb1
154.	652335.3	334090.4	1110.865	bb1c

Pt. No	Northing	Easting	Elevation	Remark
155.	652340.5	334093.7	1111.545	Bb1
156.	652342.5	334076.7	1111.455	m
157.	652345.5	334082.8	1110.938	mcl
158.	652346.4	334087	1110.821	m
159.	652330	334087.8	1111.337	m
160.	652330	334087.8	1111.337	tp
161.	652289.1	334151.7	1111.659	tp..
162.	652346.3	334087.3	1110.839	m
163.	652362.9	334086.5	1111.031	m
164.	652382.5	334084.7	1111.019	m
165.	652358.9	334080.4	1110.927	m
166.	652358.6	334079.2	1112.214	m
167.	652398.1	334086.1	1110.902	m
168.	652364	334077.1	1113.219	m
169.	652413.9	334091.6	1111.646	m
170.	652366.9	334080.5	1110.95	m
171.	652434.6	334091.5	1111.679	m
172.	652383.2	334079.8	1110.904	m
173.	652382.8	334082.6	1110.811	cl-m
174.	652409.6	334078.2	1111.424	m
175.	652399.9	334082.9	1111.088	m-cl
176.	652368	334083.4	1110.813	m-cl

APPENDIX- II

Annual Maximum Daily/Hourly Rainfall of Arbaminch
Rain Fall Fitness Analysis and

Annual Peak Discharges of Kulfo River @ Sikela Near Arbaminch

Annual Maximum Daily/Hourly Rainfall of Arbaminch

Year	24h	1h
1970	-	23.1
1971	-	-
1972	-	-
1973	-	-
1974	-	-
1975	-	-
1976	-	-
1977	-	33.5
1978	-	33.7
1979	-	28.3
1980	-	-
1981	-	-
1982	-	32.5
1983	-	18.0
1984	-	20.8
1985	-	-
1986	-	-
1987	39.0	28.2
1988	46.9	33.0
1989	72.1	35.9
1990	39.3	30.0
1991	54.0	21.6
1992	71.2	-
1993	70.1	-
1994	38.0	45.5
1995	40.7	40.3
1996	66.8	28.5
1997	68.2	29.0
1998	46.6	-
1999	75.3	30.2
2000	54.3	31.5
2001	48.0	44.0
2002	40.6	-
2003	46.8	33.0
2004	38.8	-
X_M	**53.15**	
S_X	**13.26**	

Rainfall Fitness Analysis

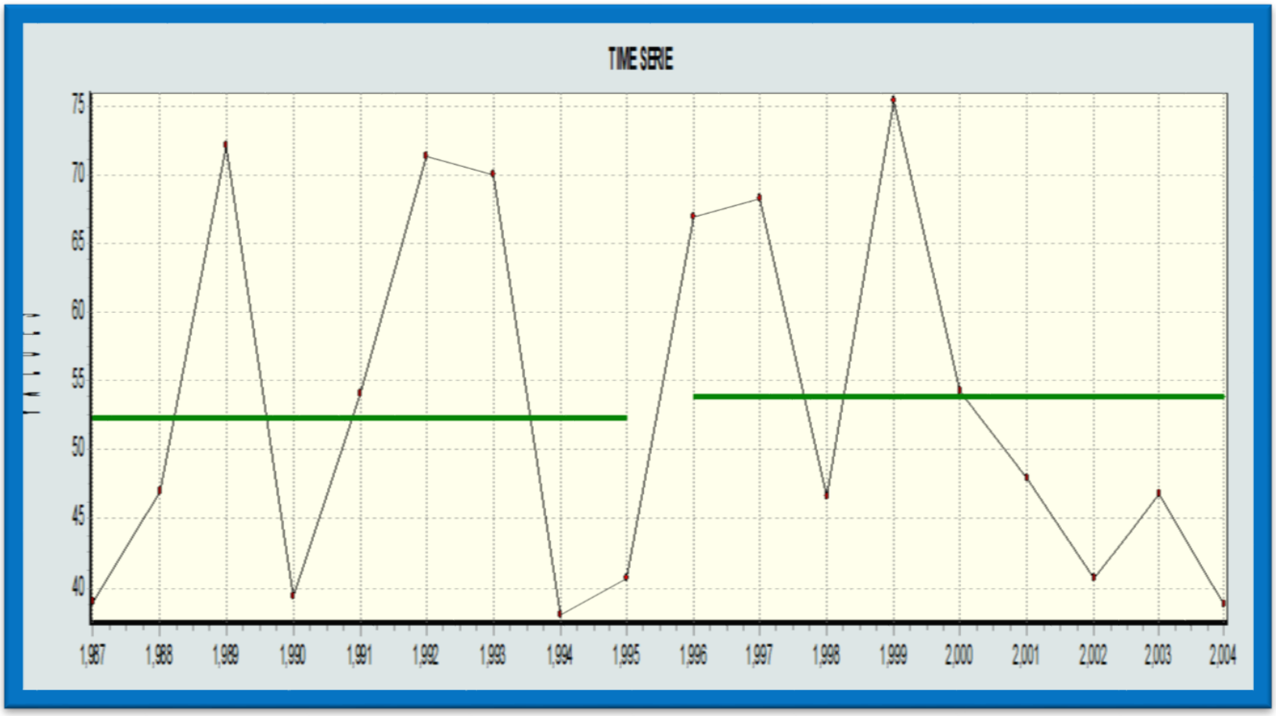

F-test Result for the Rainfall Data Analysis

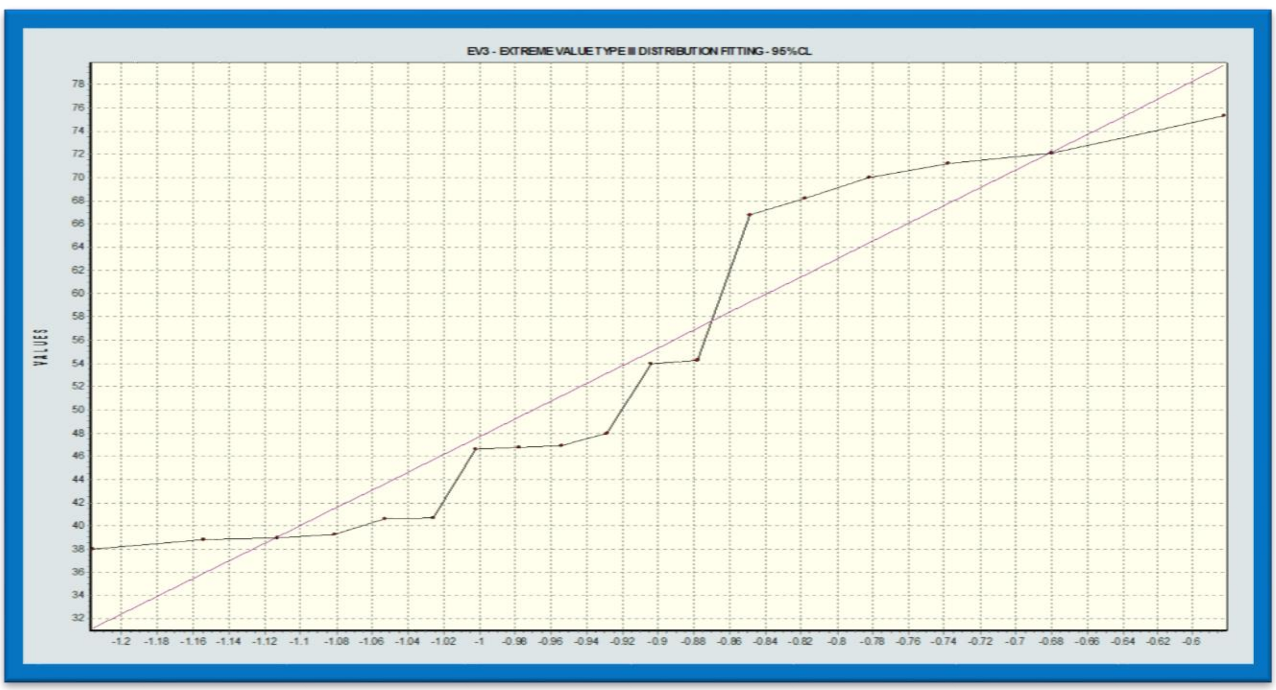

Distribution Fitting Diagram for Extreme Value Distribution III

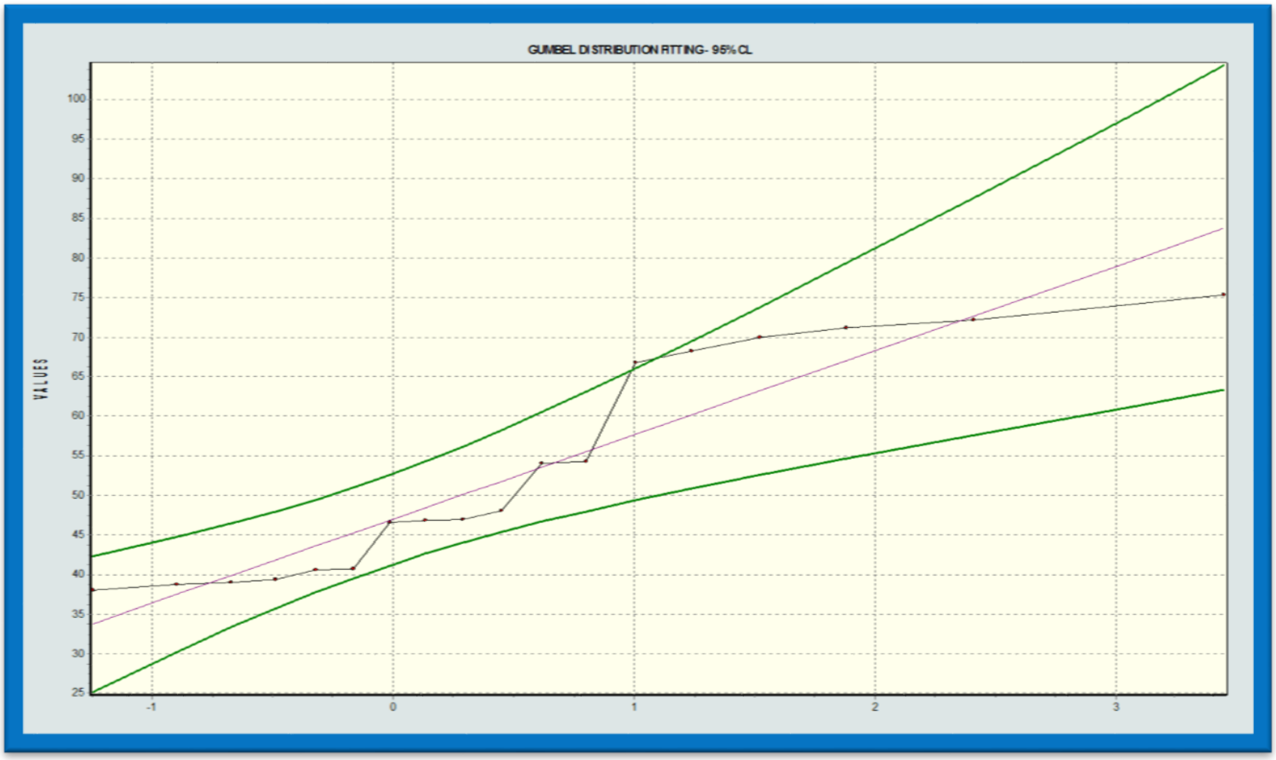

Distribution Fitting Diagram for Gumbel Distribution

Annual Peak Discharges of Kulfo River @ Sikela near Arbaminch

Annual Peak Discharge												
Station Name: Kulfo @ Sikela Near Arbaminch												
Catchment Area: 364Km2												
Y/M	**Jan**	**Feb**	**Mar**	**Apr**	**May**	**June**	**July**	**Aug**	**Sep**	**Oct**	**Nov**	**Dec**
1991			11.627									
1992						37.039						
1993					21.88							
1994					67.29							
1995										23.446		
1996						46.778						
1997										70.329		
1998					60.076							
1999										54.725		
2000					70.326							
2001							81.955					
2002								81.042				
2003								36.677				
2004						51.906						
2005					24.721							
2006										29.00		
2007									33.825			
2008				15.388								
2009									36.677			
2010					38.129							
2011									41.082			
2012									42.582			
2013					41.455							
2014	-	-	-	-	-	-	-	-	-	-	-	-
2015	-	-	-	-	-	-	-	-	-	-	-	-

APPENDIX–III
Frequency Factor (K_T) for Gumbel Extreme Distribution

Frequency Factor (K_T) for Gumbel Extreme Distribution

n (Sample Size)	Corresponding Return Period in Years						
	2	5	10	25	50	100	500
10	-0.1355	1.0581	1.8483	2.8468	3.5876	4.3228	6.0219
15	-0.1433	0.9672	1.7025	2.6315	3.3207	4.0048	5.5857
20	-0.1478	0.9186	1.6247	2.5169	3.1787	3.8357	5.3538
25	-0.1506	0.8879	1.5755	2.4442	3.0887	3.7285	5.2068
30	-0.1525	0.8664	1.541	2.3933	3.0257	3.6533	5.1038
35	-0.154	0.8504	1.5153	2.3555	2.9789	3.5976	5.0273
40	-0.1552	0.8379	1.4955	2.3262	2.9426	3.5543	4.968
45	-0.1561	0.828	1.4795	2.3027	2.9134	3.5196	4.9204
50	-0.1568	0.8197	1.4662	2.2831	2.8892	3.4907	4.8808
55	-0.1574	0.8128	1.4552	2.2668	2.869	3.4667	4.8478
60	-0.158	0.8069	1.4457	2.2529	2.8517	3.446	4.8195
65	-0.1584	0.8019	1.4377	2.241	2.8369	3.4285	4.7955
70	-0.1588	0.7973	1.4304	2.2302	2.8236	3.4126	4.7738
75	-0.1592	0.7934	1.4242	2.2211	2.8123	3.3991	4.7552
80	-0.1595	0.7899	1.4186	2.2128	2.802	3.3869	4.7384
85	-0.1598	0.7868	1.4135	2.2054	2.7928	3.3759	4.7234
90	- 0.16	0.784	1.409	2.1987	2.7845	3.366	4.7098
95	-0.1602	0.7815	1.4049	2.1926	2.777	3.357	4.6974
100	-0.1604	0.7791	1.4011	4.686	4.686	4.686	4.686

APPENDIX -IV

Summary of Reports of HEC-RAS

Reach Lengths, Manning's Values, Contraction and Expansion Coefficients

I- Summary of Reach Lengths

Reach	Station	Left	Channel	Right
Reach 1	0.26	30.62	16.06	11.56
Reach 1	0.24	13.88	11.96	11.64
Reach 1	0.23	8.04	8.04	8.09
Reach 1	0.22	9.96	9.13	8.99
Reach 1	0.21	6.72	6.72	6.79
Reach 1	0.20	30.97	6.81	1.84
Reach 1	0.19	5.79	5.79	6.39
Reach 1	0.18	16.6	7.89	23.35
Reach 1	0.17	12.11	12.11	12.66
Reach 1	0.16	7.99	17.55	29.29
Reach 1	0.159		Bridge	
Reach 1	0.14	10.39	9.87	9.75
Reach 1	0.13	11.87	10.13	10.26
Reach 1	0.12	17.11	16.35	24.35
Reach 1	0.12	20.83	13.67	13.03
Reach 1	0.09	5.1	6.33	6.55
Reach 1	0.08	20.8	20	21.65
Reach 1	0.06	26.8	20	20.76
Reach 1	0.04	40.68	41.05	45.97

II- Summary of Manning's Values

Reach	Station	n1	n2	n3
Reach 1	0.26	0.035	0.035	0.035
Reach 1	0.24	0.035	0.035	0.035
Reach 1	0.23	0.035	0.035	0.035
Reach 1	0.22	0.035	0.035	0.035
Reach 1	0.21	0.035	0.035	0.035
Reach 1	0.20	0.035	0.035	0.035
Reach 1	0.19	0.035	0.035	0.035
Reach 1	0.18	0.035	0.035	0.035
Reach 1	0.17	0.035	0.035	0.035
Reach 1	0.16	0.035	0.035	0.035
Reach 1	0.159		Bridge	
Reach 1	0.14	0.035	0.035	0.035
Reach 1	0.13	0.035	0.035	0.035
Reach 1	0.12	0.035	0.035	0.035
Reach 1	0.12	0.035	0.035	0.035
Reach 1	0.09	0.035	0.035	0.035
Reach 1	0.08	0.035	0.035	0.035
Reach 1	0.06	0.035	0.035	0.035
Reach 1	0.04	0.035	0.035	0.035

III- Summary of Contraction and Expansion Coefficients

Reach	Station	Contr.	Expan.
Reach 1	0.26	0.1	0.3
Reach 1	0.24	0.1	0.3
Reach 1	0.23	0.1	0.3
Reach 1	0.22	0.1	0.3
Reach 1	0.21	0.1	0.3
Reach 1	0.20	0.1	0.3
Reach 1	0.19	0.1	0.3
Reach 1	0.18	0.1	0.3
Reach 1	0.17	0.1	0.3
Reach 1	0.16	0.1	0.3
Reach 1	0.159	**Bridge**	
Reach 1	0.14	0.1	0.3
Reach 1	0.13	0.1	0.3
Reach 1	0.12	0.1	0.3
Reach 1	0.12	0.1	0.3
Reach 1	0.09	0.1	0.3
Reach 1	0.08	0.1	0.3
Reach 1	0.06	0.1	0.3
Reach 1	0.04	0.1	0.3

APPENDIX –V

Scour Potential Data Collection Format

Scour Potential Data Collection Format

1.UPSTREAM CONDITIONS

a. Banks

STABLE: Natural vegetation, trees; Bank stabilization measures such as riprap, paving, gabions; Channel stabilization measures such as dikes and jetties.

UNSTABLE: Bank sloughing, undermining, evidence of lateral movement, damage to stream stabilization measures, etc.

b. Main Channel

• Clear and open with good approach flow conditions or meandering or braided with main channel at an angle to the orientation of the bridge.
• Existence of islands, bars, debris, cattle guards, fences that may affect flow.
• Aggrading or degrading streambed.
Evidence of movement of channel with respect to bridge (make sketches, take pictures).
• Evidence of ponding of flow.

Floodplain

• Evidence of significant flow on floodplain.
• Floodplain flow patterns - does flow overtop road and/or return to main channel?
• Existence and hydraulic adequacy of relief bridges (if relief bridges are obstructed, they will affect flow patterns at the main channel bridge).

Extent of floodplain development and any obstruction to flows approaching the bridge and its approaches.

• Evidence of overtopping approach roads (debris, erosion of embankment slopes, damage to riprap or pavement, etc.).
• Evidence of ponding of flow.

Debris

• Extent of debris in upstream channel.

Other Features

• Existence of upstream tributaries, bridges, dams, or other features that may affect flow conditions at bridges.

2. CONDITIONS AT BRIDGE

a. Substructure

• Is there evidence of scour at piers?
• Is there evidence of scour at abutments (upstream or downstream sections)?
• Is there evidence of scour at the approach roadway (upstream or downstream)?
• Are piles, pile caps or footings exposed?
• Is there debris on the piers or abutments?
• If riprap has been placed around piers or abutments, is it still in place and in good condition?

b. Superstructure

• Evidence of overtopping by flood water (Is superstructure tied down to substructure to prevent displacement during floods?)
• Obstruction to flood flows (Does superstructure collect debris or presents a large area that would obstruct the flow?)
• Design (Is superstructure vulnerable to collapse in the event of foundation movement, e.g., simply-supported spans and non-redundant design for load transfer?)

c. Channel Protection and Scour Countermeasures

• Riprap (Is riprap adequately toed into the streambed or is it being undermined and washed away? Is riprap pier protection intact, or has riprap been removed and replaced by bed-load material? Can displaced riprap be seen in streambed beneath or downstream of the bridge?)
• Guide banks (Are guide banks in place? Have they been damaged by scour and erosion?)
• Stream and streambed (Is main current impinging upon piers and abutments at an angle? Is there evidence of scour and erosion of streambed and banks, especially adjacent to piers and abutments? Has stream cross section changed since last measurement? In what way?)

d. Waterway Area

Does waterway area at the bridge appear small in relation to the stream and floodplain? Is there evidence of scour across a large portion of the streambed at the bridge? Do bars, islands, vegetation, and debris constrict the flow and concentrate it in one section of the bridge or cause it to attack piers and abutments? Do the superstructure, piers, abutments, and fences, etc., collect debris and constrict flow? Are approach roads regularly overtopped? If waterway opening is inadequate, does this increase the scour potential at bridge foundations?

3.DOWNSTREAM CONDITIONS

a.Banks

STABLE: Natural vegetation, trees; Bank stabilization measures such as riprap, paving, gabions; Channel stabilization measures such as dikes and jetties.
UNSTABLE: Bank sloughing, undermining, evidence of lateral movement, damage to stream stabilization measures, etc.

b. Main Channel

• Clear and open with smooth exit conditions, vs. meandering or braided with bends, islands, bars, cattle guards, debris, and fences that retard and obstruct flow.
• Aggrading or degrading streambed.

Evidence of movement of channel with respect to the bridge (make sketches and take pictures).
• Evidence of extensive bed erosion.

c. Floodplain

• Clear and open so that contracted flow at bridge will expand and return smoothly to the floodplain downstream of the bridge, vs. restricted and blocked by dikes, development encroachment, trees, debris, or other obstructions.
• Evidence of scour and erosion due to downstream turbulence.

d. Other Features

• Downstream dams or confluences with larger streams which may cause variable tail water depths. (This may create conditions for high velocity flow through bridge).

Source: Site Investigation Manual-ERA, 2001